

**TECHNIQUES AND MATERIALS FOR PASSIVE
THERMAL CONTROL OF RIGID AND FLEXIBLE
EXTRAVEHICULAR SPACE ENCLOSURES**

DAVID L. RICHARDSON

ARTHUR D. LITTLE, INC.

Distribution of this document is unlimited. It may be released to the Clearinghouse, Department of Commerce, for sale to the general public.

FOREWORD

This research was performed by Arthur D. Little, Inc., Cambridge, Massachusetts, under Contract No. AF 33(615)-3533 and covers the period from February 1966 through May 1967. The work was performed under the direction of the Aerospace Medical Research Laboratories in support of Project 7164, "Aerospace Protective Technology," Task 716412, "Atmosphere and Temperature Control for Extravehicular Assemblies," with Mr. C. G. Roach as project monitor. David L. Richardson was principal investigator for Arthur D. Little, Inc.

The author acknowledges the assistance of Dr. R. P. Caren of the Lockheed Research Laboratory for assistance in procuring thermal control coatings for the louver experiment and Professor Robert C. Reid of MIT for reviewing the techniques for thermally coupling an astronaut with his thermal control system.

The author also acknowledges the assistance of Arthur D. Little, Inc., personnel: Dr. A. E. Wechsler for technical review of the project, R. W. Moore for transient evacuation of insulation, Dr. E. M. Drake for analysis of the heat transfer processes in liquid cooled garments, and E. L. Field for the thermal analysis of orbiting astronauts on or near the surface of a space station.

This technical report has been reviewed and is approved.

WAYNE H. MCCANDLESS
Technical Director
Biomedical Laboratory
Aerospace Medical Research Laboratories

ABSTRACT

This program encompassed an analytical and experimental investigation of passive and semi-passive thermal control techniques for rigid and flexible extravehicular space enclosures in 300 nautical mile earth orbits. The results of the orbit analysis indicate that when an astronaut in a flexible enclosure (soft space suit) works on the surface of a large spacecraft, the temperatures on his external surface are markedly increased over those which occur when he is not near the spacecraft. Moreover, passive thermal control of the astronaut is not possible when he is near the spacecraft. The techniques investigated for thermally coupling an astronaut with his thermal control system include liquid cooled undergarments, gas cooling, and heat transfer to the cooled walls of his enclosure. Techniques were investigated for increasing the conductance through soft space suit insulations by compressing the insulation. The insulation of a cylindrical section of a space suit arm was measured under both compressed conditions (3.7 psia) and uncompressed conditions in simulated noon and earth-umbra orbit positions. The range of conductance increased from 0.26 Btu/ft²-hr°F uncompressed to 0.81 Btu/ft²-hr°F compressed. Measurements were made in simulated noon and earth-umbra orbit positions of the thermal heat dissipating capability of a louver system which was designed for operation in the sun. A 6-inch square model had a net heat flow from the louvers for the four orbit conditions tested (open and closed in the sun and in the shade). The louver operation controls maintained the louver baseplate temperature in the range from 73.9 to 84.7°F for a steady heat dissipation rate of 95.5 Btu/ft²-hr while operating in the shade.

Contrails

TABLE OF CONTENTS

| <u>Section</u> | <u>Page</u> |
|------------------------------------------------------------------------------------|-------------|
| I. INTRODUCTION | 1 |
| II. THERMAL ANALYSIS | 3 |
| A. Flexible and Rigid Space Enclosures in a 300 n.m. Earth Orbit Near a Spacecraft | 3 |
| 1. The Model | 3 |
| 2. Results | 4 |
| B. Coupling of an Astronaut to His Thermal Control System | 12 |
| 1. Gas Cooling | 12 |
| 2. Thermal Coupling with a Liquid-Cooled Suit | 19 |
| 3. Thermal Coupling with a Cooled Wall and Gas Convection | 27 |
| 4. Decrease of Azimuthal Temperature Gradients by Heat Pipes | 31 |
| C. Thermal Control Using Phase Change Materials | 33 |
| D. Thermal Control Using LCG and the Enclosure's External Radiating Surface | 34 |
| E. Thermal Control of Flexible Space Garments | 36 |
| 1. Variable Conductance by Helium Injection | 36 |
| 2. Variable Conductance by Insulation Compression | 38 |
| 3. Thermal Effects of Folds in Space Suits | 41 |
| F. Thermal Control by Transient Injection of Gas into the Insulation Layers | 42 |
| G. Louvers for the Thermal Control of Rigid Space Enclosures | 44 |
| 1. Background | 44 |
| 2. Louver Operation in Sunlight | 45 |
| III. EXPERIMENTAL PROGRAM | 53 |
| A. Thermal Control of Flexible Space Garments | 53 |
| 1. Test Configuration | 53 |
| 2. Insulation Tested | 53 |
| 3. Test Program for Insulated Arm Section | 56 |
| 4. Test Results | 56 |

Contracts

| <u>Section</u> | <u>Page</u> |
|-------------------------------------------------------------------------------------------------|-------------|
| B. Thermal Control Louvers for Rigid Space Enclosures | 64 |
| 1. Thermal Design of the Louver Model | 64 |
| 2. Fabrication of the Louver Model | 71 |
| 3. Test Program for Louver Module | 72 |
| IV. CONCLUSIONS | 79 |
| V. RECOMMENDATIONS | 83 |
| <u>Appendix</u> | |
| I. THERMAL HEAT BALANCE FOR ORBITING ASTRONAUT ENCLOSURES IN THE PRESENCE OF A LARGE SPACECRAFT | 85 |
| A. Assumptions | 85 |
| B. Analysis | 87 |
| C. Computation Program | 88 |
| II. HEAT TRANSFER COEFFICIENT OF OXYGEN GAS TO SKIN | 93 |
| A. Oxygen Properties | 93 |
| B. Model | 93 |
| III. MAXIMUM EFFECTIVE ABSORPTANCE OF AN INFINITE V-GROOVE | 95 |
| IV. ANALYSIS OF LOUVER PERFORMANCE | 99 |
| A. Assumptions | 99 |
| B. Analysis for Open Louvers | 99 |
| 1. Louver Heat Balance | 99 |
| 2. Baseplate Heat Balance | 101 |
| C. Analysis for Closed Louvers | 102 |
| 1. Louver Heat Balance | 102 |
| 2. Baseplate Heat Balance | 102 |
| REFERENCES | 103 |

LIST OF FIGURES

| <u>Figure</u> | | <u>Page</u> |
|---------------|---------------------------------------------------------------------------------------------|-------------|
| 1. | Position of Spacecraft for Maximum Increase in Enclosure Temperature | 5 |
| 2. | Azimuthal Temperatures on a Rigid Space Enclosure--Noon Orbit | 6 |
| 3. | Azimuthal Temperatures on a Rigid Space Enclosure--Twilight Orbit | 7 |
| 4. | Azimuthal Temperatures on a Rigid Space Enclosure--Night Orbit | 8 |
| 5. | Azimuthal Temperatures on a Flexible Space Enclosure--Noon Orbit | 9 |
| 6. | Azimuthal Temperatures on a Flexible Space Enclosure--Twilight Orbit | 10 |
| 7. | Azimuthal Temperatures on a Flexible Space Enclosure--Night Orbit | 11 |
| 8. | Average Radiative Temperature vs. Internal Heat Release--Rigid Enclosure | 13 |
| 9. | Average Radiative Temperature vs. Internal Heat Release--Flexible Enclosure | 14 |
| 10. | Techniques for Coupling an Astronaut with His Thermal Control System | 15 |
| 11. | Model for Liquid-Cooled Garment on the Astronaut's Skin | 21 |
| 12. | Cooling Tube in Contact with the Skin | 24 |
| 13. | Heat Transfer Characteristics for Cooling Tubes in Contact with the Skin | 26 |
| 14. | Heat Transfer Characteristics for a Typical Liquid-Cooled Garment | 28 |
| 15. | Model for Thermal Coupling an Astronaut to a Cooled Wall by Radiation and Convection | 29 |
| 16. | Heat Transfer Characteristics for an Astronaut Thermally Coupled to a Cooled Wall Enclosure | 32 |
| 17. | Thermal Control System Using an LCG and an External Radiating Surface | 35 |

Contrails

| <u>Figure</u> | | <u>Page</u> |
|---------------|------------------------------------------------------------------------------------------------------------------------|-------------|
| 18. | Operating Characteristics of a System Comprised of an LCG and an External Radiating Surface | 37 |
| 19. | Calculated Effect of Compressive Load on an Evacuated Space Suit Insulation | 40 |
| 20. | Average and Maximum Effective Emittance and α_a/ϵ_a for Space Suit Surfaces with Folds of Angle θ | 43 |
| 21. | Schematic of Louver System for Operation in Sunlight | 47 |
| 22. | Base and Louver Temperatures for Louvers Fully Open and the Sun Overhead | 48 |
| 23. | Base and Louver Temperatures for Louvers Fully Open in the Shade | 49 |
| 24. | Base and Louver Temperatures for Louvers Closed and the Sun Overhead | 50 |
| 25. | Base and Louver Temperatures for Louvers Closed in the Shade | 51 |
| 26. | Space Suit Arm Test Section | 54 |
| 27. | Schematic of Simulated Arm Section with Insulation | 55 |
| 28. | Space Chamber Schematic | 58 |
| 29. | Calorimeter Equilibrium Temperatures for the Arm Section with Compressed Insulation | 59 |
| 30. | Azimuthal Temperature Distributions--Space Suit Section on the Earth-Sun Line--Compressed Insulation | 61 |
| 31. | Azimuthal Temperature Distributions--Space Suit Section in the Earth's Umbra--Compressed Insulation | 62 |
| 32. | Louver Test Model | 65 |
| 33. | Base and Louver Temperatures for Open Louvers in Simulated Solar Radiation | 66 |
| 34. | Base and Louver Temperatures for Open Louvers in the Shade | 67 |
| 35. | Base and Louver Temperatures for Closed Louvers in Simulated Solar Radiation | 68 |
| 36. | Base and Louver Temperatures for Closed Louvers in the Shade | 69 |

| <u>Figure</u> | | <u>Page</u> |
|---------------|--------------------------------------------------------------|-------------|
| 37. | Louver Control System | 73 |
| 38. | Louver Thermal Control Model in Simulated Solar Beam | 74 |
| 39. | Steady Heating Operating Characteristics of the Louver Model | 77 |
| 40. | Geometry for Typical Heat Balance | 86 |
| 41. | Space Suit Fold | 96 |
| 42. | Model for Open Louvers | 100 |

LIST OF TABLES

| <u>Table</u> | | <u>Page</u> |
|--------------|---------------------------------------------------------------------------------------------------|-------------|
| I. | Space Suit Insulation Layers | 39 |
| II. | Selected Louver Operation Characteristics | 46 |
| III. | Solar Absorptance, Xenon Light Absorptance, and Room Temperature Emittance for Selected Materials | 57 |
| IV. | Insulation Conductance Derived from Measured Performance | 63 |
| V. | Summary of Losses from Louver Test Model | 70 |
| VI. | Thermal Behavior of Louver Model | 75 |

Contrails

LIST OF SYMBOLS

| | |
|-------|-----------------------------------------------------------------------------------------------------------------------------------------------------------------------|
| A | heat transfer area, ft^2 |
| C | unit area conductance, $\text{Btu}/\text{ft}^2\text{-hr}^\circ\text{F}$; conductance, $\text{Btu}/\text{hr}^\circ\text{F}$ |
| C_p | effective heat capacity, $\text{Btu}/\text{lb dry air-}^\circ\text{F}$ |
| F | view factor, dimensionless |
| H | humidity, $\text{lbs water}/\text{lb dry air}$ |
| L | length, ft |
| P | pressure, lbs/in^2 (psi, psia) |
| Q | total heat flow, Btu/hr |
| R | radius of cylinder, ft |
| S | solar constant, $442 \text{ Btu}/\text{ft}^2\text{-hr}$ |
| T | temperature, $^\circ\text{F}$ |
| U | overall heat transfer coefficient, $\text{Btu}/\text{ft}^2\text{-hr}^\circ\text{F}$; absorbed radiation, $\text{Btu}/\text{ft}^2\text{-hr}$ |
| V | velocity, ft/sec |
| a | earth albedo for solar wavelengths, dimensionless |
| exp | exponential e |
| h | local heat transfer coefficient, $\text{Btu}/\text{ft}^2\text{-hr}^\circ\text{F}$ |
| i | enthalpy, Btu/lb |
| k | local mass transfer coefficient, $\text{lbs water}/\text{hr-ft}^2\text{-unit humidity driving force}$; thermal conductivity, $\text{Btu}/\text{ft-hr}^\circ\text{F}$ |
| q | heat flow per unit area, $\text{Btu}/\text{ft}^2\text{-hr}$ |
| w | flow rate, $\text{lbs dry air}/\text{hr}$, $\text{lbs water}/\text{hr}$ |
| x | length, thickness, ft |
| z | length, ft |

Contrails

| | |
|------------|-------------------------------------------------------------------------------------------|
| α | absorptance, dimensionless |
| δ | depth, ft |
| ϵ | emittance, dimensionless |
| θ | angle, degrees; temperature difference, °F |
| λ | heat of vaporization of water, Btu/lb |
| ξ | effective depth, ft |
| ρ | density, lbs/ft ³ |
| σ | Stefan-Boltzmann constant, 0.1714×10^{-8} Btu/ft ² -hr°R ⁴ |
| ψ | fraction of tube circumference touching the skin |

Subscripts

| | |
|----------|------------------------------------------------------|
| L | long wavelength; louver |
| P | projected |
| R | radiative; view factor for earth reflected radiation |
| S | solar; view factor for earthshine |
| c | enclosure wall |
| f | fluid |
| g | gas |
| in | inlet condition |
| m | metabolic; midpoint |
| o | initial conditions |
| out | outlet conditions |
| s | skin |
| w | wall |
| ∞ | infinity |
| 1 | cylinder space station; specular side of louver |
| 2 | cylinder space enclosure; diffuse side of louver |

Contrails

- 3 baseplate
- 21 view factor from sector on space enclosure to spacecraft
- 3(1)-2 view factor for surface 3 (reflected from surface 1) to surface
 2

Contrails

SECTION I INTRODUCTION

The recent experience of astronauts in extravehicular maneuvers demonstrates the need for effective thermal control of the astronaut while he orbits the earth. Present techniques of thermal control require the thermal isolation of the astronaut from his external environment through the use of an efficient insulating layer and the rejection of all metabolic heat by means of a portable cooling system. There is a time during every orbit when it is possible for the astronaut to naturally radiate away a portion of the metabolic heat generated. However, this potential has not been realized as yet.

In an earlier study (Richardson, 1965), we investigated the feasibility of varying the conductance of an extravehicular space garment by injecting helium into the garment insulation to achieve passive thermal control. Experiments were made in a simulated 300-nautical-mile noon orbit on a cylindrical section of a space suit which was tested first with an evacuated and then with a helium-filled insulation. The environment was a simulated 300-nautical-mile noon orbit. The achievable range of internal heat generation (metabolic) for comfortable suit temperatures was from 600 to 1800 Btu/hr when the evacuated insulation was filled with helium.

In this investigation, the concepts of passive and semi-passive thermal control for soft space suits are further developed, as well as a more generalized approach to thermal control of extravehicular enclosures. Our investigations covered three areas: (a) the thermal behavior of both rigid and flexible space enclosures on and near the surface of an orbiting space station, (b) techniques for thermally coupling an astronaut to an enclosing thermal control system, and (c) proposed techniques for the passive thermal control of rigid enclosures.

The objective of our work was to provide passive or semi-passive thermal control techniques for both soft anthropoform extravehicular space garments and rigid cylindrical extravehicular space enclosures and to determine the degree that thermal control can be achieved in each. Recommendations are made to aid in determining whether a flexible anthropoform garment or a rigid enclosure is optimum for extravehicular application from a thermal control point of view.

Contrails

SECTION II THERMAL ANALYSIS

A. FLEXIBLE AND RIGID SPACE ENCLOSURES IN A 300 N.M. EARTH ORBIT NEAR A SPACECRAFT

1. The Model

An analysis was undertaken to determine the maximum effect which a neighboring spacecraft could exert on the temperature distribution of a space enclosure. Accordingly, the model was set up to determine the temperature distribution around the periphery of the space enclosure under noon, twilight, and night conditions of illumination, with a spacecraft located above, next to, or below the enclosure. In each case, the spacecraft was brought up to a condition of tangency with the space enclosure.

Two types of space enclosure were to be evaluated: a flexible enclosure (cylindrically shaped with a radius of 0.58 foot and a length of 6.4 feet), and a rigid enclosure (cylindrically shaped with a radius of 1.5 feet and a length of 6.0 feet).

The various assumptions made in this analysis are outlined below:

- a. The solar constant is assumed to be $442 \text{ Btu/ft}^2 \text{ hr.}$
- b. The albedo of the earth for solar radiation is assumed to be 0.4.
- c. The absorptivity of the earth for solar radiation is assumed to be 0.6.
- d. The spacecraft can be represented as a cylinder with a 7.5-foot radius and a 16.68-foot length, maintained at a uniform skin temperature of 70°F.
- e. The emissivity of the craft and the enclosure are both $\epsilon = 0.85.$
- f. The absorptivity of the enclosure is equal to:
 - (1) $\alpha_s = 0.17$ (for solar wavelengths) and
 - (2) $\alpha = \epsilon = 0.85$ (for long wavelengths--spacecraft and earth).
- g. All reflection and radiation are assumed to be diffuse.
- h. Each 1/12 of the circumference of the space enclosure can be considered separately.

Contrails

- (1) Flat-plate view areas were taken from Stevenson and Grafton (1961) for earth reflection and earth shine.
- (2) View areas were calculated by integration for the cylindrical sectors of the enclosure to the cylindrical spacecraft to determine the effect of ship reflection and ship shine.
 - i. In all cases, the axis of the enclosure and the axis of the spacecraft are considered parallel; in all cases, the axis of the enclosure is considered to be perpendicular to the plane determined by the earth-to-sun line and the earth-to-enclosure line.
 - j. The effects of the circular ends of the cylinders are neglected.
 - k. Steady-state heat flows are assumed.

Thus, for each sector of the space enclosure, the simulation considers the effects of direct solar radiation, reflected solar radiation from the earth and from the spacecraft, and emitted thermal radiation from the earth and from the spacecraft. The effect of the space enclosure upon the spacecraft was neglected. Details of the thermal analysis are presented in Appendix I.

2. Results

Figure 1 shows the position in which the spacecraft exerts its most profound effect on space enclosure temperature. At noon (enclosure directly between earth and sun) the spacecraft exerts its maximum effect when located directly next to the space enclosure, not above or below it. At twilight (enclosure-to-sun line perpendicular to enclosure-to-earth line) the maximum effect is achieved by the spacecraft directly next to the space enclosure, on the side of the enclosure opposite from the sun. At night, as might be expected, the spacecraft exerts its maximum effect when it is overhead, blanketing the enclosure from space.

a. Azimuthal Temperature Distributions

The effect of placing the spacecraft in the indicated positions with the rigid enclosure and with the maximum estimated internal heat release of 800 Btu/hr is shown in Figures 2, 3, and 4. The similar effects for the flexible space enclosure and for the maximum estimated internal heat release of 1500 Btu/hr are shown in Figures 5, 6, and 7. These figures show how the azimuthal temperature distribution of the space enclosure can be expected to change if, in the orientation to obtain the maximum effect, the spacecraft is brought up tangent to a space enclosure. The spacecraft markedly influences the temperature on those sectors of the space enclosure which can "see" the spacecraft.

Contrails

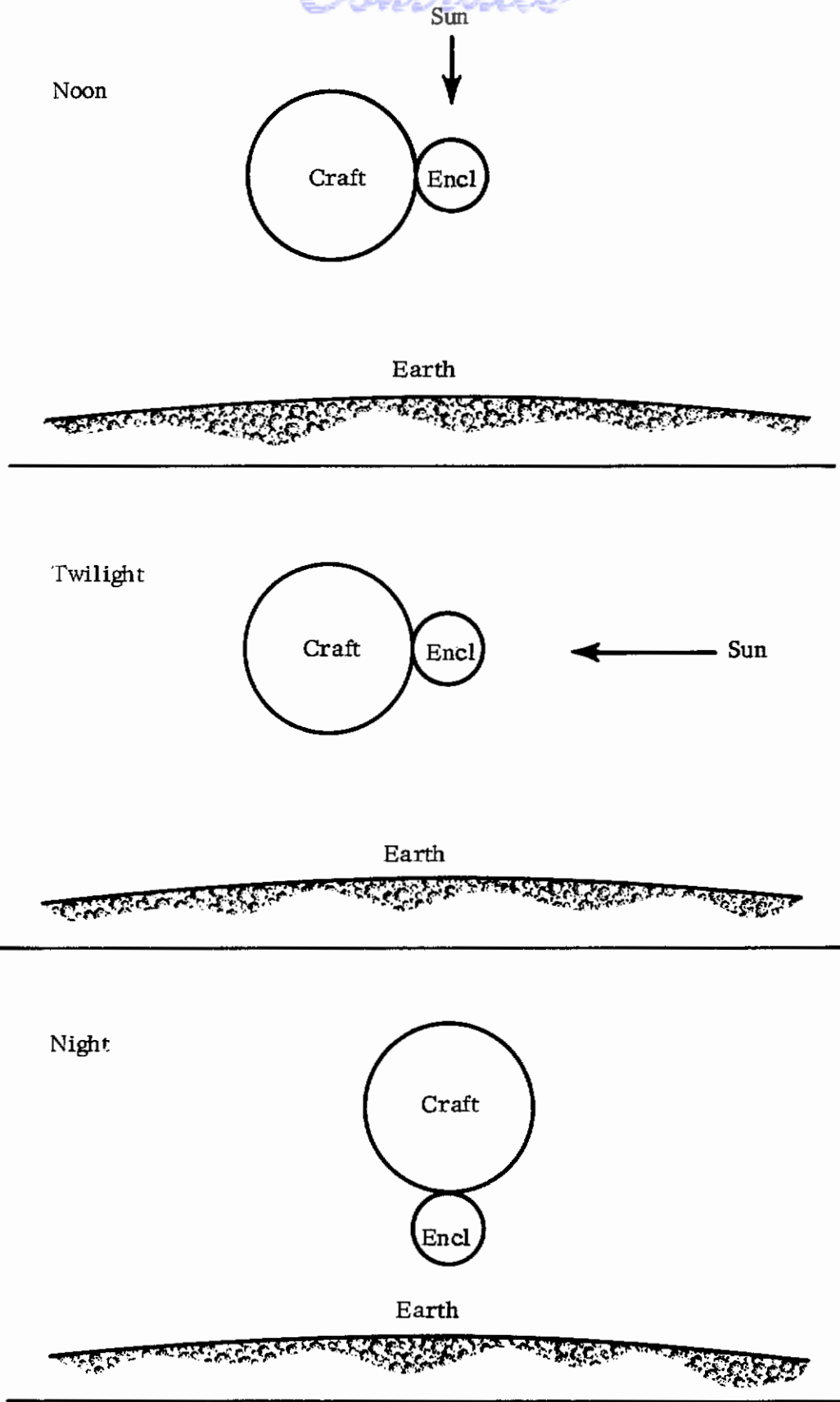


FIGURE 1. POSITION OF SPACECRAFT FOR MAXIMUM INCREASE IN ENCLOSURE TEMPERATURE

Contrails

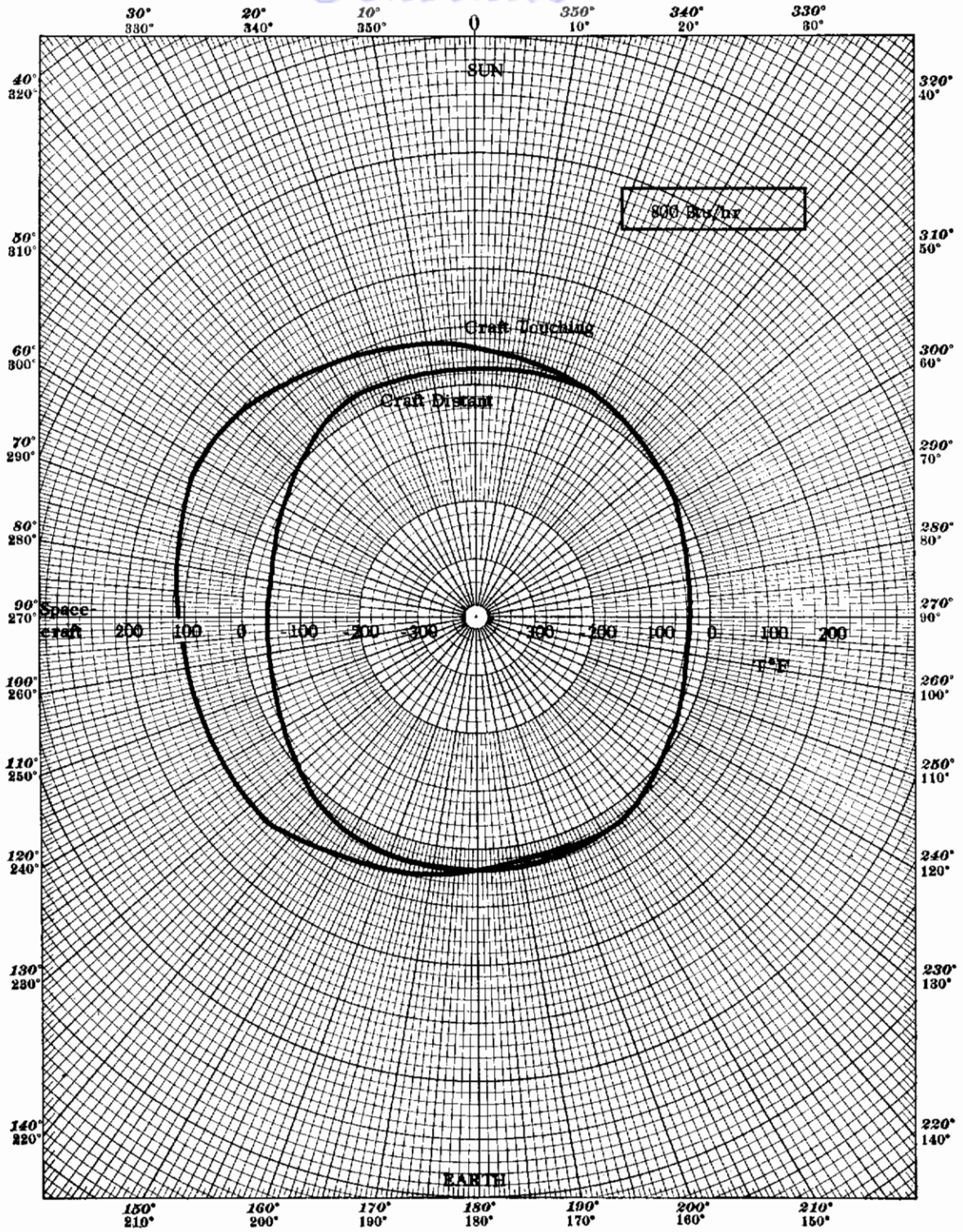


FIGURE 2. AZIMUTHAL TEMPERATURES ON A RIGID SPACE ENCLOSURE - NOON ORBIT

Contrails

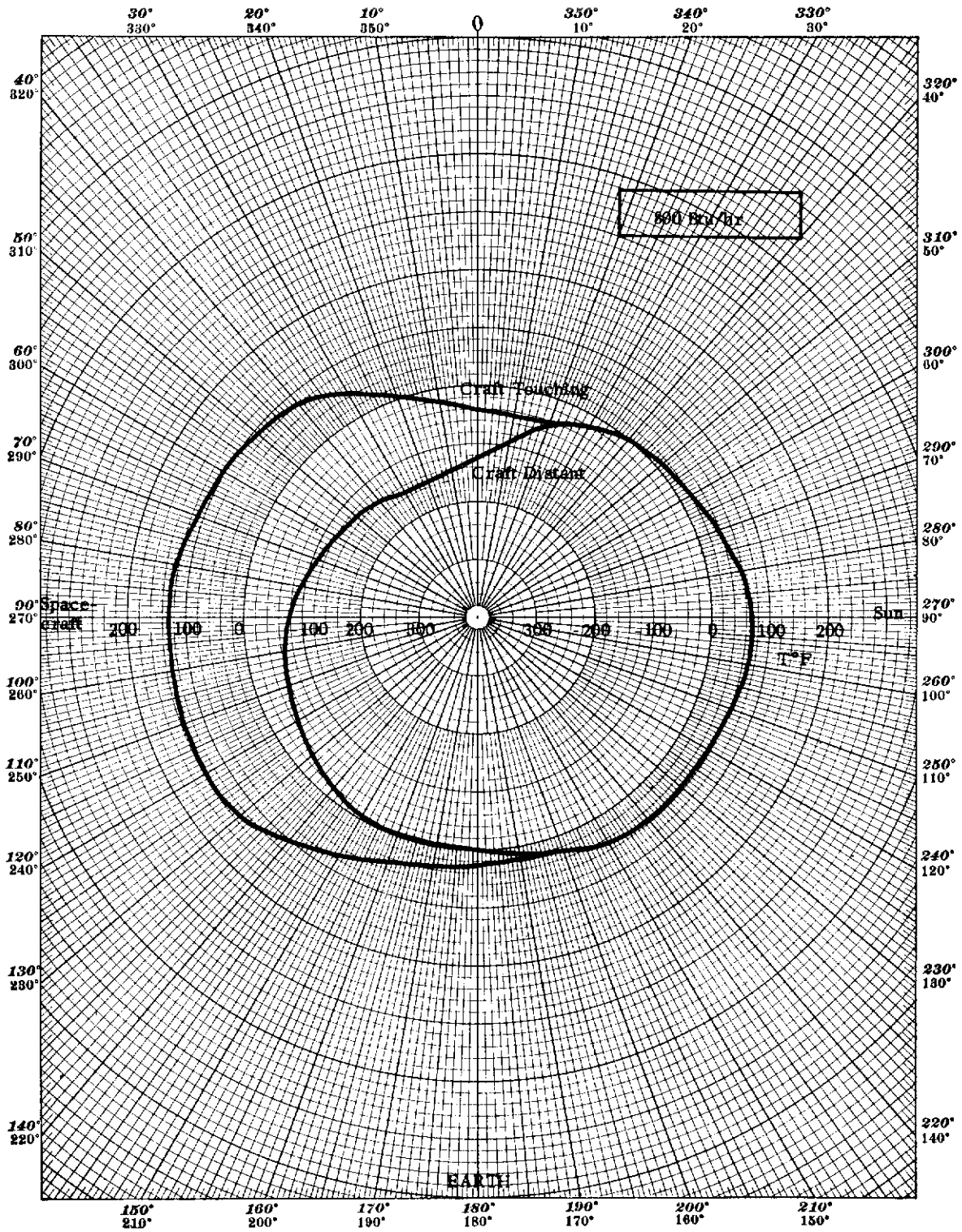


FIGURE 3. AZIMUTHAL TEMPERATURES ON A RIGID SPACE ENCLOSURE - TWILIGHT ORBIT

Contrails

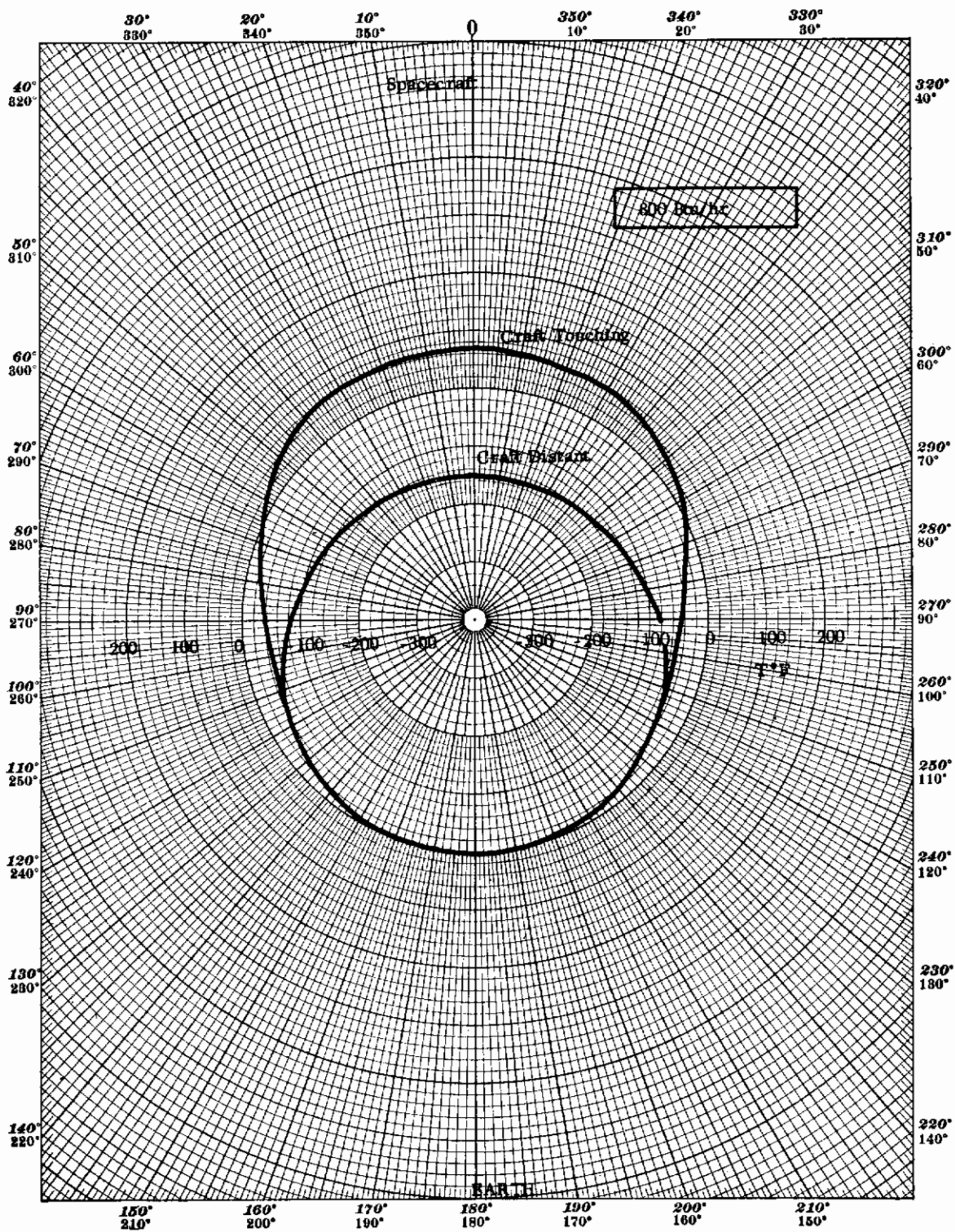


FIGURE 4. AZIMUTHAL TEMPERATURES ON A RIGID SPACE ENCLOSURE - NIGHT ORBIT

Contrails

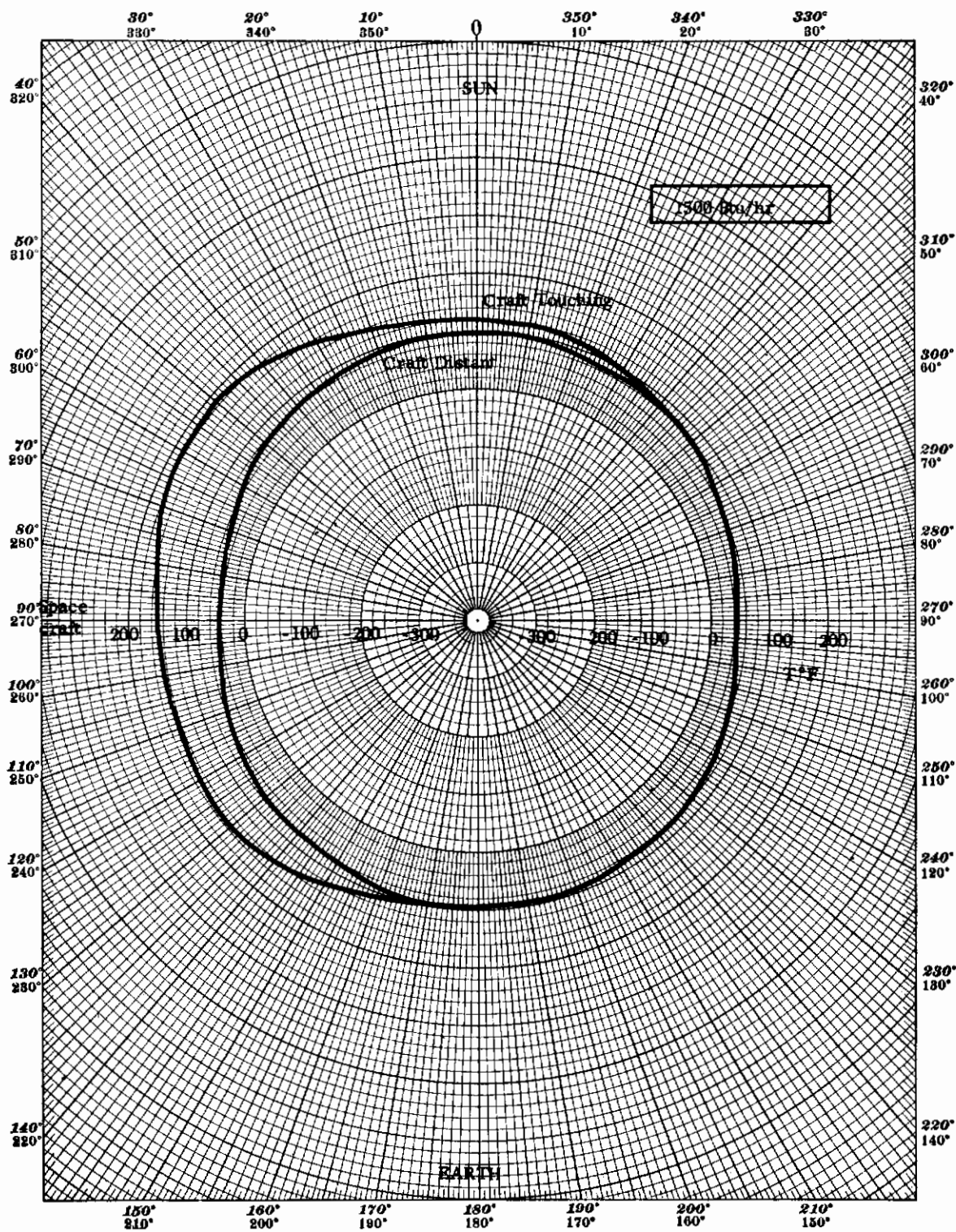


FIGURE 5. AZIMUTHAL TEMPERATURES ON A FLEXIBLE SPACE ENCLOSURE - NOON ORBIT

Contrails

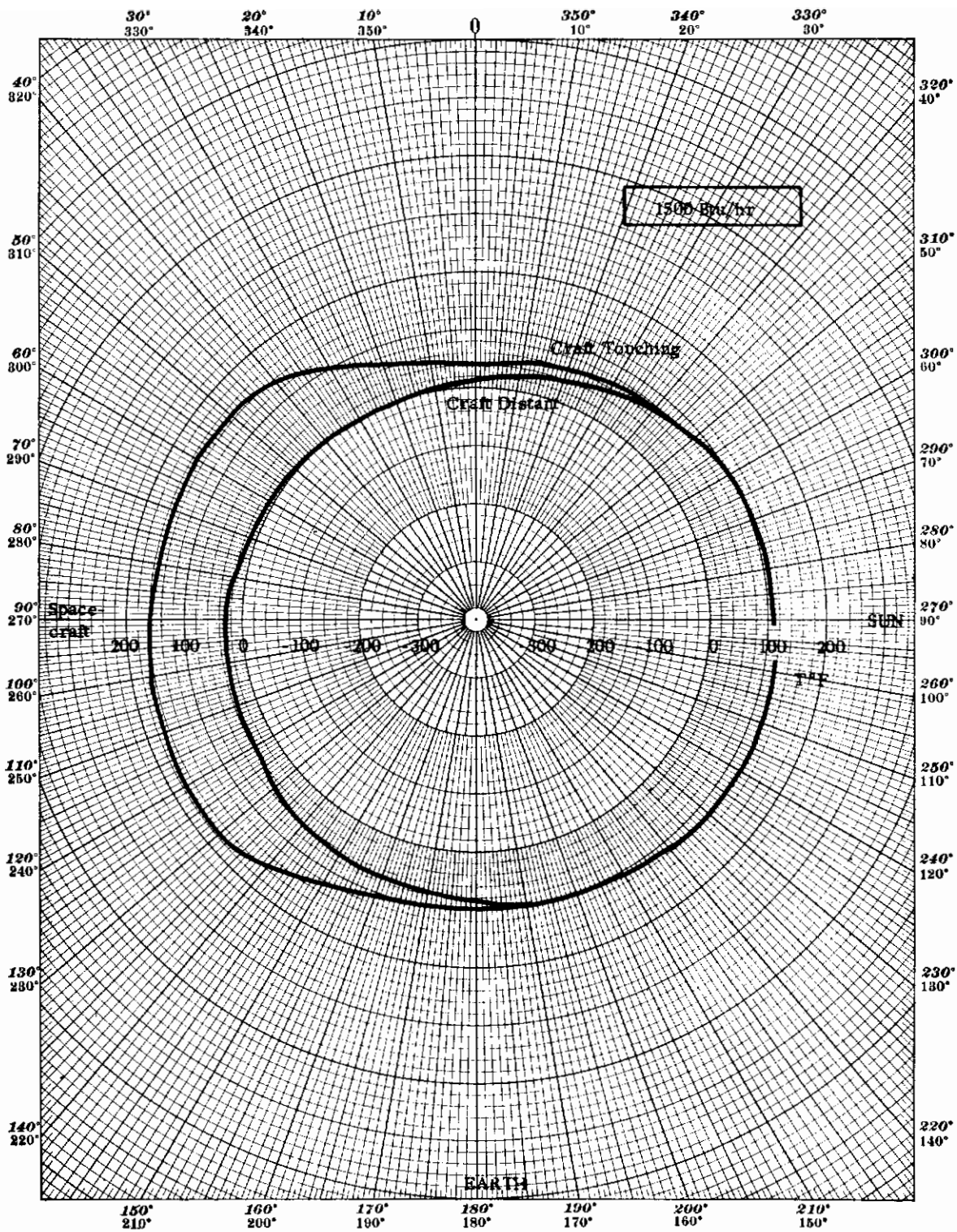


FIGURE 6. AZIMUTHAL TEMPERATURES ON A FLEXIBLE SPACE ENCLOSURE TWILIGHT ORBIT

Contrails

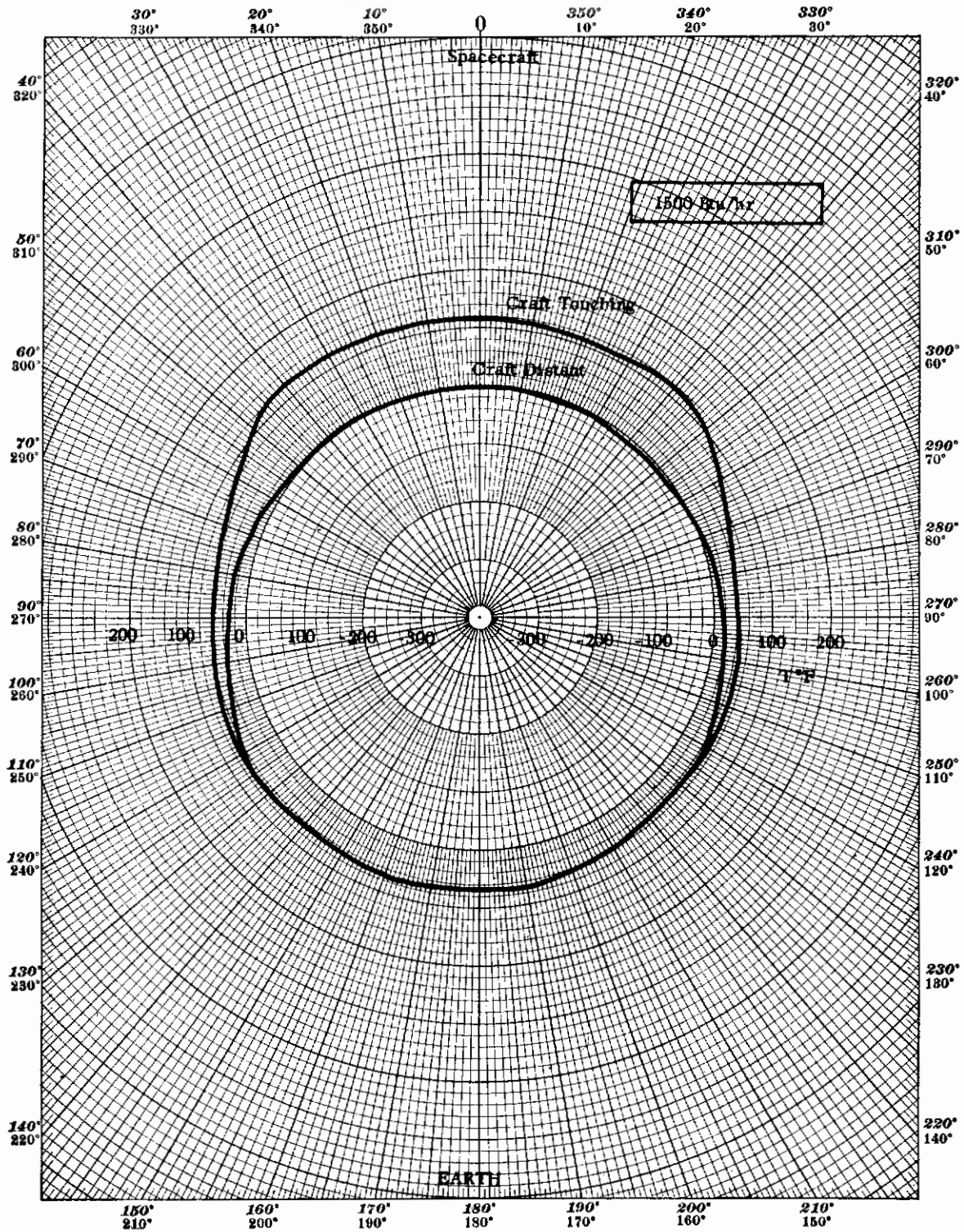


FIGURE 7. AZIMUTHAL TEMPERATURES ON A FLEXIBLE SPACE ENCLOSURE - NIGHT ORBIT

b. Average Temperature

The calculated sector temperatures shown in these graphs assume the independence of each sector. If the temperature differences between sectors are allowed to level, either by increasing the azimuthal conductivity or by employing some internal fluid heat distribution system, it is possible to calculate the effective average temperature which the skin of the space enclosure must reach to radiate the total energy emitted by all of the sectors. This effective average radiative temperature has been plotted in Figures 8 and 9 as a function of the internal heat release rate for each of the space enclosures.

Figure 8 shows that the maintenance of a comfortable temperature within the rigid enclosure poses no problem, even when the effect of the adjacent spacecraft is considered. On the other hand, Figure 9 shows that the presence of the spacecraft greatly reduces the maximum metabolic rate which is allowed before temperatures within the flexible enclosure become uncomfortable, even with the favorable values of absorptivity and emissivity assumed. Thus, if an average enclosure skin temperature of 90°F is the maximum allowable, an internal heat release of 1750 Btu/hr would be permissible in the absence of a spacecraft; but a tangent spacecraft would limit the permissible internal heat release to only 900 Btu/hr.

B. COUPLING OF AN ASTRONAUT TO HIS THERMAL CONTROL SYSTEM

The metabolic heat generated by an astronaut orbiting the earth within an enclosure (either a soft space suit or a rigid space enclosure) must be removed from the boundaries of his body and disposed of through the cooling system of the enclosure. This section summarizes several possible methods for thermal coupling an astronaut to his thermal control system. Summarized in Figure 10 are schematic diagrams for the techniques discussed in the following sections.

1. Gas Cooling

The simplest way to couple an astronaut thermally to a heat sink is to blow a cool gas over his body. The gas would then be cooled, dehumidified if necessary, and recycled. Gas cooling can be evaluated analytically if certain ground rules are first postulated. The results can also be compared with experience obtained in the various astronaut tests in which the only technique used for thermal control was gas cooling.

In our analysis, we have assumed that the exterior boundaries of the suit or capsule are adiabatic (i.e., there is no net energy flow to or from the environment). These adiabatic conditions are achieved by the multi-layer insulations used in space suits and enclosures which effectively isolate the astronaut from his external environment.

Coolant gas enters at temperature, T_{in} , and humidity, H_{in} . Both of these values are independent variables. The values used for gas leaving the suit or capsule at T_{out} , H_{out} , are dependent variables. When the gas

$\alpha_s = 0.17$

$\epsilon = 0.85$

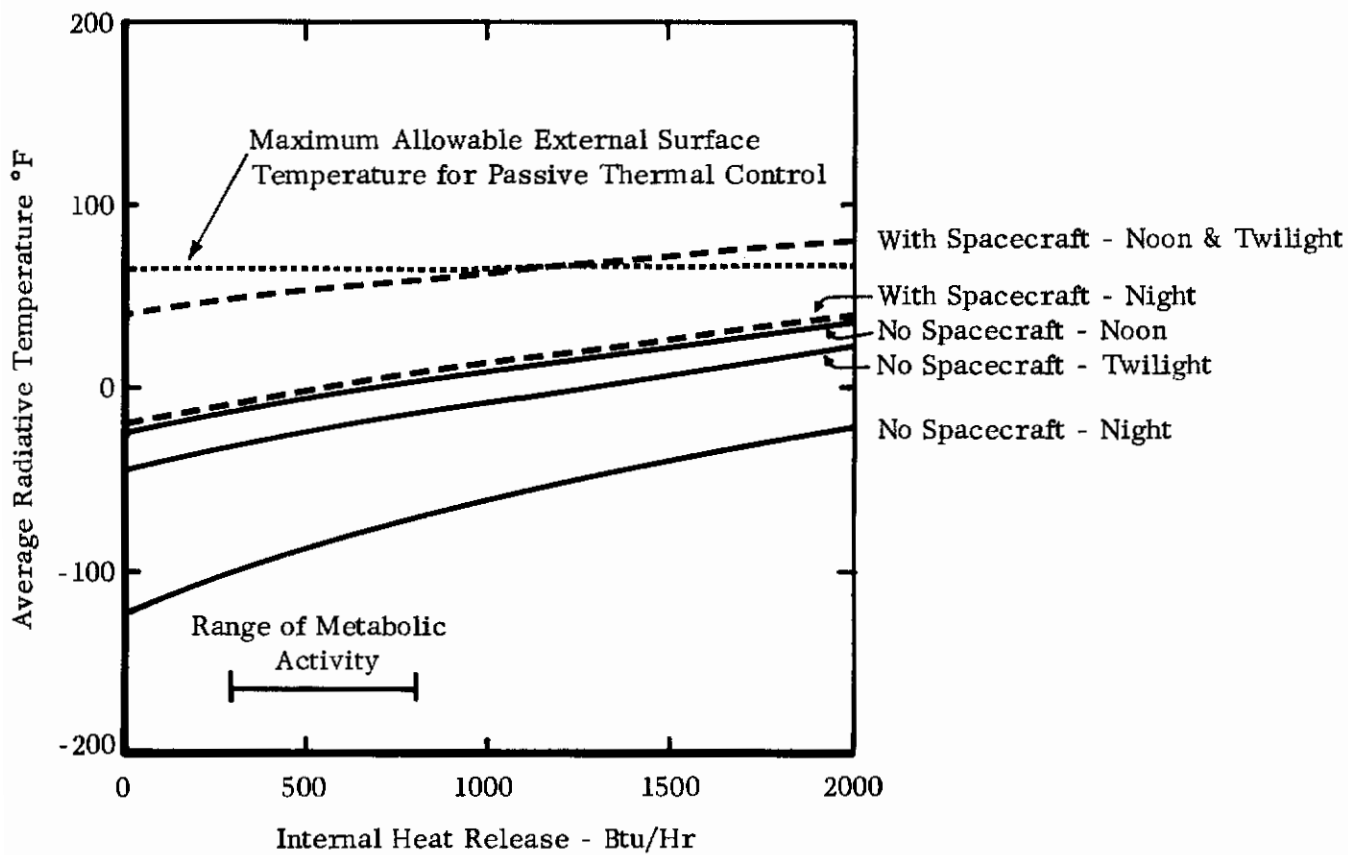


FIGURE 8. AVERAGE RADIATIVE TEMPERATURE VS INTERNAL HEAT RELEASE - RIGID ENCLOSURE

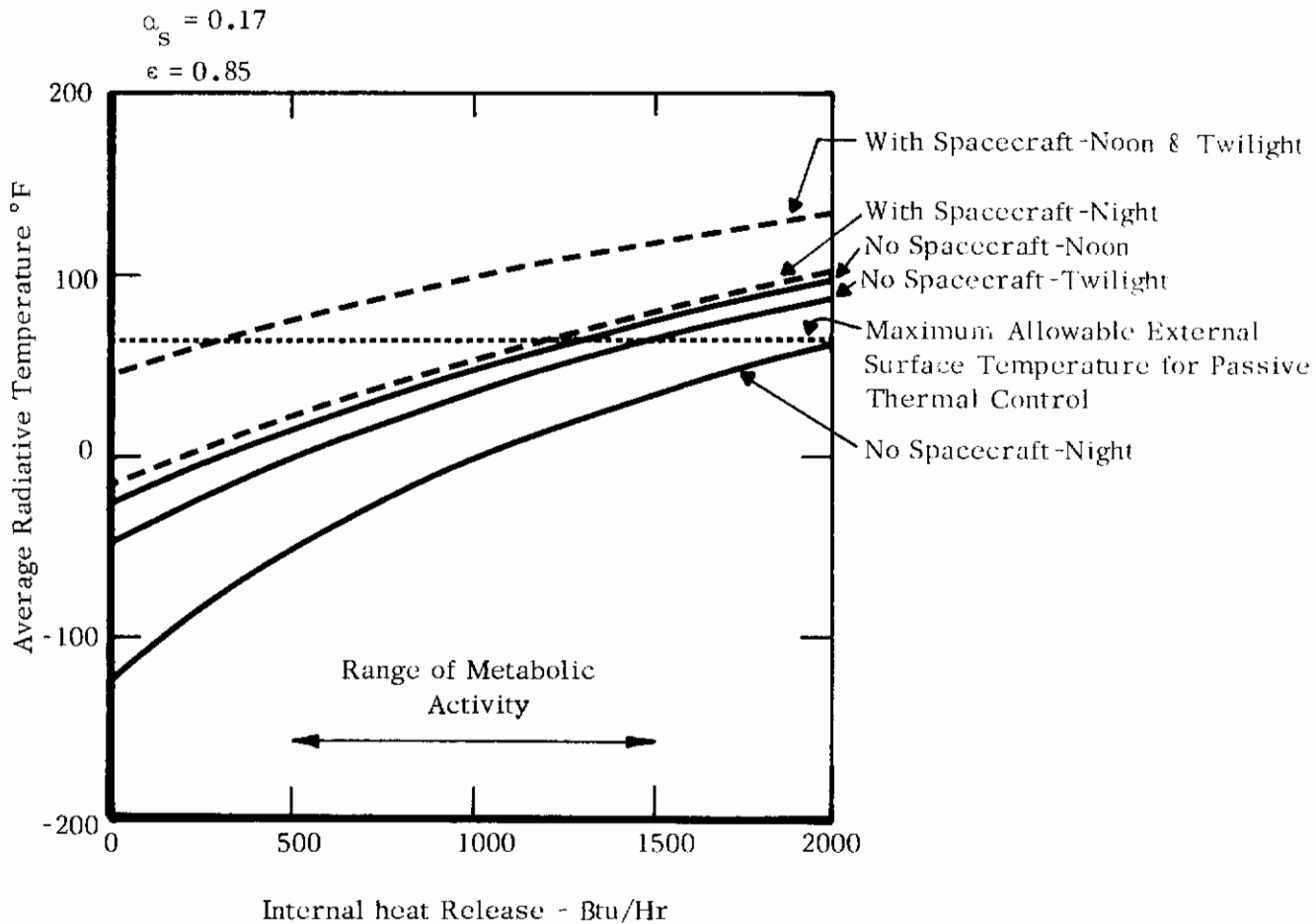
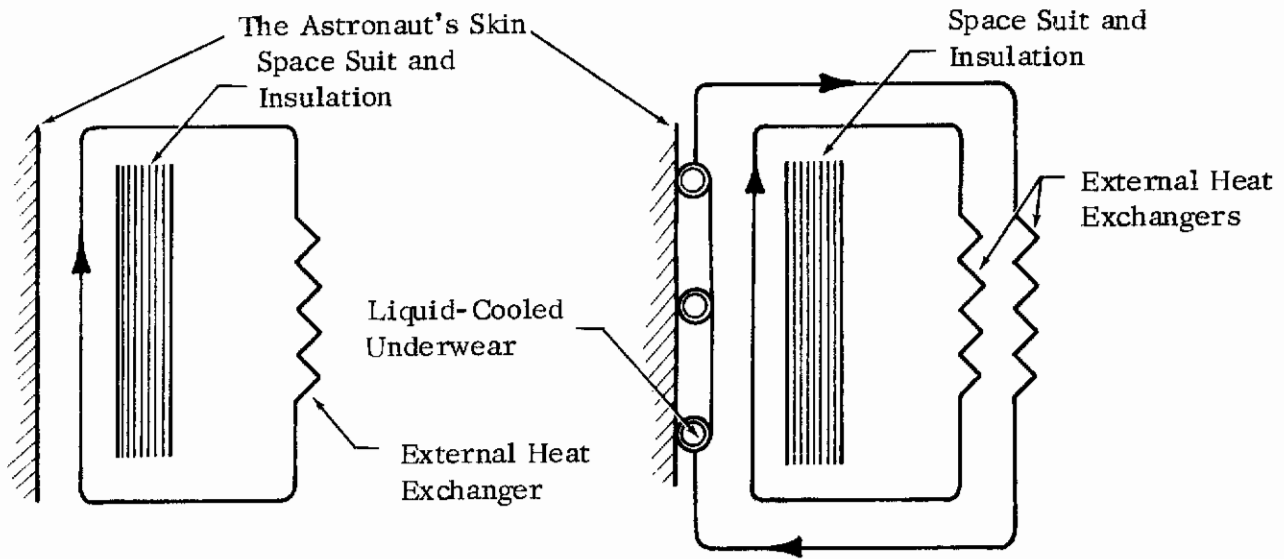
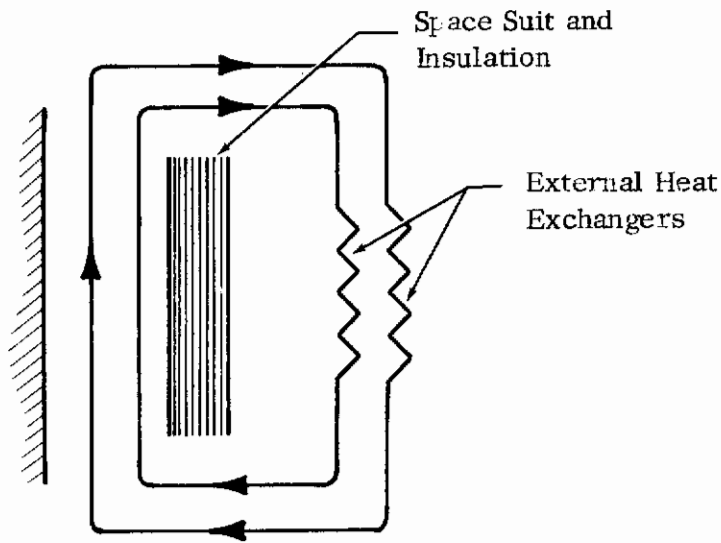


FIGURE 9. AVERAGE RADIATIVE TEMPERATURE FLEXIBLE ENCLOSURE



1. Gas Convection

2. Liquid-Cooled Garment and Gas Convection



3. Cooled Wall and Gas Convection

FIGURE 10. TECHNIQUES FOR COUPLING AN ASTRONAUT WITH HIS THERMAL CONTROL SYSTEM

comes in contact with the skin of the astronaut, it is warmed and humidified. The temperature of the skin will vary both in position and time; however, we have assumed the temperature to be constant at 91°F (33°C). This temperature is close to the measured average-comfort skin temperature of a man. Cooling by sweat evaporation is more difficult to assess. Two possible states will be considered. In the first, no evaporative cooling will be allowed. In the second, the skin always will be wet with water at 91°F.

In addition, realistic flow areas and velocities must be chosen to determine heat and mass transfer coefficients. A meaningful analysis becomes very difficult, if not impossible, if the body contours and subsequent flow patterns are taken into consideration. The alternative, an assumption of a constant velocity at all points, is also difficult to defend. However, this alternative can be analyzed, and the results will still be useful if interpreted in the light of the assumptions.

a. Summary of Analysis

Gas flowing by an element of area dA , transferring heat by convection, and evaporating water from the surface exchanges energy at a rate:

$$dQ = [h (T_{\text{skin}} - T_g) + k\lambda (H_{\text{skin}} - H_g)] dA \quad (1)$$

$$dQ = (C_p dT_g + \lambda dH) w \quad (2)$$

If we define the enthalpy, i , as:

$$i \equiv C_p T + \lambda H \quad (3)$$

then $di = C_p dT + \lambda dH$, neglecting variations in C_p and λ (4)

With equations 3 and 4, and the Lewis Relation for O_2 - H_2O systems:

$$h \approx k C_p \quad (5)$$

then equations 1 and 2 become:

$$dQ = (h/C_p)(i_{\text{skin}} - i_g) dA = w di_g \quad (6)$$

Contrails

Equation 6 may be integrated from the inlet conditions to the outlet conditions, assuming some average \bar{h} and C_p to give:

$$(i_{\text{skin}} - i_{\text{out}})/(i_{\text{skin}} - i_{\text{in}}) = \exp(-hA/C_p w) \quad (7)$$

or
$$(i_{\text{out}} - i_{\text{in}})/(i_{\text{skin}} - i_{\text{in}}) = 1 - \exp(-hA/C_p w) \quad (8)$$

From equation 7, it is obvious why the exponential term is often termed the effectiveness factor: if it is small (due to large h and/or A or due to a small w), then i_{out} becomes essentially equal to i_{skin} , and the outlet gas is in temperature and humidity equilibrium with the skin and represents the maximum energy transfer. Equation 6 integrates to:

$$Q = w (i_{\text{out}} - i_{\text{in}})$$

and substitution of equation 8 yields:

$$Q = w (i_{\text{skin}} - i_{\text{in}}) [1 - \exp(-hA/C_p w)] \quad (9)$$

Since i_{skin} is known from the assumed properties of the skin and i_{in} is an independent variable, then Q is determined by w , h , and A . (Reasonable values of the product hA are discussed in Appendix II.) Several limiting cases are discussed below to indicate the magnitude of the terms.

b. Enthalpy of Oxygen and Helium-Water Mixtures

The use of either oxygen or helium is feasible for suit cooling. The enthalpy of mixtures of these gases with water vapor is given by equation 3, and neglecting the contribution due to water vapor, $C_p(O_2) = 0.22$ Btu/lb°F and $C_p(He) = 1.25$ Btu/lb°F. For any reasonable situation, the minimum value of T_{in} would be about 40°F, and the minimum inlet humidity would correspond to saturated gas at this temperature (e.g., 0.0205 lb water/lb oxygen at 3.7 psia). Thus:

$$i_{\text{in}} = (0.22)(500) + (1000)(0.0205) = 130.5 \text{ (Btu/lb)}$$

The maximum enthalpy out would correspond to the gas in equilibrium with a wet skin ($H = 0.121$ lb water/lb oxygen at 91°F, saturated, and $P = 3.7$ psia).

Thus, $(Q/w)_{\text{maximum}} = 0.22(91-40) + 1000(0.110-0.018)$
 $= 11 + 92 = 103$ Btu/lb oxygen.

In other cases, by equation 9, for oxygen:

$$(Q/w) = 103 [1 - \exp(-hA/C_p w)] \quad (10)$$

Similarly for helium:

$$\begin{aligned} (Q/w)_{\text{maximum}} &= 1.25 (91-40) + 1000 (0.87-0.15) \\ &= 64 + 760 = 824 \text{ Btu/lb He} \end{aligned}$$

$$(Q/w) = 824 [1 - \exp(-hA/C_p w)] \quad (11)$$

Although helium appears at an advantage on a mass basis, oxygen has a slightly better $(Q/w)_{\text{maximum}}$ on a mole basis. Furthermore, because h of helium at the same Reynold's number is only about twice h , oxygen, we will limit further discussion solely to oxygen.

c. Oxygen-Water Gas Coolants

As shown in Appendix II, the heat transfer coefficient depends on the gas velocity, which in turn depends upon the flow rate and flow-passage area. For a typical average minimum area of 0.5-inch, heat transfer coefficients are in the range of 1 Btu/hr-ft²°R at 5 ft/sec to 2 at 30 ft/sec. To ensure comfort the gas velocity should be kept under 5 ft/sec; whereupon the value of h is close to 1.05 Btu/hr-ft²°F, and the flow is laminar. Furthermore, the maximum area of a man exposed to coolant gas is about 20 ft². For a velocity of 5 ft/sec, $P = 3.7$ psia, the actual cfm is near 40 and $w = 50$ lbs/hr. Thus, $hA/C_p w = 2.0$ and $[1 - \exp(-hA/C_p w)] = 0.87$; $q = 50 \times 103 \times 0.87 = 4500$ Btu/hr.

The value $50 \times 0.87 \times (0.092) = 4.0$ pounds of water evaporated from the skin is obviously an excessive quantity, but it results from our previous assumption that the skin is completely wet at 91°F. Experiments indicate that water losses are much less. In fact, if the skin were completely dry, then equation 10 becomes:

$$Q = 11 [1 - \exp(-hA/C_p w)]$$

so that for a flow of 50 lbs/hr, $T_{in} = 40^\circ\text{F}$, and the heat dissipated at the skin is $Q = 50 \times 11 \times 0.87 = 480$ Btu/hr.

d. Discussion

In the case of cooling with oxygen gas, we have arbitrarily chosen 40°F as the lowest reasonable value of T_{in} . Also, the gas in contact with the

man must maintain a velocity of about 5 ft/sec through a 0.5-inch cross section. As much as 4300 Btu/hr could be removed when the skin is wet at 91°F; however, the heat transfer decreases to about 500 Btu/hr when the skin is dry.

A very complicated parametric study could be carried out, but the merit of such an undertaking is doubtful. First, our approximate calculations indicate that refinements in determining h are not worthwhile, since the effectiveness factor is close to unity. Second, there are two limits of sweating. If there is no sweating, the concept of gas cooling can be rejected because it requires too much gas flow and compressor power to remove reasonable amounts of metabolic heat. If the skin is completely wetted, a large amount of heat can be extracted but at a cost of severe dehydration. However, the actual situation is very complex. The man probably releases sweat to cool himself depending upon the exertion and psychological state, but the flow values used above (i.e., 5 ft/sec or 40 acfm) are much larger than those used previously in air-cooled suits (Whisenhunt and Knezek, 1962). Also, large fans and power sources would be required. Although gas cooling is technically feasible if power and dehydration penalties are allowable, there are more satisfactory thermal control techniques available. These alternative techniques will be discussed in the following sections.

2. Thermal Coupling with a Liquid-Cooled Suit

Because the use of gas circulation cooling for high metabolic heating rates demands high flow rates and pumping power, a liquid-cooled undergarment has been developed (Burton and Collier, 1964, 1965; Burton, 1965; Jennings, 1966; Kincaid, 1965; and Bowen, 1963). Several basic concepts for a liquid-cooled garment (LCG) have been suggested, but the one which has received the most attention is that which circulates the liquid through small diameter tubes. These tubes are rather closely spaced and woven directly into a close-fitting undergarment. A small temperature rise is tolerated in the liquid.

Men who have worn these liquid-cooled garments in experiments found they could control their own comfort zones rather easily by varying the inlet temperature, although they often overcompensated; thus, fluctuated between feeling too cold and too warm (Burton, 1965). The experiments also revealed that various individuals had very different comfort zones. It was also noted that the body adjusts the blood flow to match the position of the cooling tubes (i.e., almost any arrangement is satisfactory; however, the usual pattern is to proportion the cooling tubes to match body mass). Furthermore, although tests indicated that the men were more comfortable when their extremities were cooler than their torso (Burton and Collier, 1964), there did not appear to be any real comfort advantage in introducing the cold inlet fluid at the extremities and removing the fluid at a torso manifold (Jennings, 1966). However, clothing worn under the LCG was definitely detrimental to comfort (Burton and Collier, 1965).

Most tested and projected LCG's circulate 200 to 300 lbs/hr of fluid through 30 to 50 parallel passages, with each passage 4 to 8 feet long. Temperature rises less than 10°F appear to be desirable (Burton and Collier, 1964); with this rise, a metabolic and ambient heat load of 2000 to 3000 Btu/hr is possible if the fluid has the heat capacity of water. Pressure drops and pumping power are low, and dehydration is not serious. Manifolding is somewhat complex and, even if the skin temperature is maintained less than about 91 to 93°F (Beaumont and Bullard, 1965; Benzinger, 1961; and Welch, et al., 1963), some insensible perspiration is still present and must be removed by a small flow-gas circulation system or by a water absorbent built into the suit or capsule wall (Robinson, 1963). About 0.2 lb/hr of water is lost by insensible perspiration and 0.1 lb/hr by respiration (Jennings, 1966).

In our analysis of the heat transfer between the man and LCG, we have assumed the subject is in an adiabatic enclosure. Heat energy flows from various depths of the skin to the surface area at the tube vicinity. There is also an additional thermal resistance in the tube wall. Finally the liquid side coefficient must be considered. We present an approximate model of this heat transfer problem below and conclude that the thermal resistance of the tube wall is the controlling or limiting factor in the entire heat transfer process:

a. Heat Transfer through Skin

Two tubes shown in Figure 11 are separated by a distance L . There is an outer layer of skin of depth, δ , which behaves as a fin (i.e., T is a function of x only). This fin is fed with energy from below by the blood flow. There is some effective heat transfer coefficient h_s which can be expressed as a ratio (k_s/ξ) , where k_s is the skin thermal conductivity and ξ is an effective depth. The skin is isothermal throughout the depth δ at $x = 0$, $x = L$. The maximum skin temperature occurs at $x = L/2$. Below ξ , there is some constant temperature, T_∞ , which is probably close to the deep-body temperature.

Denoting the fin temperature at any point x as T then the heat flow:

$$Q(x) = (k_s/\xi)(T_\infty - T) \quad (12)$$

Defining $\theta_o = T_\infty - T_o$; $\theta_m = T_\infty - T_m$ (where $T_m = T_{x=L/2}$); $\theta = T_\infty - T$, then the fin equation becomes, per unit dz in the direction parallel to the tubes:

$$-k \frac{d^2\theta}{dx^2} dz dx + (k_s/\xi) \theta dx dz = 0$$

or

$$\frac{d^2\theta}{dx^2} - \frac{\theta}{\xi\delta} = 0 \quad (13)$$

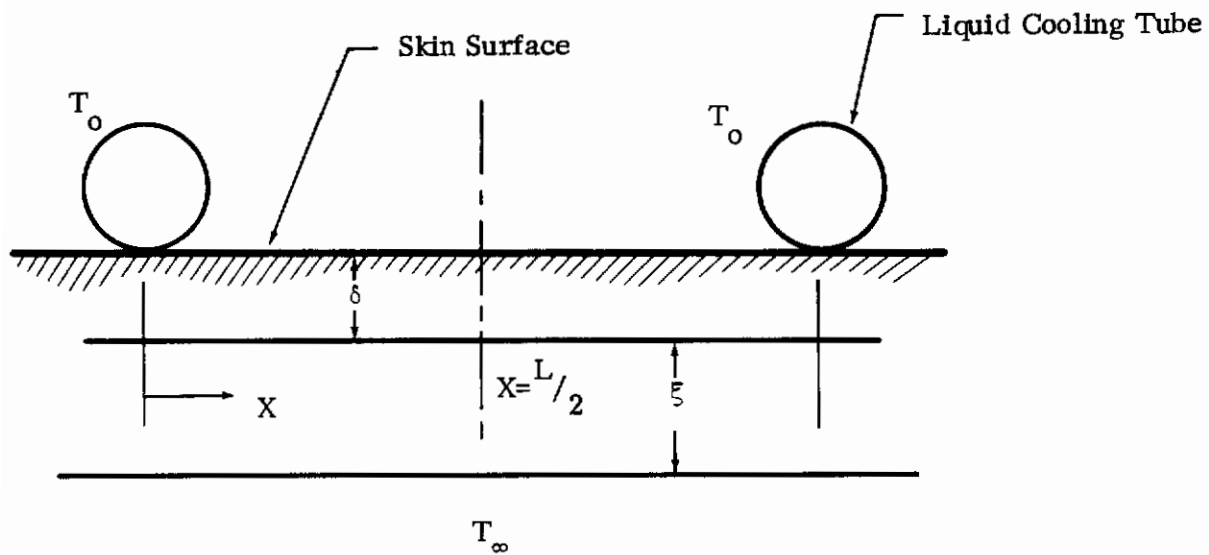


FIGURE 11. MODEL FOR LIQUID COOLED GARMENT ON THE ASTRONAUT'S SKIN

Contrails

with the boundary equations as:

$$x = 0, \theta = \theta_o$$

$$x = L/2, d\theta/dx = 0$$

The solution is:

$$(\theta/\theta_o) = \cosh x' = \tanh (L'/2) \sinh x' \quad (14)$$

The values x' and L' are non-dimensional values; that is:

$$x' = x/\sqrt{\xi\delta}; L' = L/\sqrt{\xi\delta}$$

Reasonable values of T_∞ , T_o , and T_m are:

$$T_\infty = 98.6^\circ\text{F (average deep body temperature)}$$

$$T_o = 89^\circ\text{F (lowest skin comfort temperature)}$$

$$T_m = 93^\circ\text{F (highest skin temperature to prevent active perspiration)}$$

Thus, $\theta_m = 5.6^\circ\text{F}$, $\theta_o = 18.6^\circ\text{F}$, $\theta_m/\theta_o = 0.3015$.

At $x = L/2$, using the θ ratio given above, equation 14 reduces to an equation with only one unknown, L' . Solving:

$$L' = 3.74 \text{ or } \sqrt{\xi\delta} = 0.2675L \quad (15)$$

The heat flow into any tube, from both sides, is:

$$\begin{aligned} q \text{ (tube, per unit length)} &= 2 k_s \delta (d\theta/dx)_{x=0} \quad (16) \\ &= 2 k_s \delta [(\theta_o/\sqrt{\xi\delta})(\sinh(0) - \tanh(1.87) \cosh(0))] \\ &= (2 k_s \delta \theta_o/0.2675L)(0 - 0.954) \end{aligned}$$

Contrails

k_s is in the range of 0.36 Btu/hr-ft²-F, although this varies with vaso constriction so:

$$q = 2 \times 0.36 \times 18.6 \times (-0.954)/0.2675L = 48 (\delta/L) \text{ Btu/hr-ft} \quad (17)$$

To obtain a better understanding of equation 17, suppose $\delta \sim \xi$, then by equation 15 $\delta/L = 0.2675$ and $q = 12.9$ Btu/hr-ft of tube.

Most spacings of L are less than 1 inch. However, to be conservative let L = 1 inch (i.e., 12 tubes/ft) and $q = 154$ Btu/hr-ft².

Some 15 ft² of surface (excluding head, hands or feet) will be covered (Burton and Collier, 1964), so $Q_{\text{total}} \sim 2300$ Btu/hr ($\xi/\delta = 1.0$). For other ratios of ξ/δ ,

| ξ/δ | q (Btu/hr-ft ²) | Q_{total} (15 ft ²) |
|--------------|-------------------------------|------------------------------------------|
| 5 | 69 | 1030 |
| 2 | 109 | 1620 |
| 1 | 154 | 2300 |
| 0.5 | 218 | 3250 |
| 0.2 | 345 | 5140 |

This analysis is based upon some educated guesses for the fictitious lengths δ and ξ . However, the estimated value of Q is reasonable and probably in the correct range. We have attempted to obtain better estimates of ξ and δ and, though approximate, probably ξ/δ is in the range of from 1 to 2.

b. Heat Transfer from Skin to Liquid

The problem of heat transfer from skin to liquid is significant because only a small fraction of the tube area acts as a heat transfer area (Figure 12).

We assume that the value of the outside skin temperature (T_w) is essentially constant but the fluid temperature (T_f) changes during flow. Let the flow rate be w and the overall heat transfer coefficient be U. A simple energy balance over length dz yields:

$$dQ = U (T_w - T_f) dA = w C_p dT_f \quad (18)$$

$dA = \psi \pi D dz$, ψ = fraction of circumference touching the skin. Integrating from $z = 0$, $T_f = T_{f, \text{in}}$, to z , T_f :

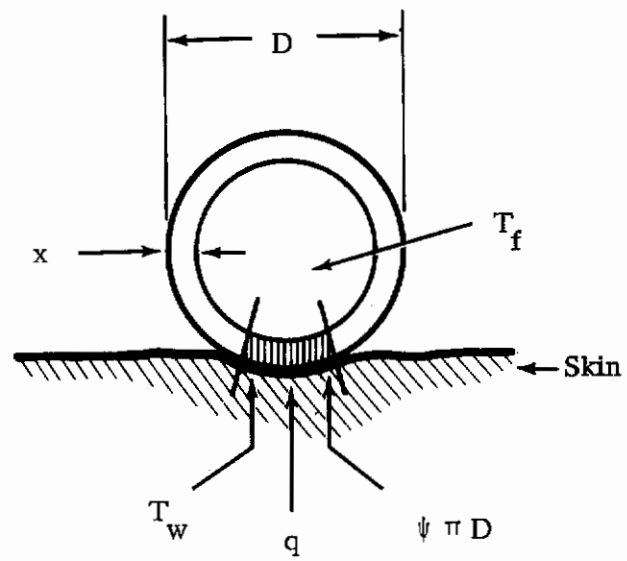


FIGURE 12. COOLING TUBE IN CONTACT WITH THE SKIN

Contrails

$$T_w - T_f = (T_w - T_{in}) \exp(-U \psi \pi D z/w C_p) \quad (19)$$

and
$$dQ = h (T_w - T_{in}) \exp(-U \psi \pi D z/w C_p) \psi \pi D dz$$

$$Q = w C_p (T_w - T_{in}) [1 - \exp(-U \psi \pi D z/w C_p)] \quad (20)$$

Some experiments have grouped the term $(U \psi \pi D z)$ as an overall conductance C (including skin and wall resistance) and report values in the range of 36 to 37 Btu/hr $^{\circ}$ F (Burton and Collier, 1965). Using quoted values for Q (1600 Btu/hr), T_{in} (45 $^{\circ}$ F), w (240 lb/hr), for the Hamilton-Standard LCG, and assuming $T_w \sim 80^{\circ}$ F, the value of the conductance is about 50 Btu/hr $^{\circ}$ F. These are in very good agreement. (Note, the small amount of gas cooling carried out simultaneously with the liquid cooling is not significant; that is, it probably accounts for less than 5% of the total heat flow.)

Concerning equation 20, note the effect of varying w on Q for values of $(U \psi \pi D z)$ given above. For example, Figure 13 shows Q plotted vs. w for several conductances and $(T_w - T_{in})$ temperature differences. The increasing w has little effect on Q at large values of w ; however, for all values of the conductance, varying the inlet temperature has a pronounced effect on Q . One might suspect that thermal control would best be handled by varying the inlet temperature and choosing a fixed, constant flow rate.

(1) Estimate of ψ . The portion of the circumference of a relatively soft plastic tubing in contact with the skin can be measured, and this calculation determined ψ . We carried out experiments with tubes varying in diameter from 1.6 to 10 mm o.d. and found ψ to vary from about 0.26 to 0.29. An average of 0.27 was chosen.

(2) Estimation of U . We estimated U from the design values of the Hamilton-Standard LCG (Jennings, 1966, and Kincaide, 1965) and arrived at a conductance of 71 Btu/hr $^{\circ}$ F for a cooling load of 2000 Btu/hr. The actual heat transfer area, including the ψ values discussed above, gave about 2.56 ft 2 . Thus, the experimental value for the overall heat transfer coefficient is $U = 71/2.56 = 27.8$ Btu/hr-ft 2 $^{\circ}$ F. Values of U estimated from more fragmentary data were in the same range.

(3) Estimation of Liquid-Side Coefficient. The data used to estimate U were also used to determine a liquid-side heat transfer coefficient from standard correlations. We found the flow to be laminar but h values as high as 250 Btu/hr-ft 2 $^{\circ}$ F. Note that $h \gg U$ so that the liquid-side heat transfer is not controlling.

(4) Tube Resistance. The equivalent thermal resistance for that portion of the plastic tube which touches the astronaut is simply k/x , where k is the thermal conductivity of the tube wall and x is the thickness. (k values range around 0.07 to 0.1 Btu/hr-ft $^{\circ}$ F and x values about 1/32 inch or 2.6×10^{-3} ft.) Thus, (k/x) ranges from about 27 to

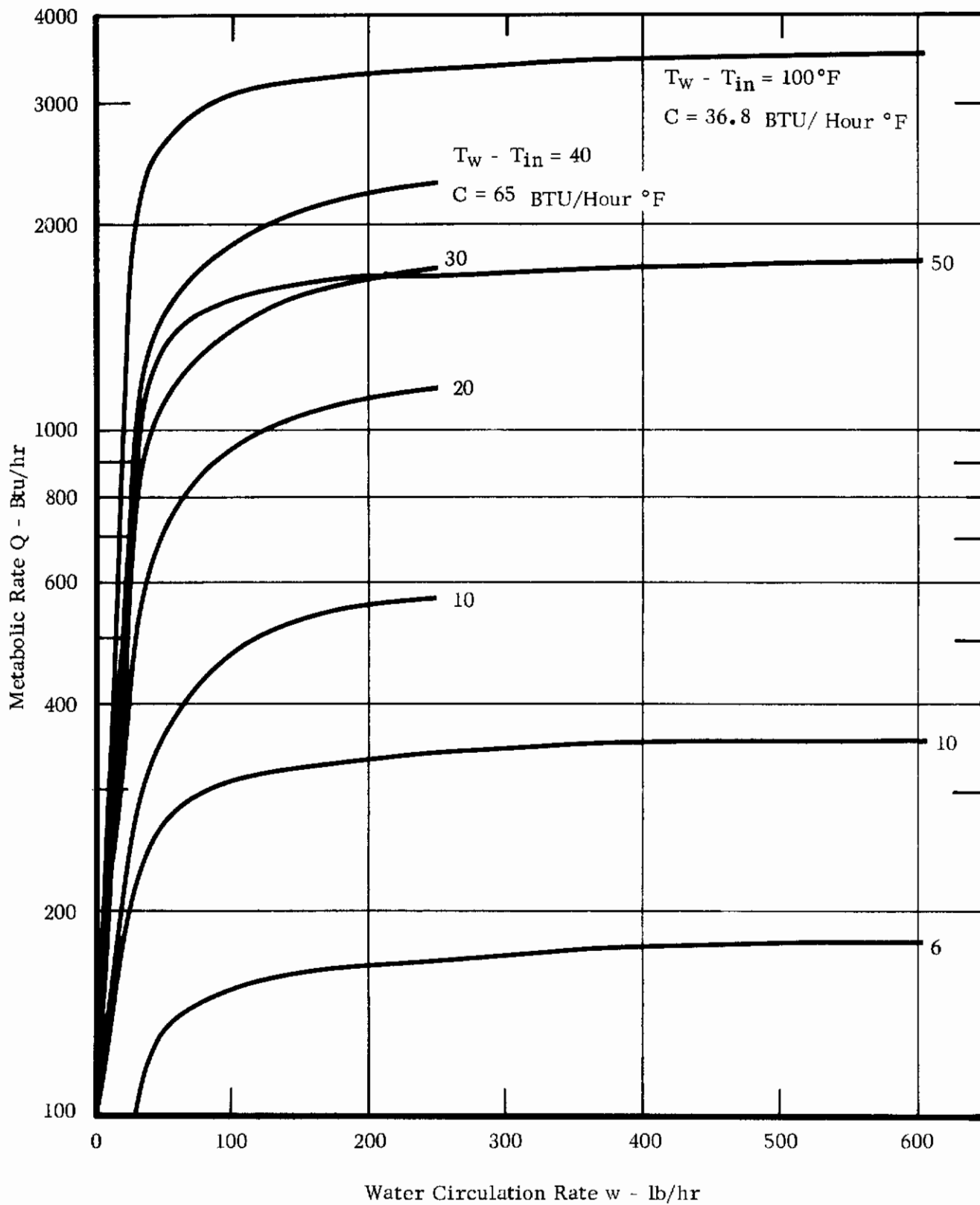


FIGURE 13. HEAT TRANSFER CHARACTERISTICS FOR COOLING TUBES IN CONTACT WITH THE SKIN

38 Btu/hr-ft²°F. This value is close to the measured overall heat transfer coefficient ($U = 27.8$ Btu/hr-ft²°F). Thus, the resistance between the skin and the tube must be small (skin heat transfer coefficient must be large), and the conductance of the plastic tube wall is heat flow controlling heat-flow resistance.

(5) Discussion. The controlling resistance to heat transfer in the present LCG units apparently is due to poor thermal conductance across the tube walls. Even so, the present LCG concept appears to be quite capable of removing normal metabolic heat loads. We show the results of our calculations in Figure 14 where we have calculated the total heat removal by equation 20 for a specific set of conditions as noted in the plot. As emphasized previously, the inlet temperature is a very critical variable, whereas at large flow rates, Q is relatively insensitive to flow.

3. Thermal Coupling with a Cooled Wall and Gas Convection

One possible environment for an astronaut is a rigid capsule. The astronaut is placed in a semi-fixed position (either sitting or lying down). Metabolic heat is removed from the body to cooled walls of the capsule by convective and radiative heat transfer. The astronaut should be lightly clothed; therefore, it can be assumed that the outer surface of the man is about average skin temperature. The walls of the capsule may be taken as an isothermal sink at some lower temperature. Water or other coolant is circulated in tubes placed on the inner wall surface.

The mathematical model for this case is based on the concept shown in Figure 15. The bulk (mixed mean) temperature of the gas is $T(x)$. The velocity of gas in the annulus is V . A steady-state energy balance written over a differential length dx and unit breadth is:

$$Vw \rho C_p (dT/dx) = U (T_s - T) - U (T - T_c) \quad (21)$$

separating variables and integrating from $x = 0, T = T_o$ to x, T , gives:

$$\frac{(2T - T_s - T_c)}{(2T_o - T_s - T_c)} = \exp (- 2U x/Vw \rho C_p) \quad (22)$$

The heat transfer from the astronaut to the gas and capsule wall at any x is:

$$q_x = U (T_s - T) + U_R (T_s - T_c) \quad (23)$$

where U_R is an effective radiation coefficient given by:

$$Q = w C_p (T_w - T_{in}) [1 - \exp(-U \psi \pi D Z / w C_p)]$$

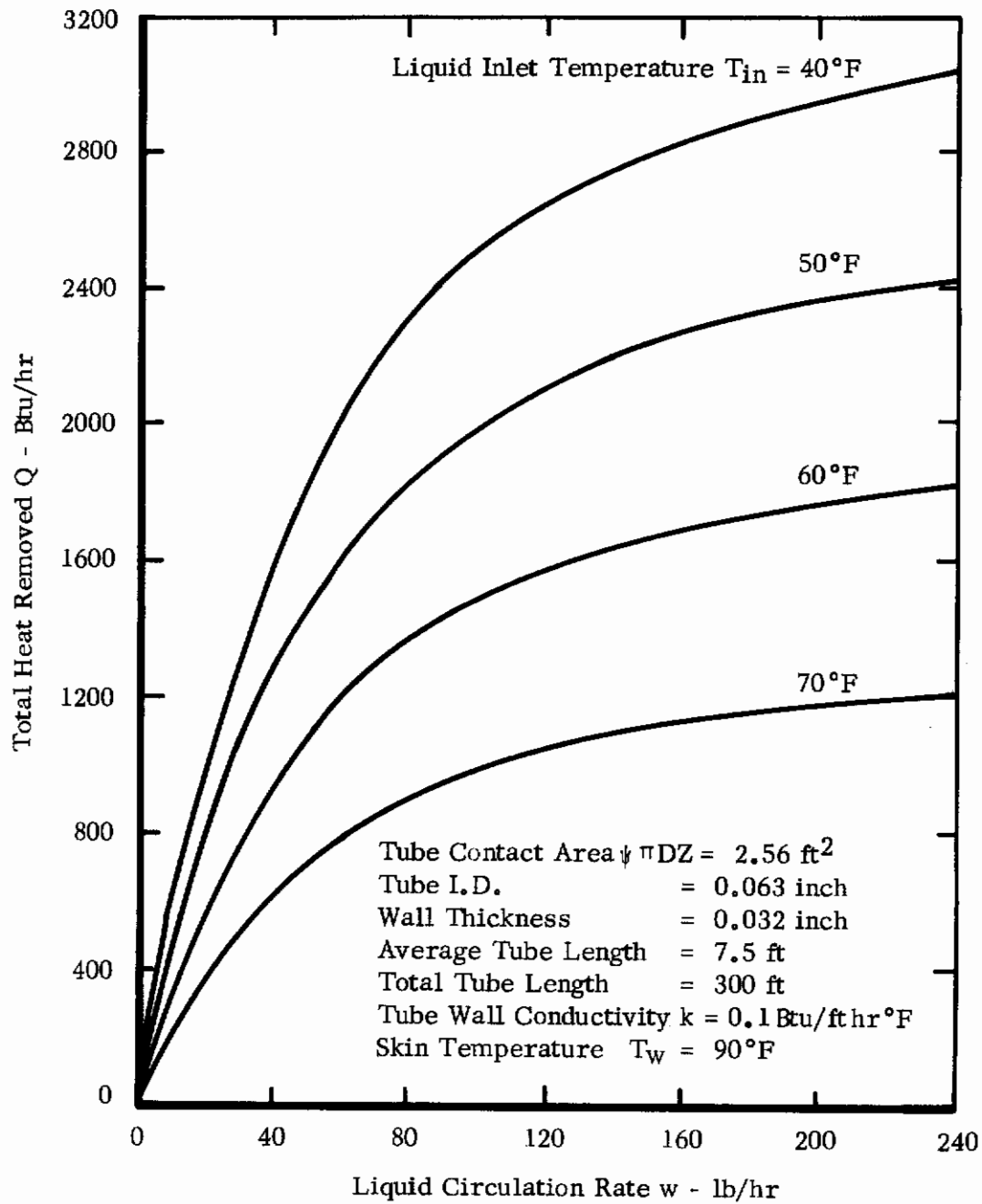


FIGURE 14. HEAT TRANSFER FOR A TYPICAL LIQUID COOLED GARMENT

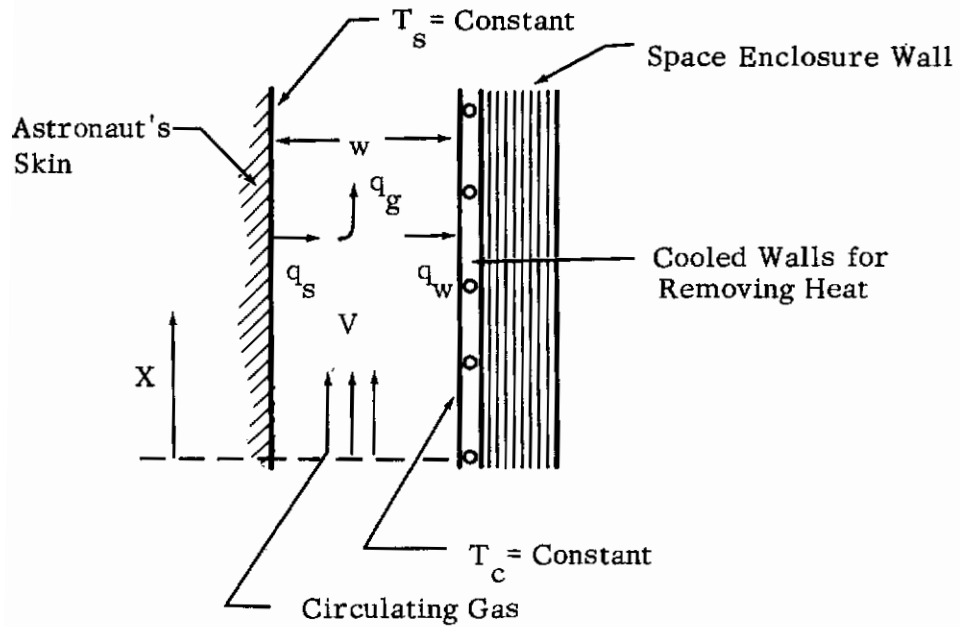


FIGURE 15. MODEL FOR THERMAL COUPLING AN ASTRONAUT TO A COOLED WALL BY RADIATION AND CONVECTION

Contrails

$$U_R = 4 \epsilon \sigma T_s^3 \quad (24)$$

Rearranging equation 22 to solve for $(T_s - T)$ and substituting in equation 23 gives:

$$\frac{q_x}{U (T_s + T_c)} = \frac{1}{2} \left\{ \left[1 - \frac{2 T_o}{(T_s + T_c)} \right] e^{-\frac{2 U x}{V_w \rho C_p}} - 1 + \frac{2 T_s}{T_s + T_c} + \frac{2 U_R}{U} \frac{(T_s - T_c)}{(T_s + T_c)} \right\} \quad (25)$$

Multiplying by dx and integrating over the interval $x = 0$ to $x = L$,

$$Q/\text{unit breadth} = \frac{V_w \rho C_p}{4} (T_s + T_c - 2T_o) \left(1 - e^{-\frac{2 U L}{V_w \rho C_p}} \right) + \frac{U}{2} (T_s - T_c) L + U_R (T_s - T_c) L \quad (26)$$

To extract some useful information from equation 26, several variables must be specified. First, we assume that the skin temperature, T_s , is close to a typical skin temperature of an extremity (with no active perspiration) at 90°F . We leave T_c as a variable and allow 40 to 70°F as reasonable values. The length, L , may be about 4 feet for a sitting astronaut. The width of circulating air flow annulus is very difficult to delineate and varies considerably for a sitting man in a cylindrical capsule. If we assume the capsule to be about 3 feet in diameter and the average diameter of the astronaut is about 1 foot, then $w = 1$ foot. The average breadth is then about $2\pi = 6.28$ feet.

The properties ρC_p vary somewhat with the gas and capsule pressure. For example:

| | <u>P (psia)</u> | <u>ρC_p (Btu/ft³°F)</u> |
|----------------------------|-----------------|-----------------------------------------------------|
| O ₂ | 3.5 | 4.5×10^{-3} |
| He | 3.5 | 3.6×10^{-3} |
| 30% He, 70% O ₂ | 5 | 4.3×10^{-3} |

Since these values are similar, we used O₂ at 3.5 psia to obtain the best performance.

Contrails

These values may be used in equation 26 to yield a plot of Q as a function of T_c for various values of gas velocity. (Once V is chosen, U may be determined.) Note the behavior of T for various values of T_o . If $T_o = T_s - (1/2)(T_s - T_c)$, i.e., is the arithmetic average, then it is easy to see from equation 22 that $T = \text{constant} = T_o$. Also, if $T_o = T_c$, the lowest value, it will exponentially approach the arithmetic average temperature. In fact, with reasonable values of velocity, equation 22 indicates that the rate of approach of T to the arithmetic mean value is quite slow. For example, if the gas enters at T_c and if $x = L = 4$ ft, $V = 10$ ft/sec, $U = 0.86$ Btu/hr-ft²°F, $w = 1$ ft, $\rho C_p = 4.5 \times 10^{-3}$ Btu/ft³°F, then $\exp[-2Ux/Vw\rho C_p] = \exp(-0.043) = 0.95$; that is, the temperature at the outlet differs only slightly from the inlet temperature.

In the convective heat transfer, an increase in velocity results in the value of U being increased, though not linearly. We do not expect velocities in excess of 20 ft/sec to be tolerated, and in Figure 16 we have plotted values of Q for several velocities and values of T_c . In all cases, $T_o = T_c$ was assumed. Both oxygen at 3.5 psia and 30% helium-70% oxygen at 5 psia are shown.

The proposal to thermally couple an astronaut in a capsule with cold walls appears feasible. Only a small gas flow would be required. This gas flow primarily would serve to transfer heat from the astronaut to the cooled wall and to remove insensible perspiration and metabolic products. The heat removed from the capsule by the gas flow will not be large. Most of the 500-1500 Btu/hr removed will be extracted at the cold wall of the enclosure.

4. Decrease of Azimuthal Temperature Gradients by Heat Pipes

Maintaining a reasonable and uniform outer suit temperature for an astronaut may be difficult. Surfaces exposed to solar radiation may become excessively warm, while those surfaces exposed to deep space may become too cold. Also, the surfaces will not remain in fixed orientations because of the astronaut's movements in accomplishing his mission requirements. Therefore, the radiation characteristics of the outer suit material are important in defining a maximum azimuthal temperature gradient (see discussion in Section II.A). In this section we explore the feasibility of employing heat pipes to prevent severe azimuthal temperature gradients.

A heat pipe contains a liquid kept in contact with a warm surface. This liquid vaporizes and absorbs energy from the warm surface. The vapor is transported to a cool surface where it condenses to the liquid phase and releases energy. The liquid is returned to the warm surface by the capillary action of a wick or by gravity forces, and the cycle begins again. The heat transported by the vapor can be controlled by regulating the capillary return flow of liquid.

In the present concept, one might visualize lightweight circumferential heat pipes fitted around the astronaut or astronaut capsule. A low-

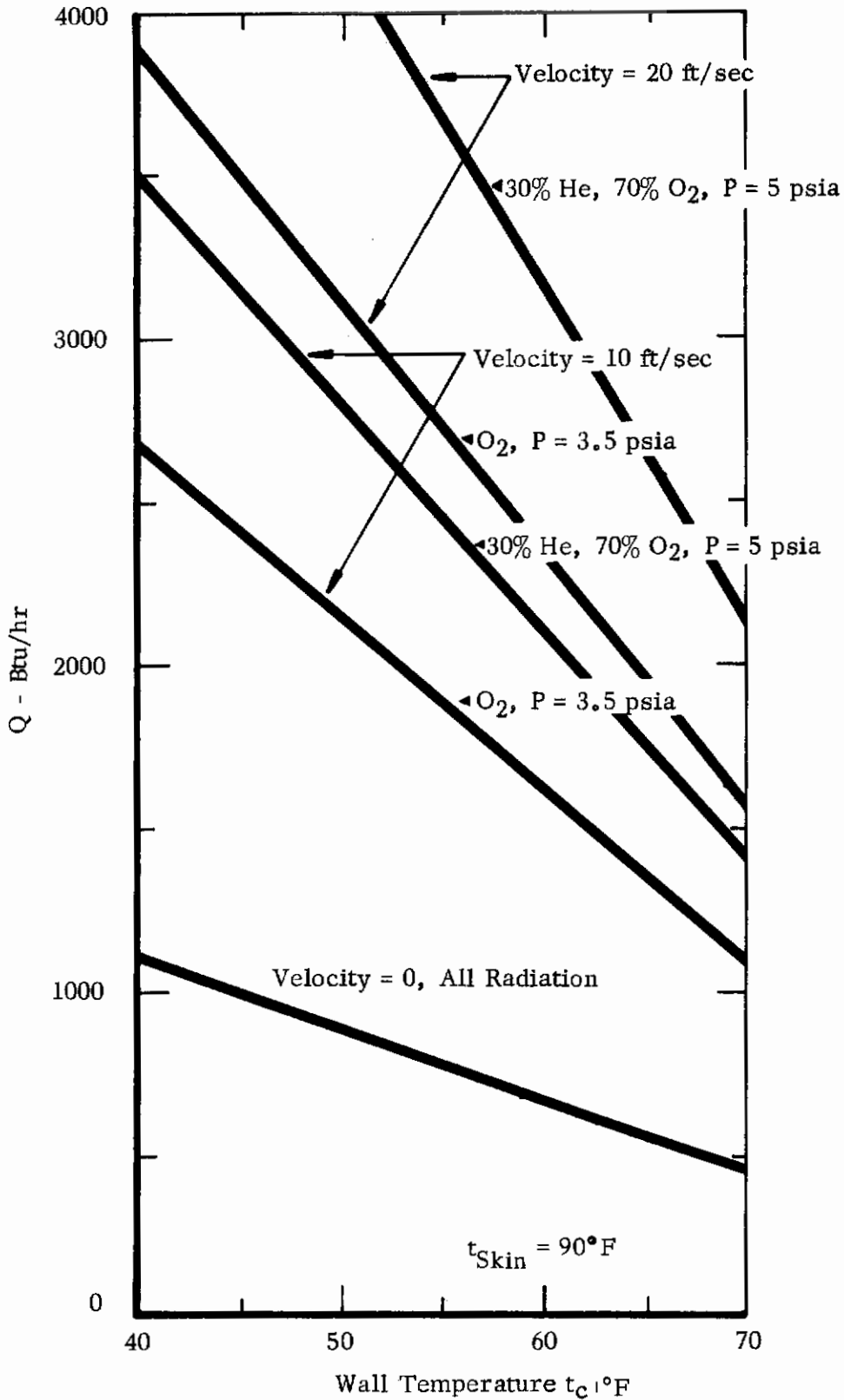


FIGURE 16. HEAT TRANSFER CHARACTERISTICS FOR AN ASTRONAUT THERMALLY COUPLED TO A WALL ENCLOSURE

freezing-point fluid (e.g., alcohol) is added and allowed to vaporize at a low pressure; however, all other gases, especially those which are non-condensable, must be removed.

The ability of a heat pipe to reduce azimuthal temperature gradients is illustrated by an example from Katzoff (1967). He considered an orbiting spacecraft with a circular cylinder of aluminum 10.4 feet in diameter and wall thickness of 0.020 inch. Without heat pipes to redistribute the heat load, the subsolar point on the spacecraft reached a temperature of 250°F and the shaded side reached a temperature of -240°F ($\alpha = \epsilon = 0.4$). With 75°F heat pipes 16 inches apart, and with an adiabatic inner wall, the corresponding temperatures reached 130 and 50°F. Thus, the uniformity of the temperature has been greatly improved.

To control the heat flow from the astronaut within the enclosure, it should be possible to control the flow of vapor to zones on the outside wall of the enclosure where heat can be dissipated by radiation. However, the difficulty with this technique is that good lateral conduction of heat is required from the heat pipe onto the surface of the enclosure so that it can be dissipated. Furthermore, the external surface of the enclosure must be made of a good conductor such as aluminum.

Thermally coupling a heat pipe to the exterior surface of a flexible space garment will be the drawback to the application of this technique.

C. THERMAL CONTROL USING PHASE CHANGE MATERIALS

Fusion thermal control may be feasible for damping periodic orbit temperatures (Leatherman, 1963, and Fixler, 1966) in unmanned satellite missions where the heat to be dissipated is small.

Shlosinger and Woo (1965) have suggested that a heat sink integrated with the space suit could be used for reasonable total heat loads. The heat sink would store metabolic heat during the EV mission and, after the mission, when the suit is regenerated the heat would be rejected. Various investigators have suggested endothermic phase change materials, and interest has centered on materials which liquefy near body temperatures.

The concept of a heat sink is appealing because of its simplicity. However, this concept has three basic disadvantages which will limit its application for either soft flexible enclosures or rigid space enclosures:

First, weights are excessive for high heat load missions. In most cases, high molecular weight hydrocarbons such as the paraffins have been suggested. These materials have low heats of fusion (less than 100 Btu/lb). Fixler (1966) discusses a proprietary formulation (Transit Heat 86) which has a heat of fusion of 130 Btu/lb and melts at 86°F. For an astronaut with a metabolic load of 500 to 1500 Btu/hr, the weight of this material alone will exceed 5 to 15 pounds for every hour of activity.

Second, when a layer of fluid material insulates the unmelted solid, thermal coupling is not sensitive to changes in the metabolic rate and the only control for heat removal is to allow the skin temperature to rise and thereby increase the temperature gradient. Often this solution is very unsatisfactory since it may lead to undesirable active sweating and a decrease in the astronaut's comfort.

Third, regeneration of the heat absorption material is difficult. The material must be cooled below the freezing point to be regenerated. This requirement means that the whole garment must be removed from the astronaut and placed in a cool place until all of the material resolidifies. There appears to be no way in which to reactivate this system while the astronaut remains extravehicular; thus, his activity time cannot be extended.

These comments are especially applicable to manned missions where typical metabolic rates may vary from 300 to greater than 2500 Btu/hr in a short period of time. Therefore, other thermal control systems appear preferable for most applications involving manned missions.

D. THERMAL CONTROL USING LCG AND THE ENCLOSURE'S EXTERNAL RADIATING SURFACE

In this thermal control system, a liquid-cooled garment (LCG) is coupled with an external heat exchanger (i.e., cooling tubes imbedded in the external wall of the garment or the enclosure). The arrangement is shown schematically in Figure 17 and is applicable primarily to rigid space enclosures.

Metabolic heat is extracted from the astronaut's skin by the liquid-cooled garment, thus increasing the temperature of the circulating liquid. The warmed liquid is piped through the garment insulation to the external heat exchanger. The tubes in the exchanger are arranged so that the natural flow reduces any azimuthal temperature gradients which may exist. The astronaut's comfort is maintained by controlling the amount of cooled liquid returned from the external heat exchanger to the LCG. The amount of heat extracted is controlled by the liquid flow valve shown in Figure 17.

In our analysis of this system, we assumed that the cooled liquid returning to the LCG from the external heat exchanger is at the average radiative temperature of the external surface of the enclosure. Average temperatures as a function of the internal heat released are given in Figures 8 and 9 for rigid and flexible space enclosures in the various worst orbit situations. The liquid circulation rates and total heat removed in an LCG are given in Figure 14 for a range of liquid inlet temperatures.

We calculated the liquid circulation requirements for the worst orbit situation where the astronaut is working on the surface of his space station in either a twilight orbit or at the noon position, with the

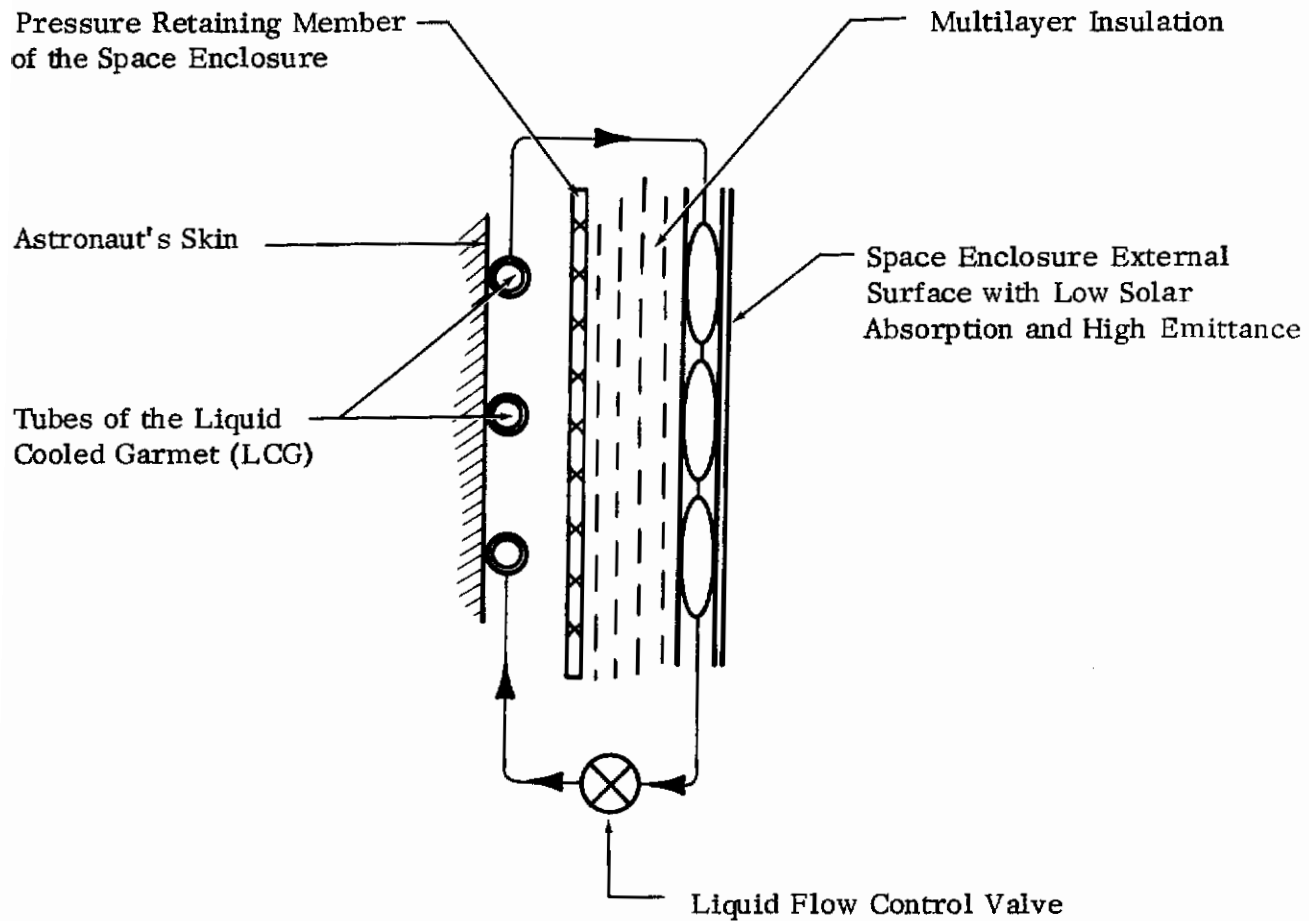


FIGURE 17. THERMAL CONTROL SYSTEM USING A LIQUID COOLED GARMENT AND AN EXTERNAL RADIATING SURFACE

stipulation that the astronaut's skin is always maintained at 90°F. (See Figure 18.) In addition to the LCG, there must be a small circulation of gas through the enclosure to remove the insensible evaporation. The operation limitation of this system occurs when the temperature of the cooled liquid returning from the external heat exchanger approaches 75 to 80°F and the liquid circulation rate, consequently, becomes large (greater than about 200 lbs/hr).

Figure 18 shows the impossibility of maintaining thermal control throughout the desired range (500 to 1500 Btu/hr) of an astronaut in a flexible enclosure if he works on the surface of the spacecraft in a worst twilight orbit. Control can be maintained only when the internal heat generated is below 650 Btu/hr. However, if the astronaut works a small distance from the space station, for the same orbit, it is possible to work successfully at rates up to 1500 Btu/hr. However, the rigid enclosure would enable the astronaut to work on the space station surface during worst orbit conditions throughout the desired range of metabolic activity (300 to 800 Btu/hr).

E. THERMAL CONTROL OF FLEXIBLE SPACE GARMENTS

In this section we discuss techniques for thermally controlling flexible space garments. In an earlier study (Richardson, 1965), we demonstrated the feasibility of increasing the conductance of soft space suit insulations by injecting helium into the insulation layers. Here, we further discuss the helium injection concept and propose a mechanical compression concept for increasing the conductance of soft space suit insulations. In a later section, we estimate the effects which wrinkles and folds in the outer surface of a soft space suit might have on the thermal performance and well being of the space suit.

1. Variable Conductance by Helium Injection

The effectiveness of good multilayer insulations depends to a large extent on the evacuation of gas from between the radiation shields. By injecting a small amount of gas such as helium into the space between the insulation layers, the conductance and thus the heat flow can be increased by more than three orders of magnitude. In our previous work (Richardson, 1965), we found that to effectively remove heat from within a space suit to the external surface, the conductance of the insulation should be maximum when helium is present. Therefore, we developed an insulation which at all times has good radiant heat transfer characteristics, and which has an apparent thermal conductance of greater than 10 Btu/ft²-hr°F when filled with helium at 3.7 psia and thermal conduction less than 0.01 Btu/ft²-hr°F when well evacuated.

When applied to a section of a space suit arm, the maximum average conductance of the insulation when it was filled with helium at 3.7 psia was about 4 Btu/ft²-hr°F; the minimum conductance of the insulation was about 0.3 Btu/ft²-hr°F when it was evacuated. Although this range of control of conductance is less than predicted, development of application techniques should gain the desired range of operation.

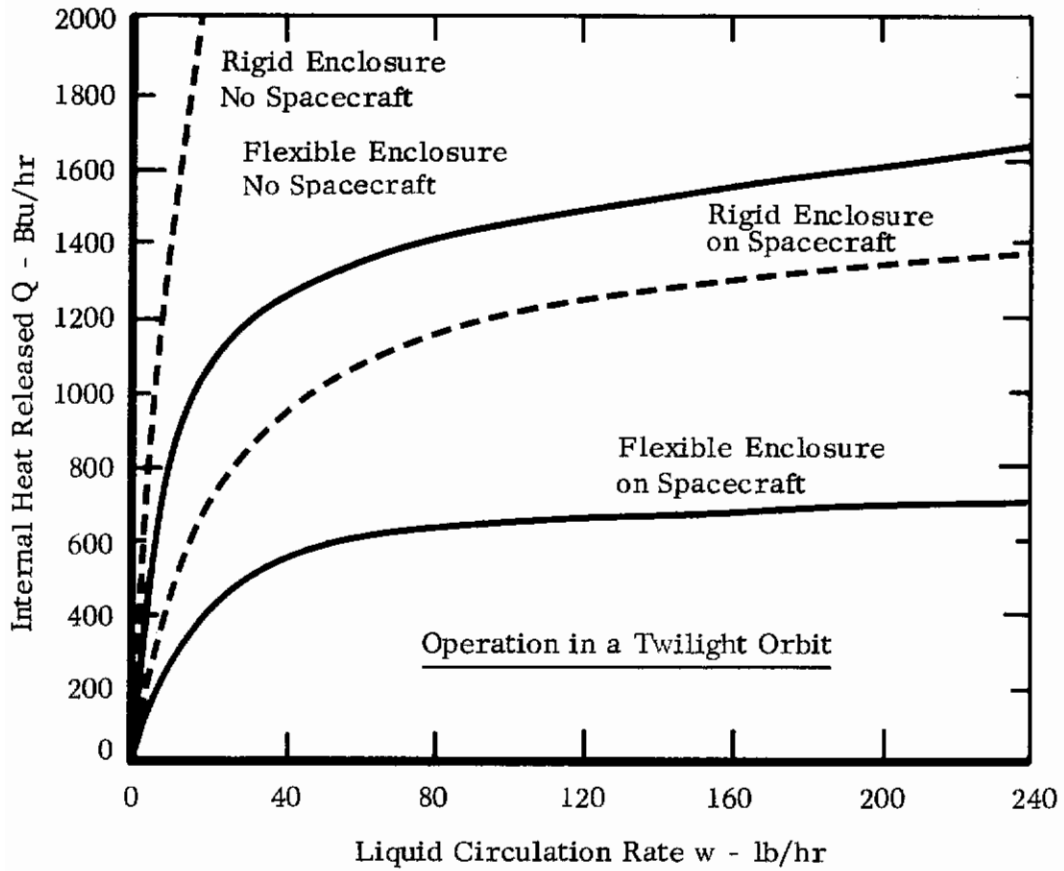


FIGURE 18. OPERATING CHARACTERISTICS OF A SYSTEM COMPRISED OF A LIQUID COOLED GARMENT AND AN EXTERNAL RADIATING SURFACE

We became more concerned with the means for controlling the injection and evacuation of helium into the insulation layers in response to the thermal needs of the astronaut. We investigated the time it takes for the helium gas to flood the insulation if it is injected at the waist section and the time it takes for the insulation to regain low heat flow conditions when again exposed to vacuum. In both cases, the time required for either high conductance or low conductance to be achieved was about 10 seconds. As a model, we considered the average evacuation path length to be 3 feet and the total open space in the insulation layers to be 0.033 inch.

Thus, for all practical applications, the response time of the insulation can be considered instantaneous. It is, therefore, possible to utilize zone control of the heat flow from the space suit. For example, those portions of his space suit which have a "cool" view will be used to dissipate heat, while those sections which have a "hot" view can be evacuated to reduce heat flow into the suit. The control system would need only an external temperature sensor to determine if the outside temperature of the space suit is low enough for heat to be dissipated and an internal temperature sensor to determine if there is excess heat which must be dissipated.

2. Variable Conductance by Insulation Compression

We next investigated the feasibility of controlling the flow of heat through soft space suit insulations by applying small compressive loads. By compressing the insulation, the spacers and radiation shields are brought into close contact with each other, and the point-to-point solid conduction through the insulation is increased. In conjunction with basic and applied studies of insulations for cryogenic tankage (Arthur D. Little, Inc., 1964, 1966), we have found that the heat flux per unit of area through insulations varies with pressure according to the relation:

$$q \approx P^n \quad (27)$$

where $0.5 < n < 0.66$.

With equation 27, we calculated the effect of varying the compressive load on the insulation summarized in Table I by using the results of flat plate calorimeter tests of the insulation (Richardson, 1965), an estimate of the compressive load which the insulation experienced in these tests, and an estimate of the radiative heat transfer contribution. The results (Figure 19) indicate that the maximum conductance which may be achieved when the insulation is compressed at the standard soft suit pressure of 3.7 psia is 8 Btu/ft²-hr°F and that the minimum conductance will be about 0.4 Btu/ft²-hr°F which corresponds to a residual compression of about 0.02 psia. Thus, by varying the compression in the space suit insulation, we should be able to achieve about the same degree of control as is possible with helium injection.

TABLE I SPACE SUIT INSULATION LAYERS

P-1807-A neoprene-coated rip-stop nylon fabric
(black side facing the center of the insulation)
0.003-inch nylon netting
SRD-5905 neoprene-coated dacron fabric (5 oz)
0.003-inch nylon netting
SRD-5905 neoprene-coated dacron fabric (5 oz)
0.003-inch nylon netting
P-1807-A (black side facing the center of the
insulation)
6-oz Nomex HT-1 fabric

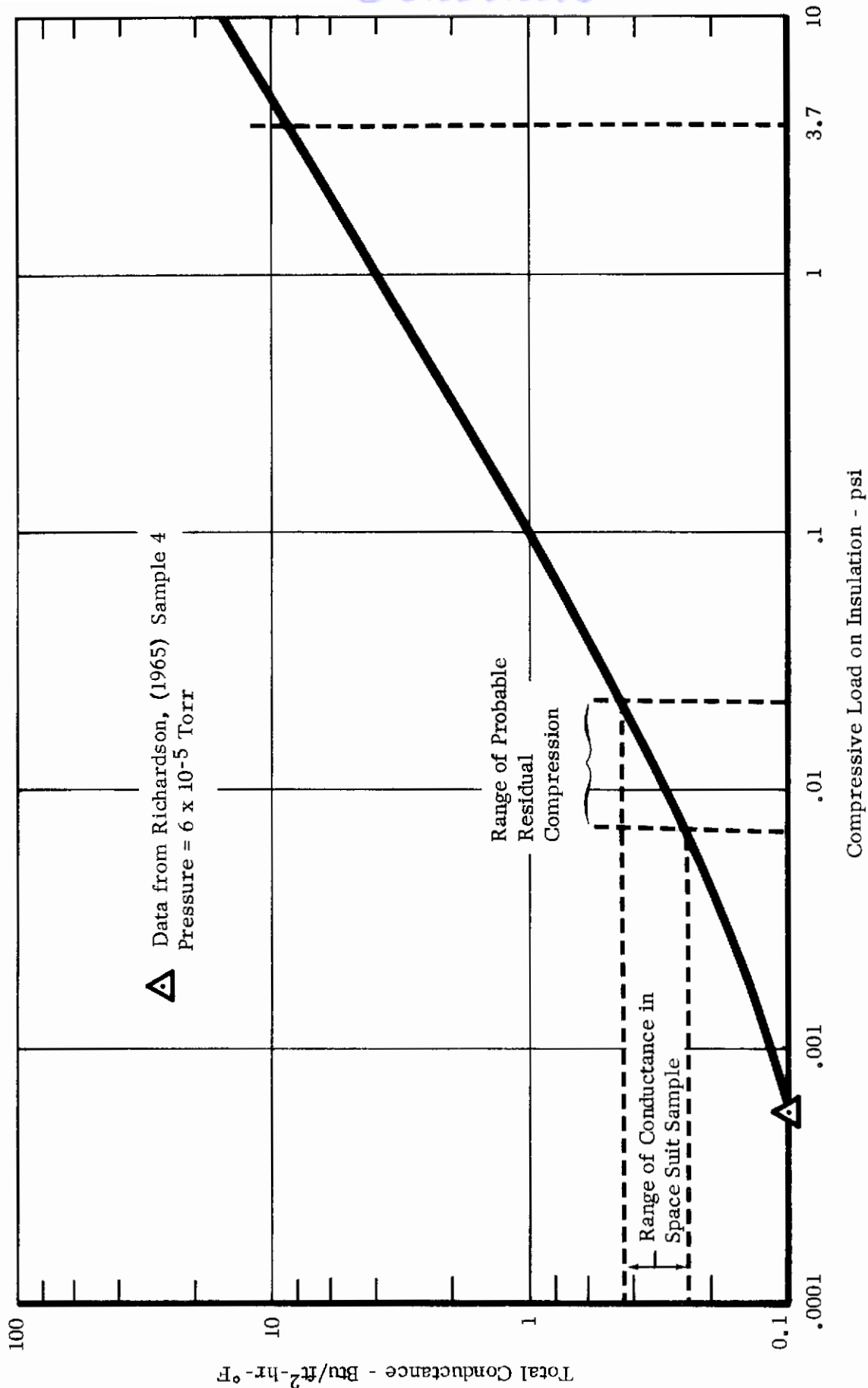


FIGURE 19. CALCULATED EFFECT OF COMPRESSIVE LOAD ON AN EVACUATED SPACE SUIT INSULATION

One scheme for applying compression to a soft suit whose insulation is located outside of the gas restraint layer is to transfer the load-bearing function from the gas restraint layer to the outermost layer of the insulation. The insulation then will become compressed to the pressure within the space suit (currently 3.7 psia). When it is desired to insulate the astronaut, the load is transferred back to the internal restraint layer, thereby releasing the insulation from compression.

An experimental evaluation was made of the heat flow through an insulation which was compressed at 3.7 psia on the arm-section calorimeter. Results are summarized in Section III.A.

Although compression of the insulation appears to be a feasible means for increasing the heat flow through the insulation, there are several major drawbacks to its application to a space suit. By simply transferring the load from an inside layer to the outside layer, the insulation around the space suit section becomes compressed. It is, therefore, impossible to increase the conductance of just the front of the suit without increasing that of the back also. There appears to be no way of locally increasing the compression in the insulation.

Another drawback of compressing the insulation is that the mobility of the space suit will be greatly compromised when the outer layer is load-bearing and the insulation is in compression, because the added layers of the insulation must then be flexed with the gas retaining layers of the space suit.

3. Thermal Effects of Folds in Space Suits

In this section we considered the possible adverse effects which folds in a space suit might have on the radiative thermal balance. Folds act like blackbody (or dark-gray body) cavities and present to space a substantially different solar absorptance-to-thermal-emittance ratio than does the open flat surface of the suit material. Although local hot spots in folds are possible, the fraction of a space suit which will be wrinkled at any time is small compared to the entire surface area. Thus, we do not believe that folds will have a large effect on the overall thermal balance of a space suit.

a. Average Effects

To determine the fold's effect, we assumed the fold to be represented by a V-groove with included angle θ and the space suit surface to have diffuse reflectance properties. Two cases were considered: (1) where parallel radiation enters the V-groove and (2) where diffuse radiation either enters or leaves the V-groove. Sparrow and Lin (1962) discuss the case of parallel rays entering a diffuse V-groove, and present the effective solar absorptance as a function of the original surface absorptance and θ . They also discuss the absorptance of diffuse incident radiation for a diffuse cavity. Sparrow (1965) shows that for diffuse

radiation and a diffuse cavity, the effective absorptance and emission of a V-groove are equal, provided the incident and emitted radiation are of the same spectral quality. Since the surface temperature of a space suit is approximately that of the earth's surface, the diffuse earthshine radiation and that emitted from the V-groove are spectrally the same. The solar radiation diffusely reflected from the earth (albedo) and, subsequently, absorbed on the suit is not of the same spectral quality as that radiated from the space suit. However, for simplicity we assume that the effective absorptance of the albedo component of solar radiation is the same as the effective absorptance of parallel solar radiation.

b. Maximum Effects

We determined the maximum effects on the effective absorptance or emittance by examining the flux absorbed (or emitted) from a differential area near the point of a V-groove. The analysis is presented in Appendix III and summarized in Figure 20.

The effective absorptance and emittance of both illustrative cases approach unity as the fold angle approaches zero. For the worst orbit position, which we identified in our analysis, the radiant flux field might consist of direct solar radiation of 442 Btu/ft²-hr, albedo of 177 Btu/ft²-hr and long wavelength radiation (earthshine and heat from an adjacent space station) of about 66 Btu/ft²-hr. From these heat flow combinations and with a V-groove, which has an angle approaching zero, ($\alpha \rightarrow 1.0$, $\epsilon \rightarrow 1.0$), the maximum equilibrium temperature in a fold might approach 370°F if there is no lateral heat flow through the folded material. In actual space suit EV garments, there will be lateral flow of heat in the material of the fold which will reduce this maximum temperature. Although the temperature would be uncomfortable on an astronaut's skin, it is localized on the outer layer of the EV garment outer wall. Under normal circumstances, the maximum temperature which will exist on the astronaut will be 180°F (see Figure 5). Although the maximum temperature in the fold is considerably greater than the unfolded maximum temperature, it is about equal to the design temperature limit for EV space garment materials.

F. THERMAL CONTROL BY TRANSIENT INJECTION OF GAS INTO THE INSULATION LAYERS

We investigated the feasibility of thermal control in a flexible soft space suit by transiently increasing the heat flow through the insulation. In the technique considered, a small amount of gas (helium) is injected into the evacuated layers of the space suit insulation. Previous work had shown that the presence of a small amount of gas increases the thermal conductivity by almost a factor of three (Richardson, 1965). Thus the feasibility of transiently increasing the conductance by injecting gas into the insulation will depend upon how well the heat flow can be controlled and how fast the system will respond. We calculated the time required for the insulation to outgas and regain the original low heat flow conditions which existed before the gas was injected into the insulation.

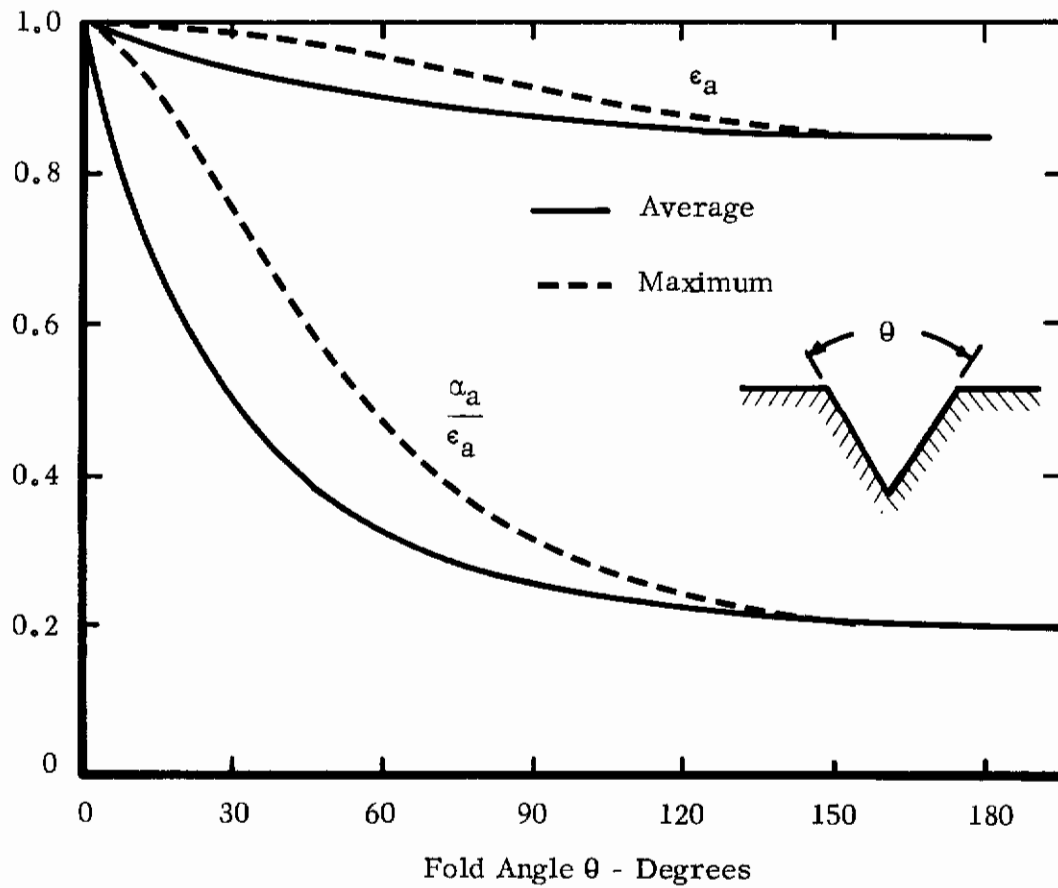


FIGURE 20. AVERAGE AND MAXIMUM EFFECTIVE EMITTANCE AND α_a/ϵ_a FOR SPACE SUIT SURFACES WITH FOLDS OF ANGLE θ

In the model used for transient evacuation, gas is injected into the insulation at a location near the astronaut's waist and flows laterally through the spaces between radiative shields until it exits at the edges near the extremities of the body (i.e., the wrists, ankles, and neck). The average path length was assumed to be 3 feet and the total effective open space in the insulation layers to be 0.033 inch.

To obtain a conservative estimate of the time required to evacuate the insulation from 100 to 10^{-4} torr, we assumed that the evacuation process is by free molecular flow through the whole range (actually, two flow regimes occur in the transient evacuation; laminar flow occurs in the pressure range 100 to 1 torr and free molecular flow occurs in the pressure range 1 to 10^{-4} torr). The pressure is calculated to drop from 100 to less than 10^{-4} torr in less than 7 seconds when the edge of the insulation is suddenly exposed to the hard vacuum of space.

For purposes of thermally controlling the heat flow through space garment or enclosure insulations, this evacuation time is instantaneous. Thus, transiently injecting a small amount of gas into an insulation in response to a need for an increase in the heat flow will not significantly affect the heat flow. To become effective, the gas must be either continuously injected (a wasteful procedure) or retained by not allowing it to escape until low heat flow through the insulation is again desired. The latter is a feasible technique and has been discussed (Section II.E, and Richardson, 1965).

G. LOUVERS FOR THE THERMAL CONTROL OF RIGID SPACE ENCLOSURES

All of the techniques described for the thermal control of flexible space enclosures are directly applicable to the thermal control of rigid space enclosures; however, louvers are uniquely applicable for thermal control of rigid space enclosures.

1. Background

Active thermal control by a louver system was first used in the Mariner II Venus Fly-By. The louver systems, since used in several unmanned space explorations, are based on an array of movable vanes, which have low emittance surfaces on both sides and which are controlled thermostatically by bi-metallic sensors. These bi-metallic sensors actuate the vanes from a fully closed to a fully open position over a predetermined temperature range. Arrays of vanes are placed over surfaces of high emittance and control the effective emittance of this base surface. When the array is closed, the vanes act like a single low-emittance radiation shield against dissipation of heat from the high-emittance baseplate surface to space. As the vanes open, the effective emittance of the louver and baseplate system increases because the baseplate view to space is increased. In effect, the louvers are a heat flow valve controlling the heat flow out of the baseplate to space.

Plamondon (1964) has analyzed the thermal behavior of louvers which have the same emittance on both sides and which are always oriented so that no sunlight falls on the louver system. To simplify the analysis, he assumed that the low emittance surfaces of the louvers are diffusely emitting and diffusely reflecting. Actually, the louver surfaces are not diffusely reflecting but are highly specular reflecting.

Parmer and Buskirk (1967) analyzed the thermal behavior of louver systems in the sun as well as in the shade. They assumed that the louver vanes were diffuse emitting but specular reflecting, that the louvers had the same surface properties on both sides, and that they were polished aluminum. Their analysis shows that the temperature of polished louvers covering a diffusely emitting white baseplate can reach extremely high values for certain sun and vane orientations. For example, the louver system geometry, surface properties, and operating temperature summarized in Table II show that the vane temperature is almost 590°F when the vanes are at 45° to the baseplate and the sun is directly overhead. Further, to maintain a baseplate temperature of 70°F, approximately 70 Btu/ft²-hr of heat must be removed from the baseplate. Thus, to control the baseplate temperature, heat must be extracted from the system. The louver system as designed is, therefore, incapable of controlling the baseplate at a reasonable temperature (70°F), because the vanes absorb more solar energy than they can radiate away and, consequently, their temperature rises.

2. Louver Operation in Sunlight

By careful selection of the surfaces of both sides of the louvers and of the baseplate and of the mode of operation of the louver system, a system can be devised to provide thermal control of a baseplate at a temperature of 70°F even when operated in the sun. Figure 21 illustrates a system with a diffusely emitting baseplate covered by a system of louvers which, when closed, have a white diffusely emitting surface facing the outside and a highly polished aluminum specular reflecting surface facing the baseplate. We simplified the control system for this set of louvers by specifying that they would operate in both, the fully closed and the fully open position, depending upon whether we want to conserve the heat flux or to increase the heat flux from the system. In our analysis (see Appendix IV), we considered only operations with the louvers fully opened and fully closed, in sunlight and in shade. For sunlight conditions, we assumed the sun to be directly overhead. Intermediate orientations were not analyzed, and some difficulty might be encountered in the performance of this louver system when the sun is oriented at an angle other than directly overhead and the louvers are at angles other than open or closed. Summarized in Figures 22, 23, 24, and 25 are the predicted heat fluxes per unit area and louver temperatures for the four operating conditions. Note that in all operating conditions a net heat flow from the system is possible and that at no time do the louver vane temperatures become excessively warm.

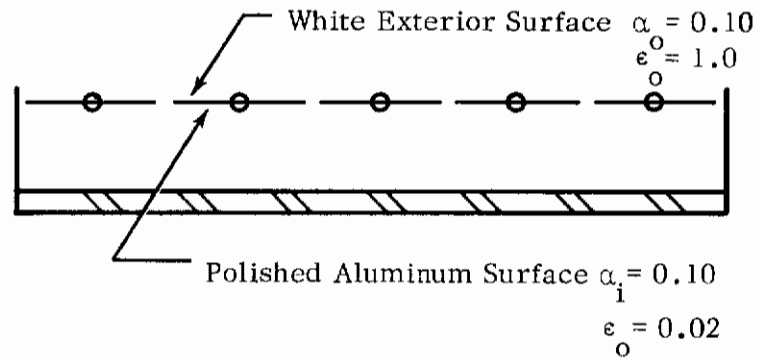
TABLE II SELECTED LOUVER OPERATION CHARACTERISTICS

Source: Parmer and Buskirk (1967)

| | |
|----------------------------------------|------------------------|
| Baseplate (white surface) | $\alpha_s = 0.20$ |
| | $\epsilon = 0.85$ |
| Louver (polished aluminum--both sides) | $\alpha = 0.17$ |
| | $\epsilon = 0.05$ |
| Baseplate Temperature | $t = 70^\circ\text{F}$ |

| <u>Sun Angle</u> | <u>Louver Position</u> | <u>Louver Temperature</u> ($^\circ\text{F}$) | <u>Net Outward Heat Flow</u> q (Btu/ft ² -hr) |
|------------------|------------------------|---------------------------------------------------|---------------------------------------------------------------|
| 0 (overhead) | open | 365 | 5 |
| | 45° | 590 | -68 |
| | closed | 415 | -40 |
| 40 | open | 465 | 20 |
| | closed | 350 | -32 |
| 80 | open | 360 | 85 |
| | closed | 140 | -10 |
| 90 (shade) | open | -- | 115 |
| | closed | -- | 0 |

Louvers Closed



Louvers Open

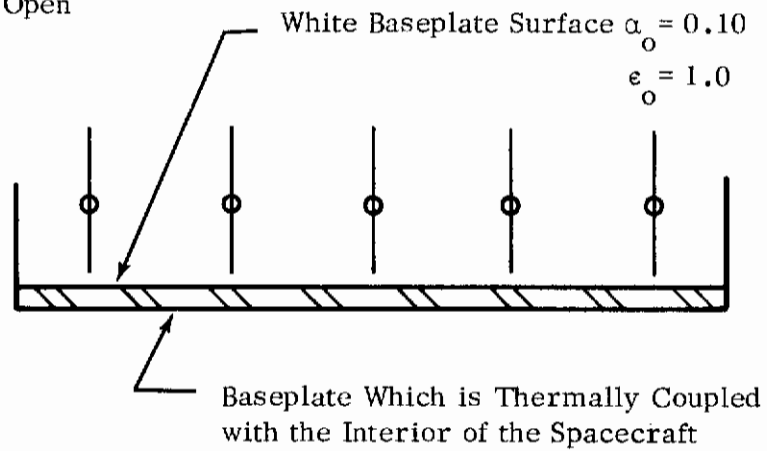


FIGURE 21. SCHEMATIC OF LOUVER SYSTEM FOR OPERATION IN SUNLIGHT

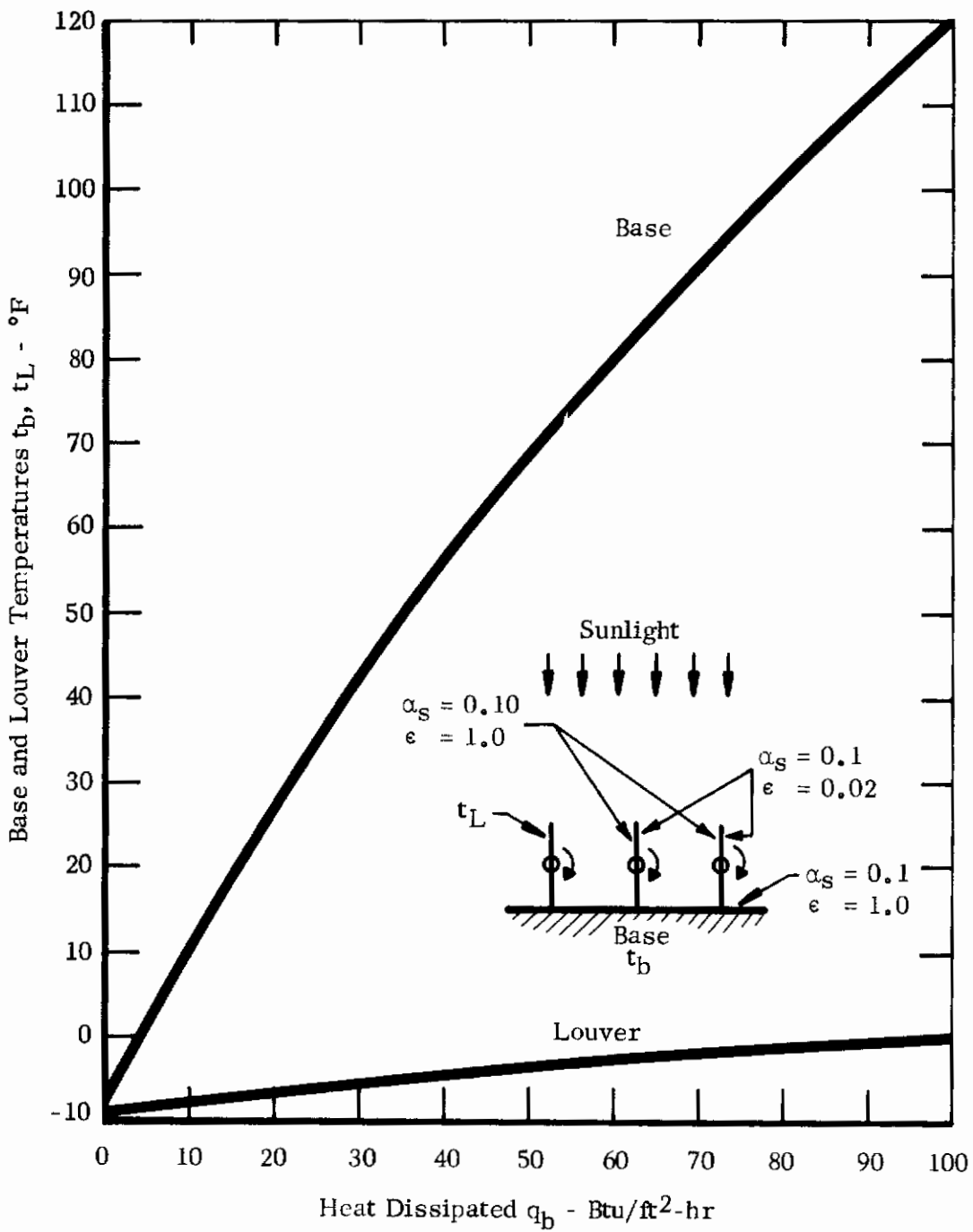


FIGURE 22. BASE AND LOUVER TEMPERATURES FOR OPEN LOUVERS AND THE SUN OVERHEAD

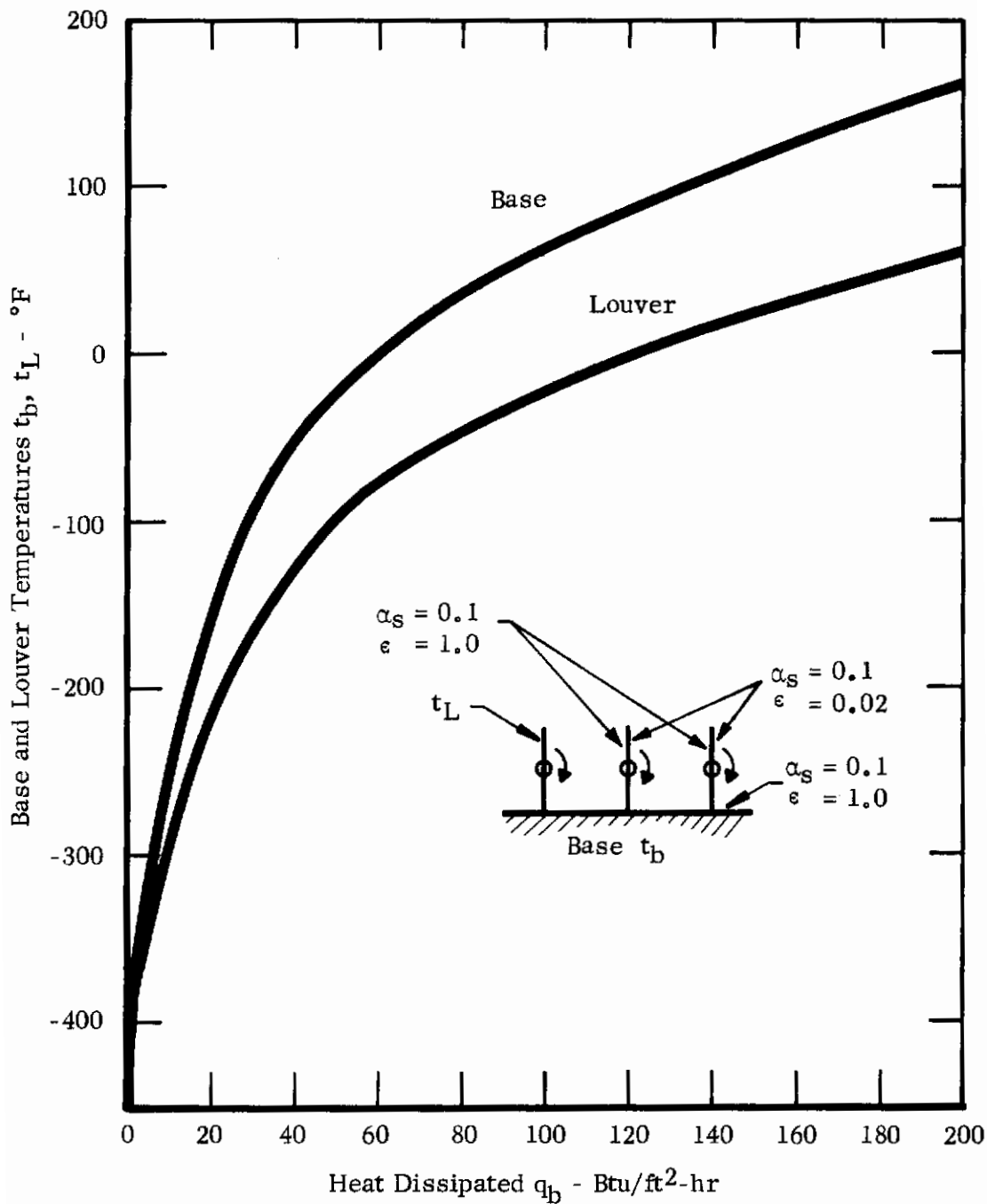


FIGURE 23. BASE AND LOUVER TEMPERATURES FOR OPEN LOUVERS IN THE SHADE

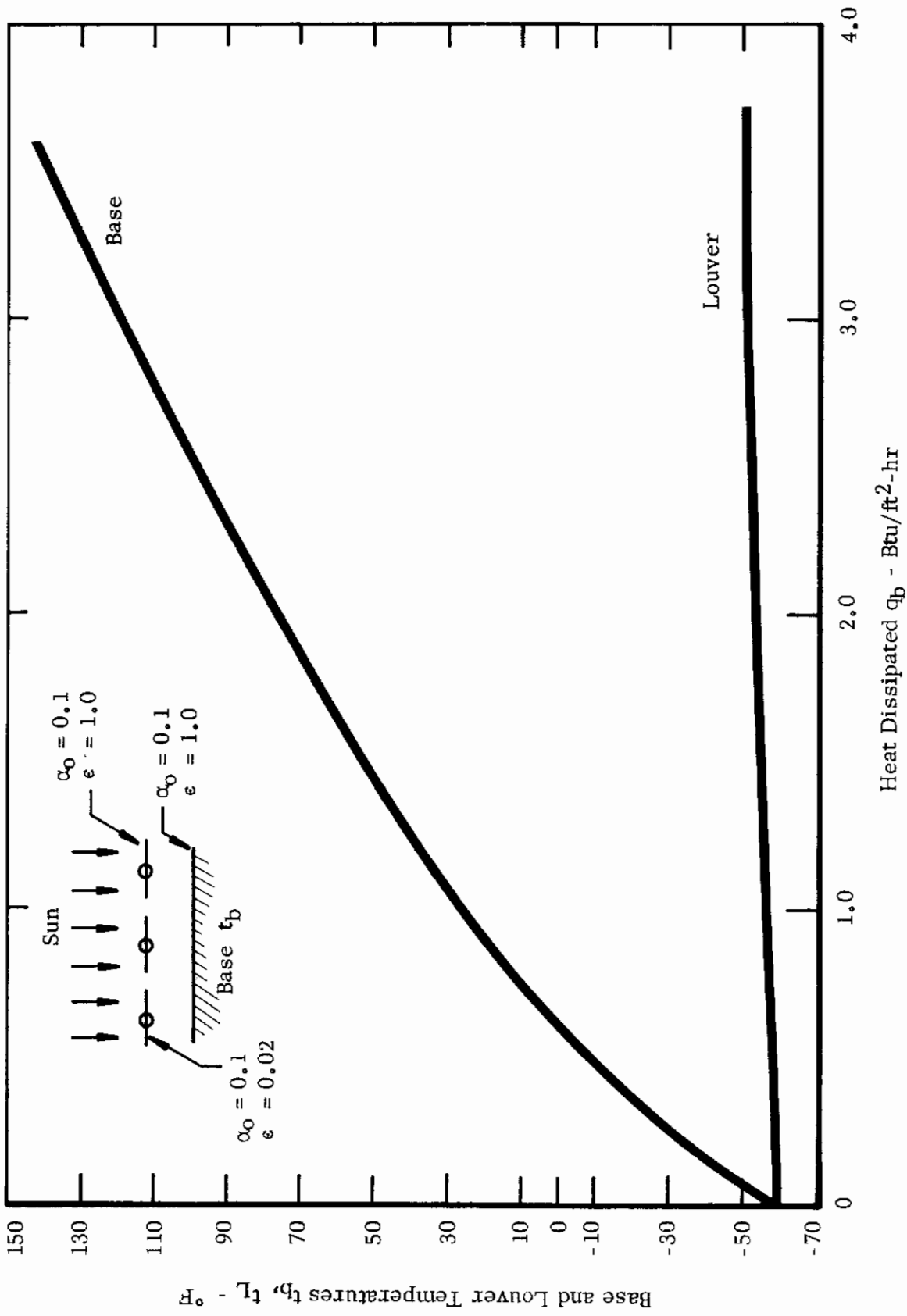


FIGURE 24. BASE AND LOUVER TEMPERATURES FOR CLOSED LOUVERS AND THE SUN OVERHEAD

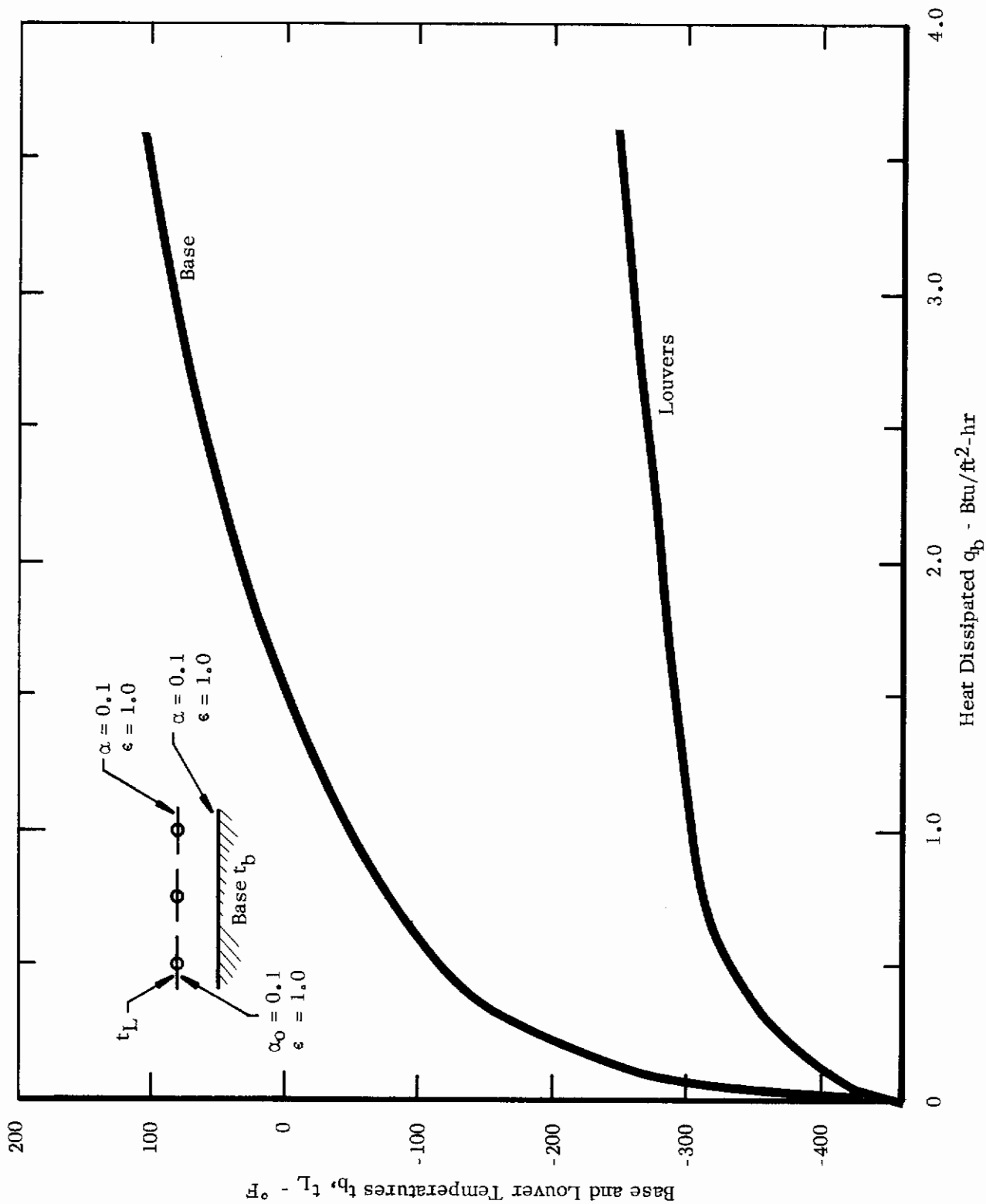


FIGURE 25. BASE AND LOUVER TEMPERATURES FOR CLOSED LOUVERS IN THE SHADE

Contrails

SECTION III EXPERIMENTAL PROGRAM

To supplement the analysis of thermal control of EV space enclosures, we fabricated a model of a soft space suit insulation and a model of thermal control louvers and tested them in simulated earth orbits. The results of the experimental program were used to verify the performance analysis and to provide engineering design data.

A. THERMAL CONTROL OF FLEXIBLE SPACE GARMENTS

In this phase of the experimental program, we investigated the feasibility of varying the conductance of a space suit insulation by compressing the insulation and measuring its heat flow in simulated earth orbits. The heat flow through the same insulation when uncompressed was also measured (Richardson, 1965), and comparisons show that compression of the insulation is a feasible technique for controlling heat flow through flexible space suit insulations, but that the predicted range of heat flow was not achieved.

1. Test Configuration

A cylindrical section representing an arm section of a soft space suit was used in the tests. Two half-cylinder calorimeters, each equipped with an electrical heater, were used in the arm section (Richardson, 1965) to simulate the metabolic heating rate of the astronaut (Figure 26). The calorimeters, 3-1/2 inches in diameter and 6 inches long, were covered by a gas-tight bladder made from neoprene-coated rip-stop nylon cloth anchored to the bulkheads of the calorimeter assembly.

The bladder was equipped with eight copper-constantan thermocouples (No. 40, 0.003-inch diameter), equally spaced circumferentially in a plane at the middle of the calorimeter assembly. They measured the circumferential temperature distribution on the inner wall of the space suit.

2. Insulation Tested

The insulation tested on the arm calorimeter was comprised of the layers summarized in Table I applied over the bladder and shown schematically in Figure 27.

The outermost layer of the insulation (6 oz nomex) was carefully secured by stitching, while the tension in the layer was kept as close to zero as possible. This outer layer absorbed the pressure load when the bladder of the arm section was inflated, and the insulation layers became compressed at the pressure of the arm section (3.7 psia). This layer also contained eight copper-constantan thermocouples, equally spaced circumferentially in a plane at the middle of the calorimeter assembly. The thermocouples were located radially above the thermocouples on the inner

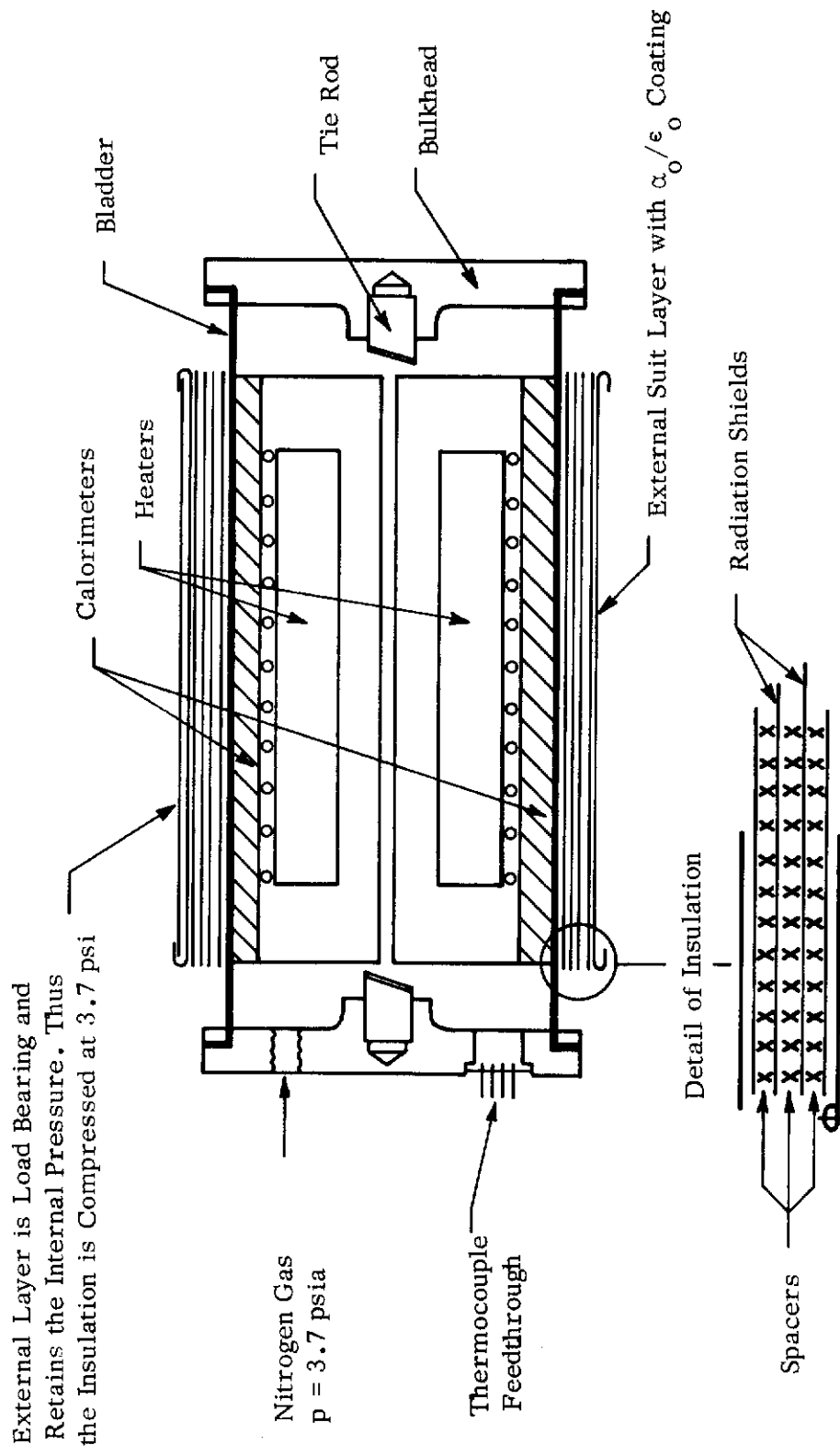


FIGURE 26. SPACE SUIT ARM TEST SECTION

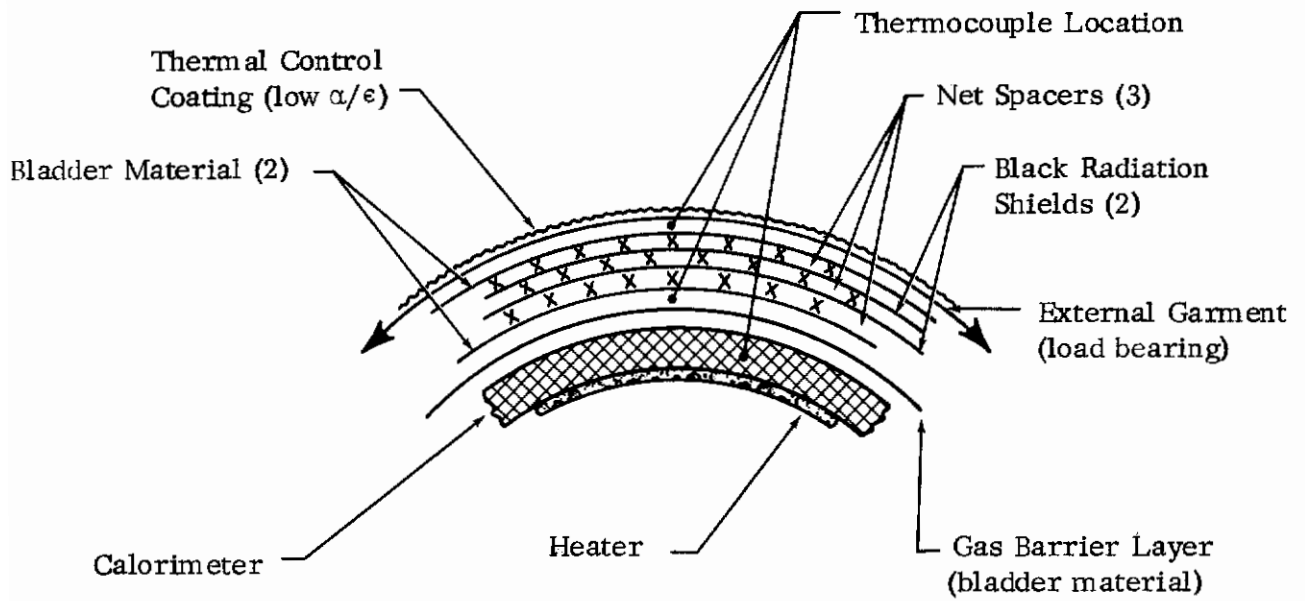


FIGURE 27. SCHEMATIC OF SIMULATED ARM SECTION WITH INSULATION

bladder layer--thus allowing the measurement of circumferential temperature differences across the insulation layer.

The outermost layer of the insulation was painted with a thermal control coating (S-13 Silicone paint). Table III summarizes the solar absorption and the emittance characteristics of this coating.

3. Test Program for Insulated Arm Section

The insulated arm section was tested in our space simulation chamber (Figure 28) at a pressure of 1.4×10^{-5} torr where solar radiation and earthshine were simulated. A complete description of the facility, its capabilities and calibration, and the test procedures can be found in our original report on thermal control in flexible space garments (Richardson, 1965). The heat input to the calorimeters was increased incrementally, and the temperatures of the calorimeters in the arm section were measured when equilibrium was reached for each heat input level. Two orbit positions were simulated: in the earth's umbra and on the earth-sun line.

4. Test Results

a. Equilibrium Temperatures

Calorimeter equilibrium temperatures were measured when equilibrium was reached for each heat input level to the calorimeters. The object of these tests was to determine the maximum metabolic rate possible before the astronaut will experience uncomfortably warm skin temperatures. It was assumed that the calorimeter temperatures would be indicative of the astronaut's skin temperature.

Equilibrium temperatures as a function of the total internal heat generated (on the basis of a whole space suit whose total area is 20.5 ft^2) are summarized in Figure 29 for operation in the earth's umbra and on the earth-sun line. Included in Figure 29 are the measured results (Richardson, 1965) for the same insulation loosely wrapped around the arm section (no compression in the insulation layers). The net increase in the internal heat which can be dissipated at a given calorimeter temperature thus results from an increase in the solid conduction through the insulation when it is compressed to 3.7 psia. Figure 29 shows the range of the astronaut's skin comfort zone (82.4 to 89.6°F).

In the case of operation in the earth's umbra, there is a substantial range of control of heat flow through the insulation when the insulation is compressed from residual to 3.7 psia. Uncompressed insulation has a maximum metabolic rate of 600 Btu/hr before the allowable skin temperature is exceeded. If the insulation is compressed to 3.7 psia, the maximum metabolic rate increases to almost 1100 Btu/hr before the same comfortable skin temperature is exceeded.

TABLE III SOLAR ABSORPTANCE, XENON LIGHT ABSORPTANCE, AND ROOM TEMPERATURE EMITTANCE
FOR SELECTED MATERIALS

| Coating and Substrate | Coating Thickness | Solar Absorptance | Xenon Light Absorptance | Room Temperature Emittance |
|---------------------------------------------------------------------------------------------------------------|-------------------|-------------------|-------------------------|----------------------------|
| | in | α_s | α_x | ϵ |
| S-13 ^a Silicone Polymer with ZnO Pigment on 6 oz Nomex | 0.004-0.005 | 0.16 ^b | -- | 0.73 ^b |
| S-13 Silicone Polymer with ZnO Pigment on 0.020 inch Aluminum | -- | 0.10 | 0.18 | 0.83 |
| Dow Corning 92-007 Thermatrol Silicon Resin with T ₁ O ₂ Pigment on 0.020 inch Aluminum | 0.004 | 0.10 | 0.06 | 0.82 |
| Aluminum 1100 H-22, Cleaned and Polished per ADL Specification A-3611-119 | -- | 0.10 | 0.08 | 0.018 |

a. Formulation; see Zerlaut, 1965.

b. Data from Richardson, 1965.

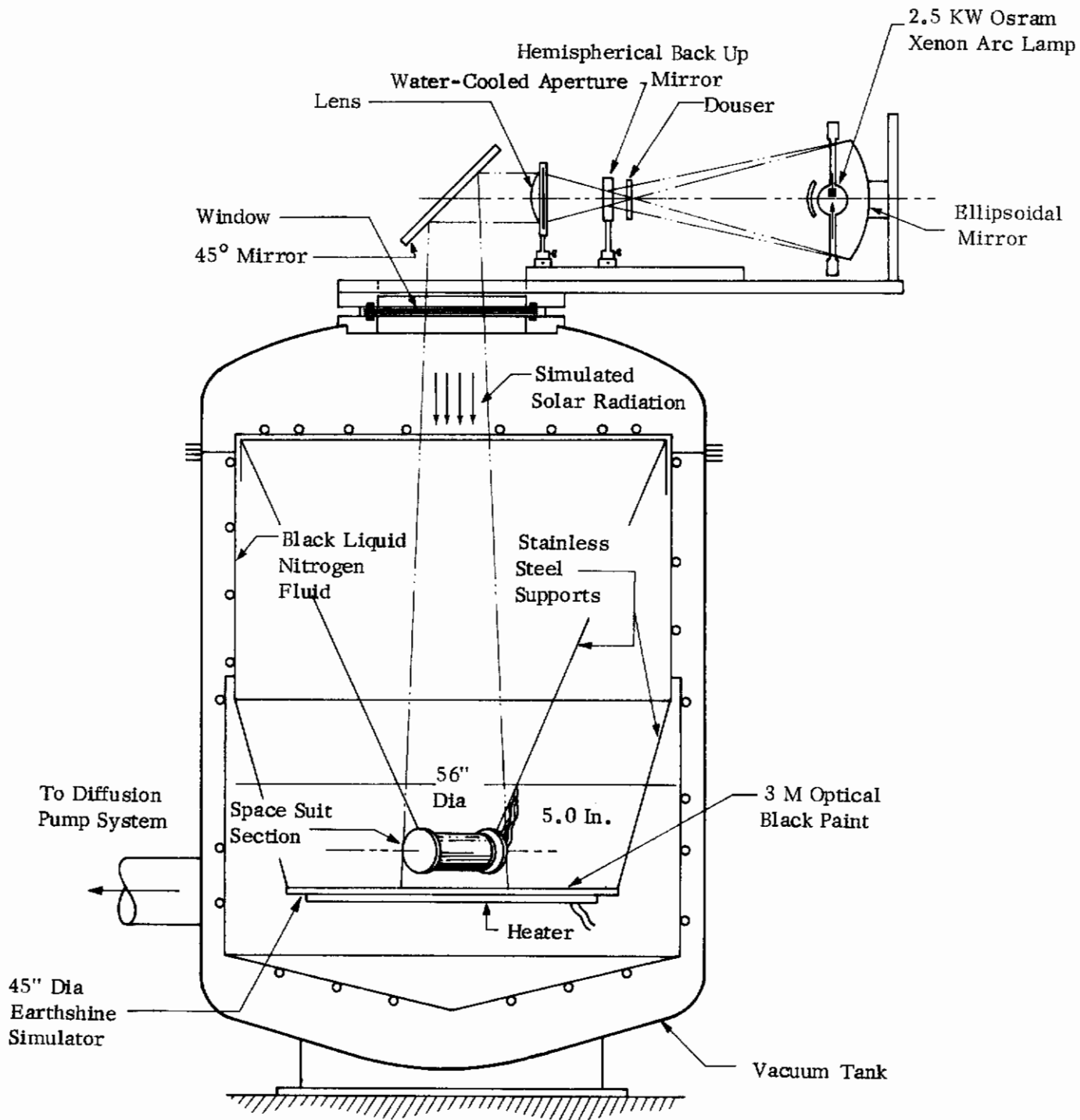


FIGURE 28. SPACE CHAMBER SCHEMATIC

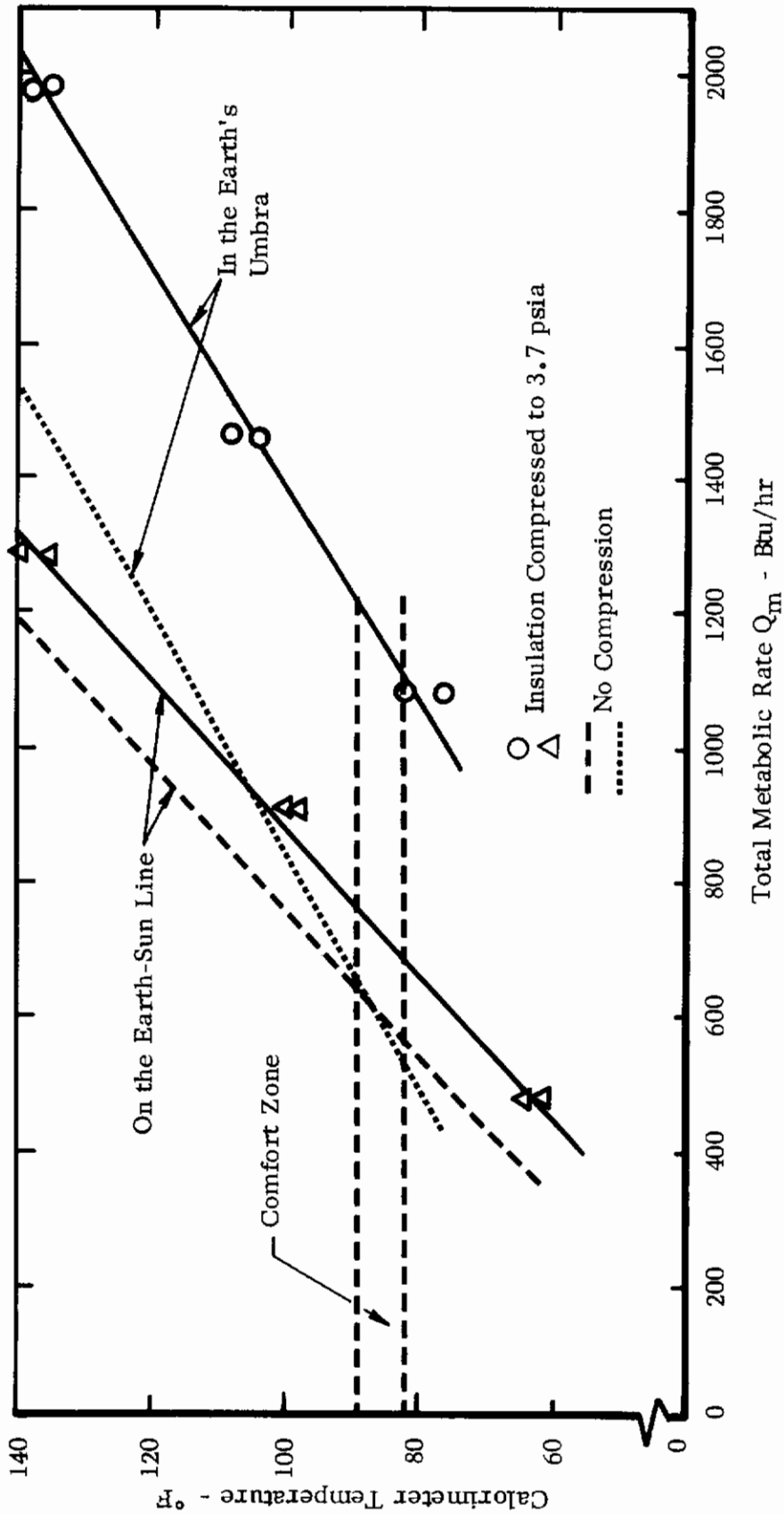


FIGURE 29. CALORIMETER EQUILIBRIUM TEMPERATURES FOR THE ARM SECTION WITH COMPRESSED INSULATION

Contrails

The other case, the earth-sun line, has a considerably narrower range of control of the heat flow through the insulation between the uncompressed and the compressed cases. As in the previous case, the maximum metabolic rate possible before the allowable skin temperature is exceeded is 600 Btu/hr. However, when the insulation is compressed to 3.7 psia, the maximum metabolic rate increases to only 750 Btu/hr before the same comfortable skin temperature is exceeded. This narrow range of heat flow control is attributable to the high skin temperatures which occur on the arm section when exposed to solar, albedo, and increased earthshine radiation when operating on the earth-sun line.

b. Azimuthal Temperature Distributions

The azimuthal temperature distributions on the inner and outer walls of the insulated space suit arm section were continuously recorded during the test program. The temperature distributions for the two orbits simulated are summarized in Figures 30 and 31. The reported azimuthal temperature distributions are for the equilibrium calorimeter temperatures in each orbit which are close to the astronaut's comfort zone.

Temperature distributions for the insulated arm section in a simulated orbit position on the earth-sun line are given in Figure 30. For a calorimeter average temperature of 98.6°F, the compressed insulation allowed a net heat flux per unit area from the arm section of 40.7 Btu/ft²-hr which corresponds to an astronaut's overall metabolic rate of 916 Btu/hr. Figure 31 summarizes the temperature distributions around the arm section for a simulated orbit position but in the earth's umbra. For a calorimeter temperature of 78.9°F, the net heat flux per unit area from the calorimeter was 52.9 Btu/ft²-hr, which corresponds to an astronaut's overall metabolic rate of 1080 Btu/hr.

c. Insulation Conductance

Point-by-point conductances around the model were calculated for all measurements of azimuthal temperature distributions on the inner and outer walls of the space garment insulation. We assumed that the heat flux per unit area through the space suit was constant, and we calculated average conductance: first, from the temperature difference between the inner and outer walls of the suit; and, second, from the temperature difference between the calorimeter and the outer wall of the suit. The second calculated conductance accounts for the resistance of the gas layer between the calorimeter and the inner wall of the insulation. The results are summarized in Table IV, as are the results of the measured conductances for the same insulation not compressed (Richardson, 1965).

Table IV also summarizes the ratio of conductance for the compressed and uncompressed insulation in both the umbra and on the earth-sun line. From this ratio we can see that it is possible to achieve control of the insulation conductance by compressing the insulation; the conductance increased by a factor of 3.1 in the earth's umbra and by a factor of 2.2 when on the earth-sun line.

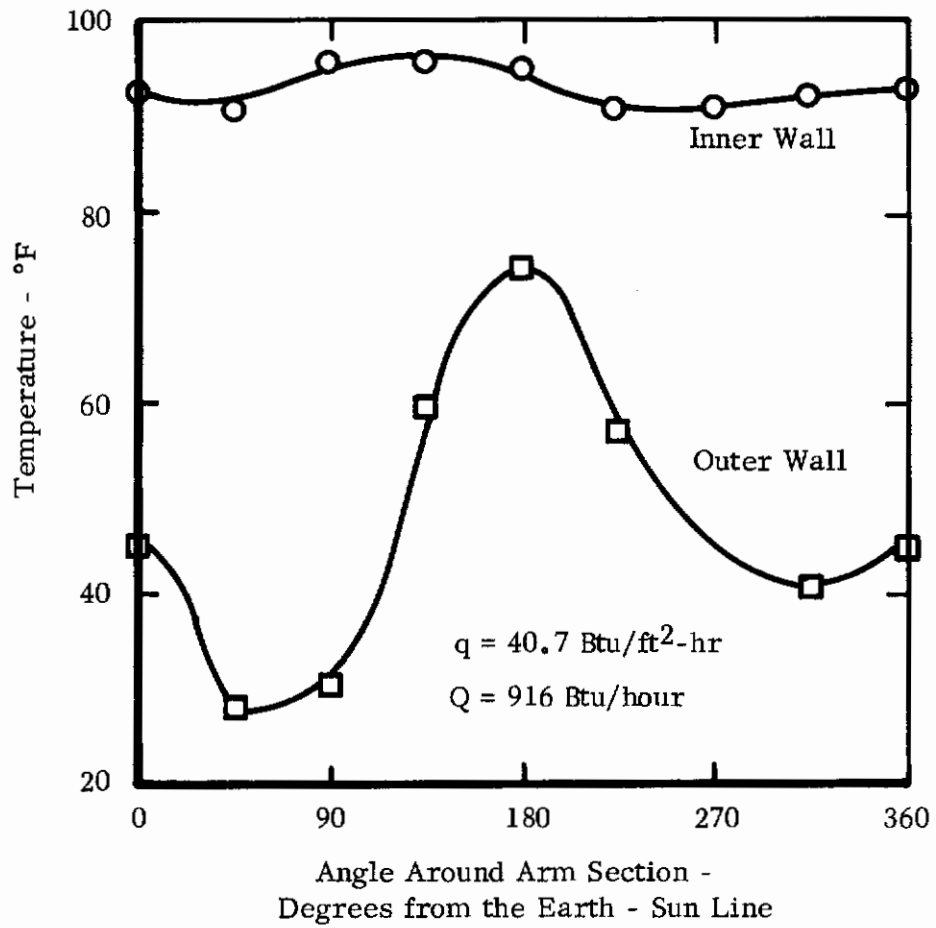


FIGURE 30. AZIMUTHAL TEMPERATURE DISTRIBUTIONS -- SPACE SUIT SECTION ON THE EARTH-SUN LINE-- COMPRESSED INSULATION

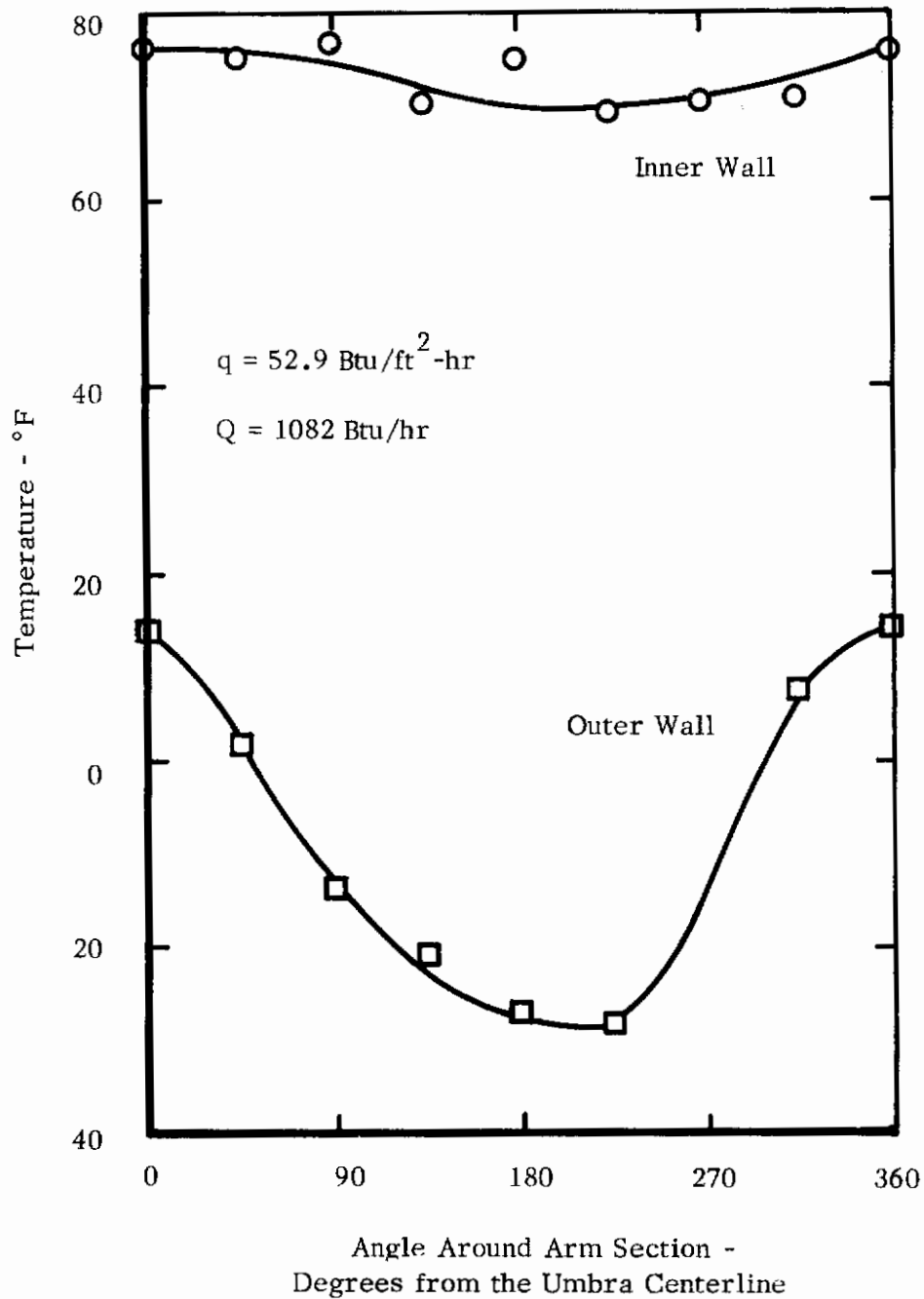


FIGURE 31. AZIMUTHAL TEMPERATURE DISTRIBUTIONS - SPACE SUIT SECTION IN THE EARTH'S UMBRA - COMPRESSED INSULATION

TABLE IV INSULATION CONDUCTANCE DERIVED FROM MEASURED PERFORMANCE

| Orbit Position | Insulation Type | Insulation Average Conductance (Btu/ft ² -hr°F) | Ratio of Compressed to Uncompressed Conductance | Calorimeter to Outer Wall Average Conductance (Btu/ft ² -hr°F) | Ratio of Compressed to Uncompressed Conductance |
|----------------|-----------------|------------------------------------------------------------|-------------------------------------------------|---------------------------------------------------------------------------|-------------------------------------------------|
| Earth Umbra | Compressed | 0.81 | 3.1 | 0.76 | 3.2 |
| | Uncompressed | 0.26 | | 0.24 | |
| Earth-Sun Line | Compressed | 1.06 | 2.2 | 0.91 | 2.0 |
| | Uncompressed | 0.48 | | 0.45 | |

B. THERMAL CONTROL LOUVERS FOR RIGID SPACE ENCLOSURES

To determine the efficiency of louvers in thermally controlling rigid enclosures, we analyzed, designed, and fabricated a 6-inch-square louver module and tested it in our space simulation chamber.

1. Thermal Design of the Louver Model

In Section II.G, we analyzed the performance of thermal control louvers operated in sunlight. We extended this thermal analysis to determine the performance of the 6-inch-square louver model shown in Figure 32 when exposed to simulated solar radiation from a xenon lamp. At the beginning of the design process, we determined the emittance and absorptance properties of the louver and baseplate surfaces.

a. Emittance and Absorptance Measurements

Measurements were made of total hemispherical emittance on the candidate materials summarized in Table III. Measurements also were made of spectral total reflectance versus the reflectance of magnesium oxide (MgO). Solar absorptance was calculated by a program which accounted for the absolute reflectance of MgO, the sample reflectance, and the measured solar spectrum. This program was modified to calculate the absorptance of the samples to our simulated solar beam which utilized a xenon lamp. Values of solar and xenon absorptance are summarized in Table III. For the baseplate and the top of the louvers, we used the Dow Corning Thermatrol white paint (silicone polymer with TiO₂ pigment). For the bottom side of the louvers, we used chemically polished aluminum.

b. Louver Performance and Estimation of Losses

The theoretical operating performance of the 6-inch-square louver module, shown in Figure 32, was calculated for both the open and closed state and in the shade as well as in simulated solar radiation (xenon solar simulation). Figures 33, 34, 35, and 36 summarize the results of these calculations, along with the surface properties which were used.

We next estimated the losses which might occur for each orbit situation from the side rails, through gaps between louver vanes, and through the insulation. These losses were then added to the theoretical performance to obtain the net heat flow from the louver module which would occur during simulated orbit tests in our space chamber. These results are summarized in Table V.

By analysis it was determined that the minimum losses would occur from the exposed aluminum framework (side rails) of the louver module if we thermally connected them to the baseplate and then polished them to achieve low emittance and low solar absorptance. Because the solar absorptance of aluminum is higher than its emittance and the side rails are maintained at about 80°F, there is a net influx of solar heat into the side rails when they are exposed to sunlight. Thus, the net heat flow from the louver module is reduced by this absorbed heat flow.

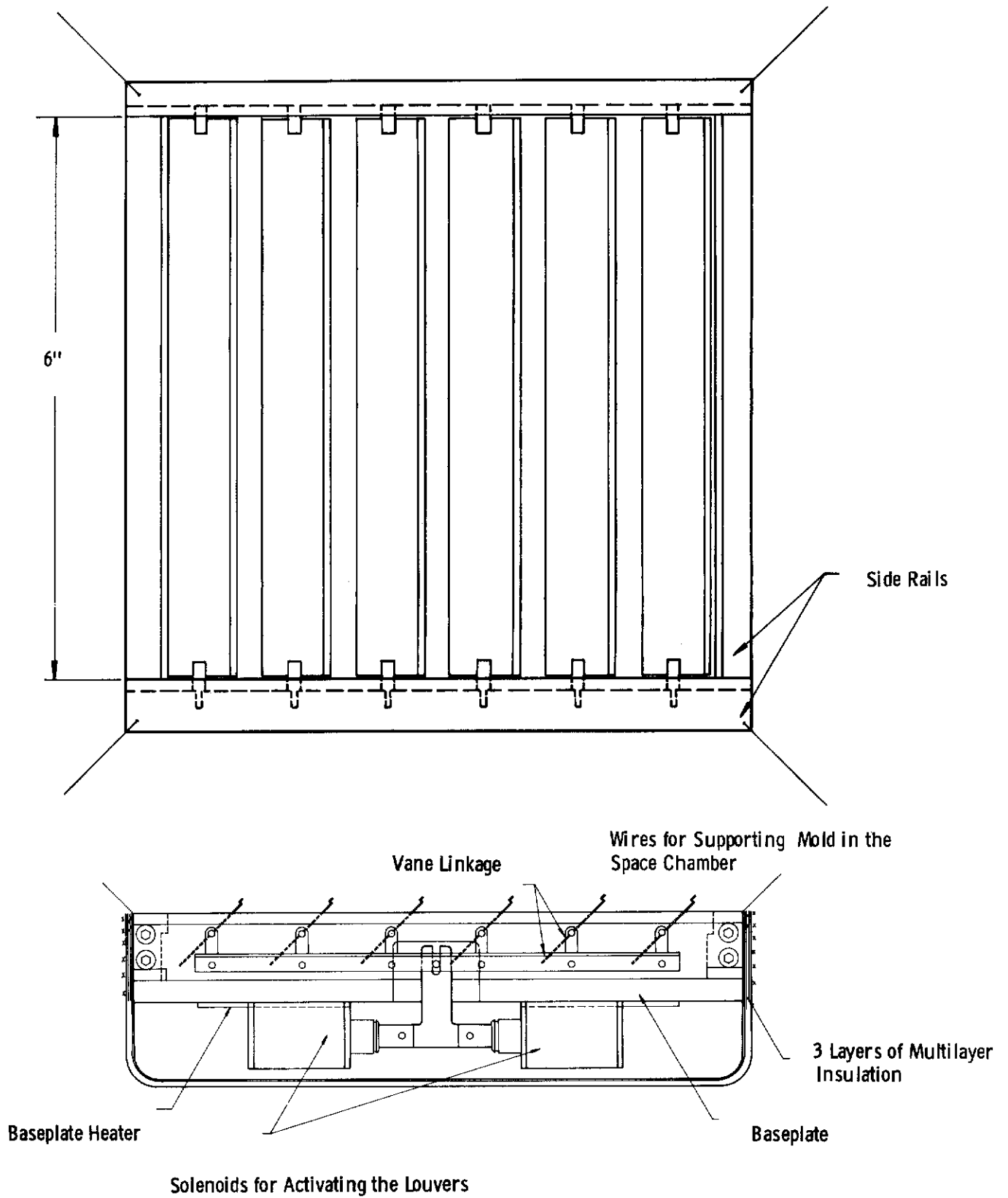


FIGURE 32. LOUVER TEST MODEL

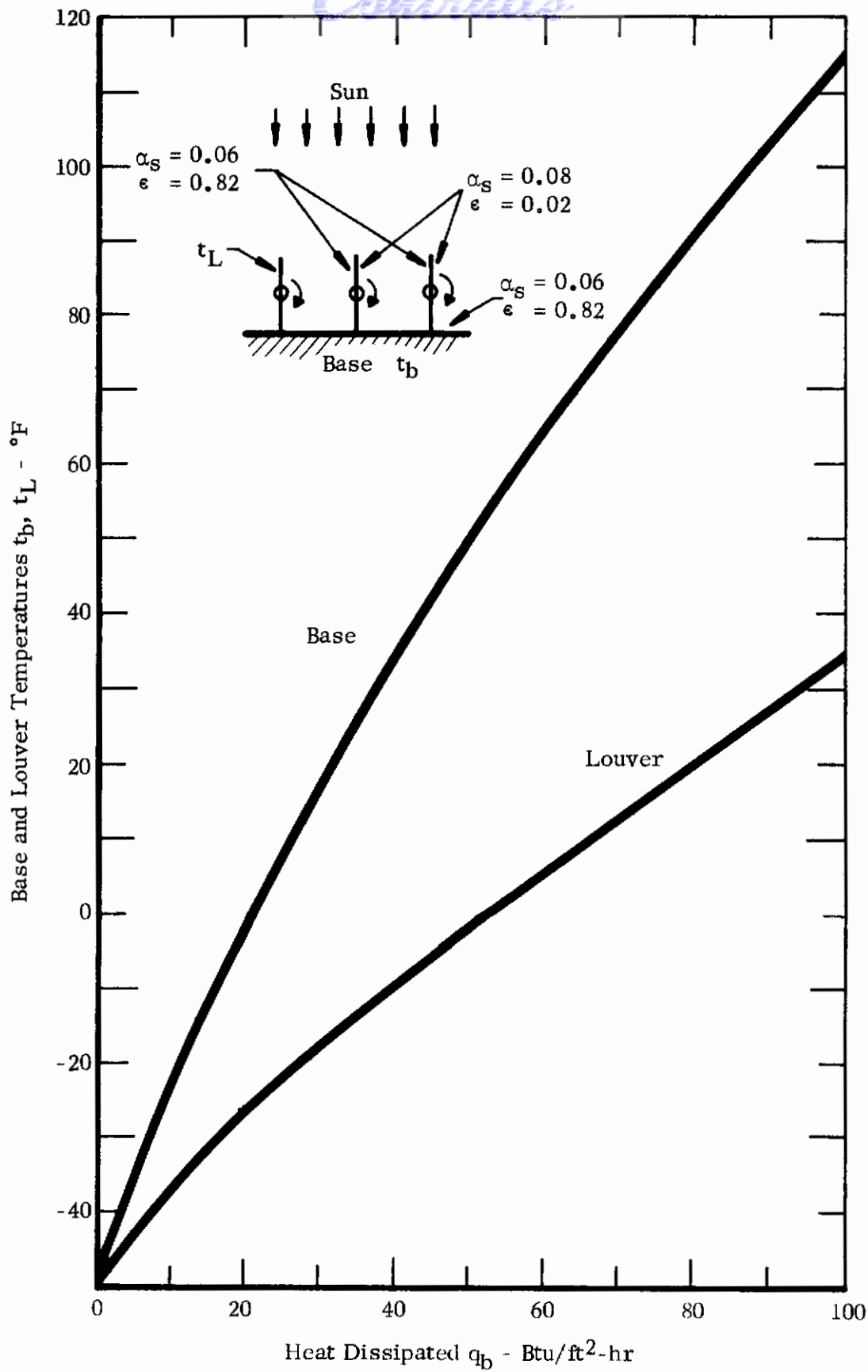


FIGURE 33. BASE AND LOUVER TEMPERATURES FOR OPEN LOUVERS IN SIMULATED SOLAR RADIATION

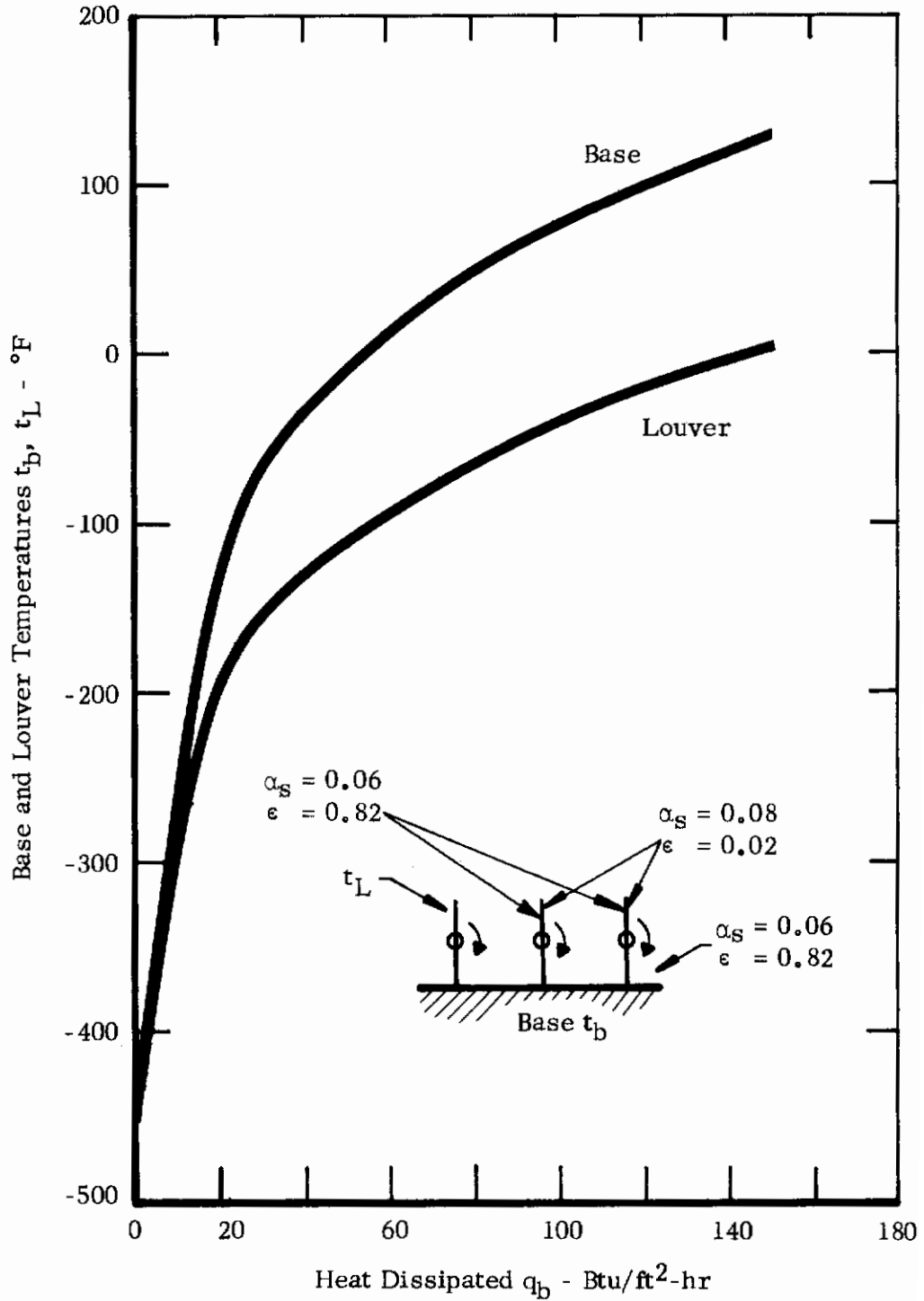


FIGURE 34. BASE AND LOUVER TEMPERATURES FOR OPEN LOUVERS IN THE SHADE

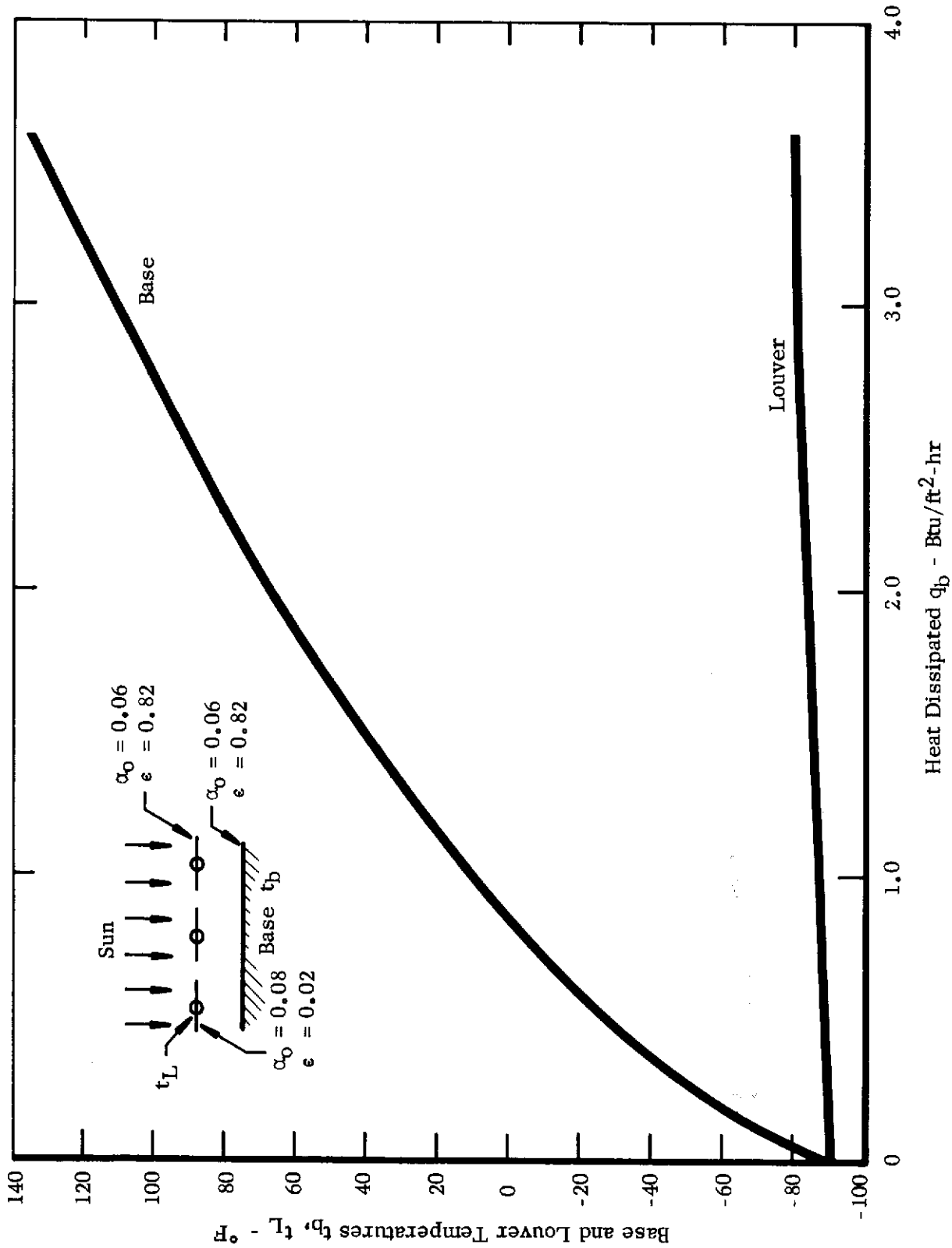


FIGURE 35. BASE AND LOUVER TEMPERATURES FOR CLOSED LOUVERS IN SIMULATED SOLAR RADIATION

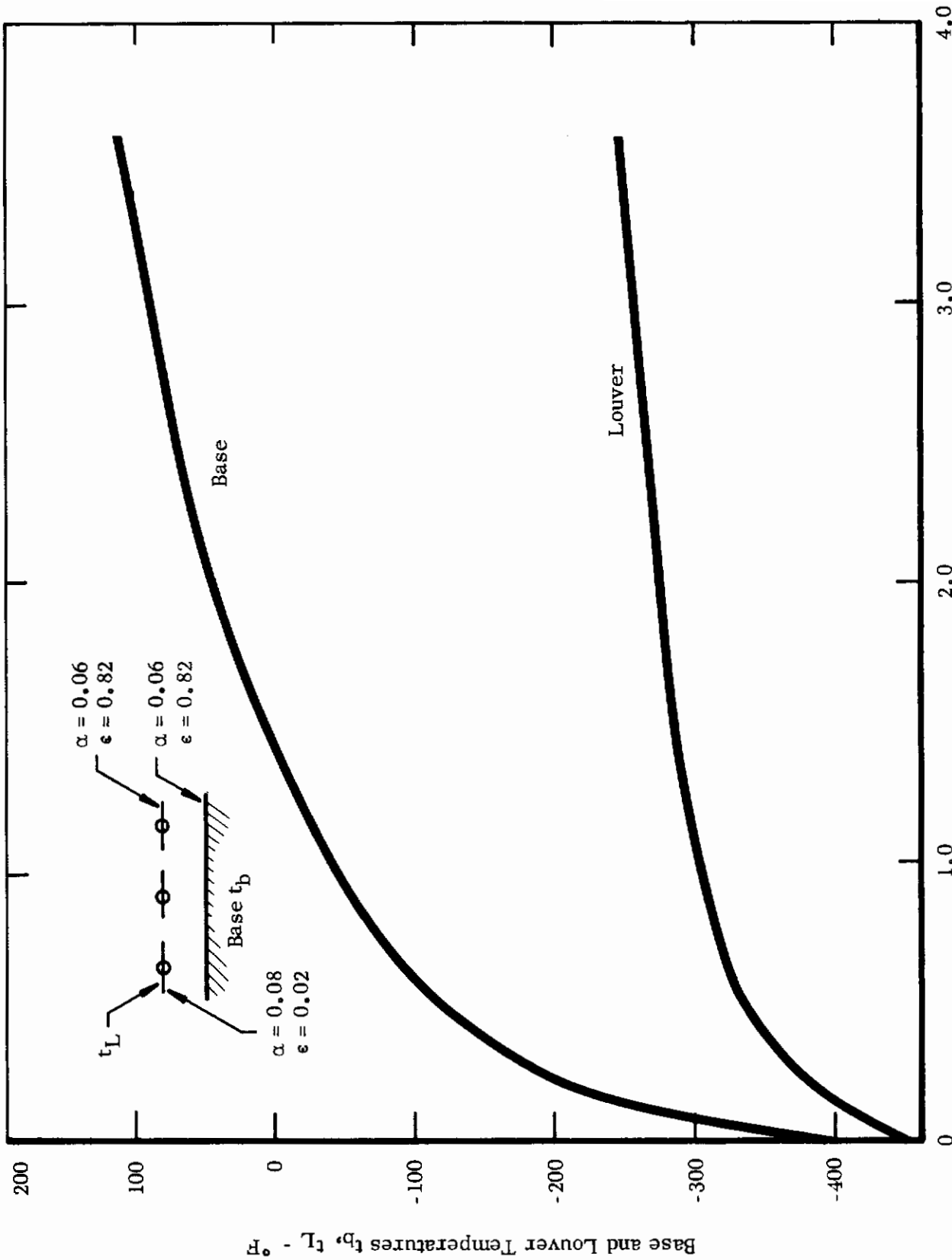


FIGURE 36. BASE AND LOUVER TEMPERATURES FOR CLOSED LOUVERS IN THE SHADE

TABLE V SUMMARY OF LOSSES FROM LOUVER TEST MODEL

| <u>Orbit Situation</u> | <u>Net Heat Flow from the Model (Btu/hour)</u> |
|------------------------|----------------------------------------------------|
| Open in the shade | 1.2 |
| Open in the sun | -1.3 |
| Closed in the sun | -1.2 |
| Closed in the shade | 1.3 |

2. Fabrication of the Louver Model

We used six louver vanes for the louver configuration, each 6 inches long and 1.04 inches wide. The vanes had pivots near the centerline of their long axis and were spaced on 1 inch centers in a framework which was attached mechanically and thermally to the baseplate. The vanes were designed with an offset on one edge which overlapped the adjacent vane to minimize the losses from gaps which might occur when assembled. The louver actuation solenoids and linkage and the thermostatic control circuits were attached to the bottom surface of the baseplate. An aluminum cover and 3 layers of insulation were placed over the back surface and sides of the louver model, each layer comprised of 0.00025-inch, double aluminized mylar radiation shields and two spacers of 0.003-inch silk netting. This insulation reduced the back losses from the louver module to less than 1 Btu/hr.

The louver system shown in Figure 32 was designed to operate with the louvers either fully opened or fully closed. Louver action was controlled by sensing the temperature of the baseplate. When the temperature increased above a fixed point, a thermostat switch actuated a control circuit which energized a solenoid attached to a mechanical linkage which opened the louvers. When the temperature of the baseplate decreased below another fixed point, a second thermostat switch actuated its control circuit to energize a solenoid which closed the louvers.

Electric heaters were attached to the baseplate and thermocouples were attached to the baseplate and the louver vanes. Heat input to the louver system was controlled by a variac and measured by means of a calibrated wattmeter.

Care was taken in selecting and preparing the thermal control surfaces of the louvers to insure that their absorptance and emittance would be the same as those which were measured during the materials screening phases of the program.

a. Theory and Operation of Louver Control System

Thermal analysis of the behavior of the louvers indicates that operation with the vanes either open or closed in direct sunlight is possible and that, by careful choice of the surfaces for the vanes, the temperature of the baseplate will always remain cool enough so that heat can be dissipated. Thus, the control system for the louvers needs to sense only the temperature of the base and to open the louvers when the temperature rises above a set point and close them when the temperature drops below another set point.

In the design of the louver controls, we used the following criteria:

| | |
|------------------------|--------|
| baseplate temperatures | |
| maximum | = 80°F |
| minimum | = 70°F |

Contrails

response time = instantaneous
cycle time = 60 seconds
continuous power = < 20 milliwatts
actuation voltage = 24 volts d.c.

For actuating the louvers, we used two solenoids, one for opening the louvers on temperature rise and one for closing them on temperature fall. A block diagram of the control circuit is shown in Figure 37. In operation, the thermostat switch actuates the switching circuit which energizes the solenoid for a long enough time so that the louvers can be fully opened or fully closed. At the end of the pulse, the power to the solenoid reaches a minimum level which holds the solenoid. The circuit works as follows:

When the thermostat contacts close, the 250 μ fd capacitor shown in Figure 37 discharges into the gating circuit and bias resistor to gate the transistor into full conduction thus applying 24 volts to the solenoid during a period of approximately 1 second, thus closing it. The solenoid remains closed by the magneto-motive force resulting from a controlled leakage current of approximately 0.2 ma through the solenoid coil from the collector circuit.

3. Test Program for Louver Module

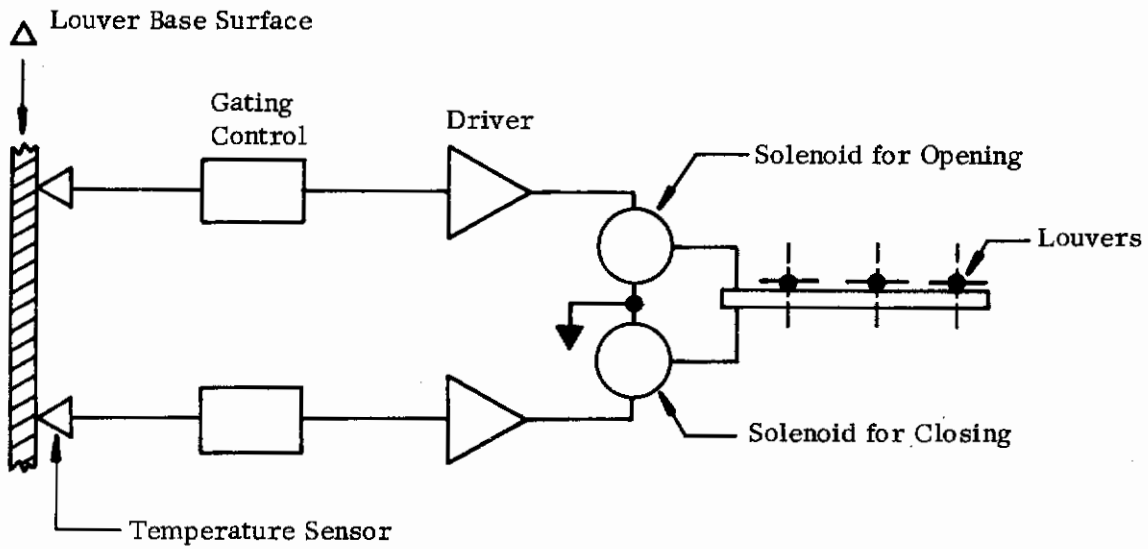
The louver module was tested in our space simulation chamber (Figure 28) at a pressure of 1.1×10^{-5} torr. The walls of the space chamber were again cooled with liquid nitrogen to simulate outer space, and solar radiation was simulated. However, earthshine and albedo were not simulated. Thus, the two orbit situations which were simulated were (a) with the louvers facing the sun and (b) with them facing outer space and with no sunlight. Figure 38 shows the louver model suspended in the space simulation chamber and with the solar simulator in operation.

With the solar simulator turned off, the heat input to the baseplate was increased until the louvers opened, and then the power was held constant until steady-state temperatures were obtained. The power input to the baseplate was then increased, and a new equilibrium temperature was achieved. This procedure was followed until the three steady-state operating points summarized in Table VI were obtained.

The solar simulator was turned on and the power level was decreased until the baseplate temperature reached a steady-state temperature near 80°F. The louvers were then closed and the power was again decreased until the baseplate again reached a steady-state temperature near 80°F. The solar simulator then was turned off and the power to the baseplate increased until a steady-state temperature near 80°F was again achieved.

At each steady-state operating condition, the power into the baseplate was measured with a wattmeter and the temperatures of the baseplate and

CIRCUIT BLOCK DIAGRAM



CIRCUIT DETAILS

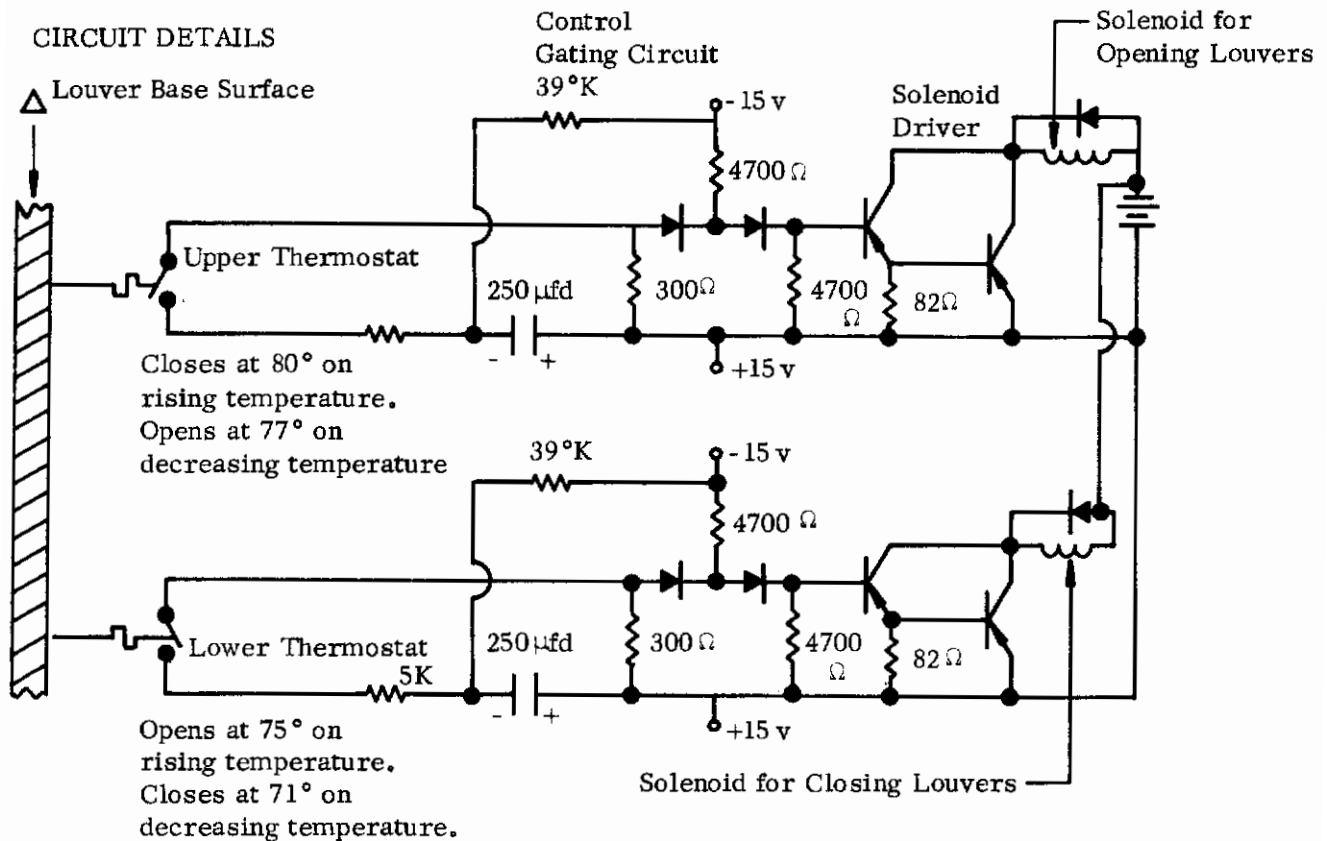


FIGURE 37. LOUVER CONTROL SYSTEM

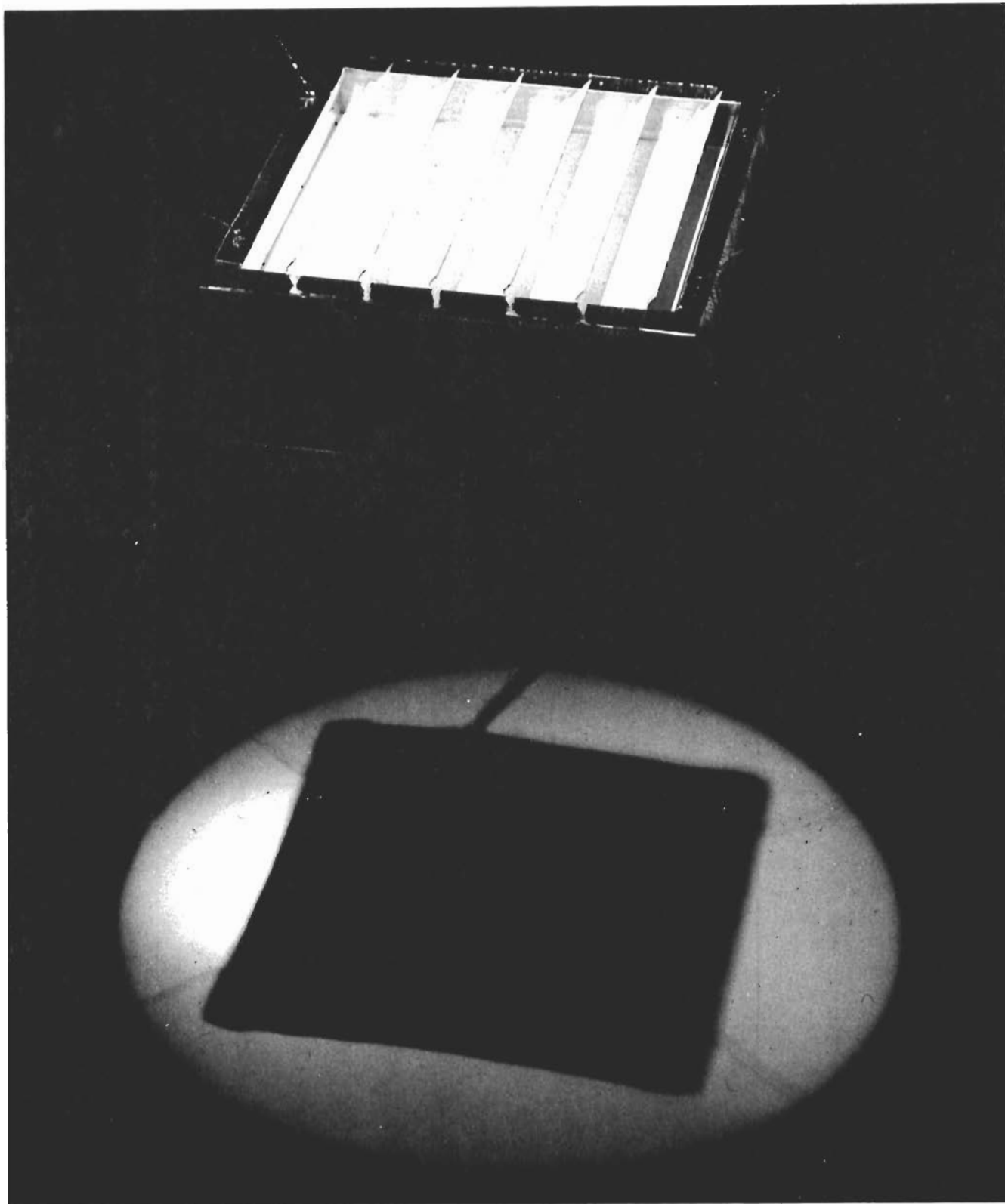


FIGURE 38 LOUVER THERMAL CONTROL MODEL IN
SIMULATED SOLAR BEAM

TABLE VI THERMAL BEHAVIOR OF LOUVER MODEL

| Test No. | Orbit Situation | Baseplate Temperature (°F) | Louver Temperature (°F) | Heat Flow Per Unit Area of Base (Btu/ft ² -hr) | Total Heat Dissipated (Btu/hr) | Calculated Total Heat Dissipated (Btu/hr) |
|----------|---------------------|----------------------------|-------------------------|-----------------------------------------------------------|--------------------------------|-------------------------------------------|
| 1 | Open in the shade | 85.0 | 2.9 | 136 | 34.2 | 26.3 |
| | | 75.8 | -3.0 | 109 | 27.3 | 25.3 |
| | | 64.9 | -11.4 | 81.8 | 20.5 | 22.3 |
| 2 | Open in the sun | 77.8 | 40.9 | 44.4 | 11.1 | 15.7 |
| 3 | Closed in the sun | 78.5 | -32.1 | 6.8 | 1.7 | -0.6 |
| 4 | Closed in the shade | 78.8 | -93.9 | 37.4 | 9.4 | 2.0 |

Contrails

two of the louvers were measured. The results of these tests for the four orbit situations are summarized in Table VI.

The heat input to the baseplate was then increased to $95.5 \text{ Btu/ft}^2\text{-hr}$ in order to determine how well the louvers can maintain the baseplate within a temperature range under steady heating conditions. The time versus temperature characteristics for the louver system operating in the shade are shown in Figure 39.

Because the baseplate temperatures were about equal for each of the four operating situations, the performance of the louvers summarized in Table VI can be compared. Note that heat always flows from the baseplate. Table VI summarizes the estimated total heat rejected from the louver model. This predicted performance comes from Figures 33 through 36 and from losses summarized in Table V.

A comparison of the total heat dissipated in Tests Nos. 1b and 4 in Table VI shows the range of control of heat flow afforded by louvers operating on the shaded side of a space enclosure. The ratio of heat rejected by open louvers in the shade to heat losses by closed louvers in the shade is 2.9. The range of control of heat flow for louvers operating on the sunlight side of a space enclosure can be obtained by comparing Tests Nos. 2 and 3, and the ratio of heat by open louvers to closed louvers is 6.5. A comparison of the heat dissipated in Tests Nos. 1b and 2 shows the effects on heat flow which occur when open louvers on the shaded side of an enclosure are suddenly moved into the sunlight. The ratio of heat rejected in this case is about 2.5.

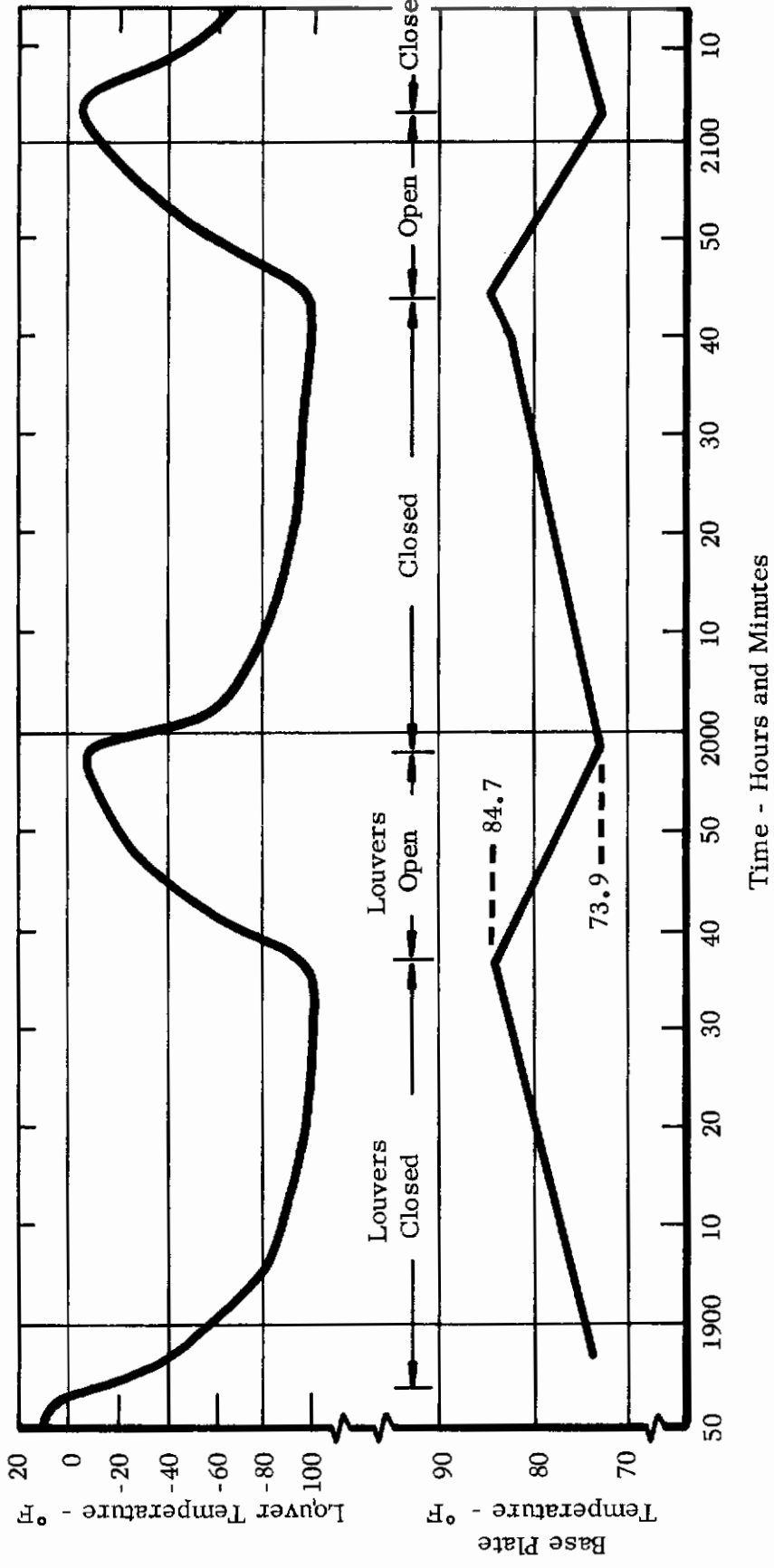


FIGURE 39. STEADY HEATING OPERATING CHARACTERISTICS OF THE LOUVER MODEL
Heat Input to the Base Plate $q = 95.5 \text{ Btu/ft}^2 \text{-hr}$

Contrails

SECTION IV

CONCLUSIONS

The analytical and experimental work performed in this program produced several conclusions about techniques and materials for the passive thermal control of rigid and flexible extravehicular space enclosures.

1. The degree to which passive thermal control can be applied to an orbiting enclosure can be determined only by performing an orbit thermal analysis which takes into account:

- a. Radiation exchange with the external environment (solar, albedo, earthshine, and radiation from other nearby objects);
- b. Heat generated internally; and
- c. The geometries of the enclosure and adjacent bodies.

Passive or semi-passive thermal control is possible only when the average external temperature of the enclosure is less than the desired internal temperature.

2. The presence of a spacecraft markedly influences the temperature on those sections of the space enclosure which see the spacecraft, and it reduces the amount of metabolic activity which an astronaut may exert before passive thermal control becomes impossible. An astronaut in a man-sized enclosure with an effective radiating area of 56.6 ft² and actively moving near a space station under the worst orbit conditions may generate metabolic heat at a rate of 1000 Btu/hr before the average temperature on the outside of the enclosure exceeds 65°F. However, an astronaut in a soft anthropoform enclosure with an effective radiating area of 23.4 ft² is allowed to generate metabolic heat at a rate of only 400 Btu/hr under the same circumstances. Thus, for soft anthropoform enclosures with presently achievable surface radiating properties, there is too little effective radiating area to maintain passive thermal control for the expected metabolic range of activity (500 to 1500 Btu/hr) when the astronaut is operating on the surface of a spacecraft. However, operation away from the surface is possible.

3. Rigid space enclosures have a sufficient effective radiating area to maintain passive thermal control for the expected metabolic range of activity (300 to 800 Btu/hr) for all orbit situations.

4. If the feasibility of applying passive thermal control to orbiting enclosures is not limited by the effective radiating area of the enclosure, several techniques are available for thermal control. The following techniques are feasible for both flexible and rigid enclosures:

- a. Control of heat flow through the enclosure insulation by injecting a high conductivity gas (such as helium) into the insulation

Contrails

layers and maintaining it there until low heat flux conditions are desired, at which time this insulation is evacuated to space. This technique is particularly applicable to soft space suits.

b. Circulation of a liquid through a liquid-cooled garment on the astronaut's skin and then through a heat exchanger on the surface of the enclosure. This technique is particularly applicable to rigid enclosures; however, if effective means for distributing heat on the outside of the space suit can be developed, this technique could be effective for soft suits.

For rigid space enclosures, louvers can be used to control the heat flow at the external surface of the enclosure. Louvers can be designed which are capable of rejecting heat to space when exposed to both sunlight and shade. The louvers can be controlled by sensing the temperature of the baseplate of the louver system. The louvers will be fully opened when the base temperature rises above a fixed point and closed when the temperature drops below another fixed point.

5. It is not feasible to thermally control an astronaut in an enclosure by storing the generated heat in materials which change phase. The weight of phase change material is excessive for the maximum metabolic rates in question (1500 Btu/hr). Furthermore, there are operational difficulties in regenerating the phase change material at the conclusion of each EV mission. The liquid phase insulates the astronaut. The thermal coupling of the astronaut to the phase change material is not sensitive to changes in metabolic rate. Thus, it is difficult to regulate the removal of heat from the astronaut's skin.

6. It is not feasible to passively thermally control an astronaut by changing the conductance of insulation by compression, because there is no way of differentially controlling the compression in various zones of the enclosure. When the insulation layer is in compression, the flexibility of a soft space suit will be impaired.

7. Wrinkles or folds in the outer surface of a soft space suit will not affect the overall heat balance on the space suit. Localized hot spots may occur in the bottom of a fold, but they will not be felt by the astronaut and will not exceed the operating temperature for the presently used soft space suit materials.

8. The liquid-cooled garment (LCG) is the most effective way to thermally couple an astronaut with his thermal control system in either a rigid or a flexible space enclosure. The LCG presently developed is capable of removing the metabolic heat loads encountered in space exploration. The thermal resistance of the LCG tube walls appears to be the limit on heat removal.

9. The thermal coupling of an astronaut with the cold walls of a rigid space enclosure can be effectively achieved by circulating a small amount of gas. The gas flow primarily serves to transfer heat from the

Contrails

astronaut to the cooled wall and to remove insensible perspiration and metabolic products.

10. Removal of metabolic heat at the astronaut's skin by gas convection is not effective. If there is no sweating, too much gas flow and power are required to remove reasonable amounts of metabolic heat. If the skin is wet from active sweating, a large amount of heat can be extracted but at a cost of severe dehydration of the astronaut.

11. It is not feasible to control the heat flow through the insulations on rigid or flexible space enclosures by transient injection of gas into the insulation layers because evacuation is too rapid. To be effective, the gas must be either continuously injected (a wasteful procedure) or retained by not allowing it to escape until low heat flow through the insulation is again desired.

Contrails

SECTION V RECOMMENDATIONS

In the design of thermal control systems for astronauts working in orbit, we recommend the following:

1. An umbilical thermal control system should be used in situations where the astronaut will be required to work on the surface of his space station because it is not possible to passively thermally control his temperature. The umbilical thermal control system will pass the astronaut's thermal load to the space station thermal control system.
2. Thermal control systems for both flexible and rigid astronaut enclosures should be developed to transfer the astronaut's thermal load from his skin to those portions of the exterior surface of the enclosure which are cool enough to effectively dissipate his metabolic heat. One promising system utilizes an insulation to thermally isolate the astronaut, a liquid-cooled garment on his skin, and a control for distributing the warmed liquid to heat exchangers integrated with the enclosure wall.
3. Louver systems capable of operating in sunlight as well as in shade should be developed for thermally controlling rigid space enclosures. One feasible system utilizes louver vanes with the outer surface painted white and the inner surface of polished aluminum. The baseplate of this system is also painted white, and the louvers are operated either in the fully open or fully closed position.
4. Materials should be developed for the exterior layer of flexible space garments which will laterally dissipate heat along the garment surface and yet will remain as flexible as present space garments.

Contrails

APPENDIX I

THERMAL HEAT BALANCE FOR ORBITING ASTRONAUT ENCLOSURES IN THE PRESENCE OF A LARGE SPACECRAFT

In this analysis, we are concerned with the azimuthal temperature distribution on the external surface of an astronaut enclosure at selected locations in earth orbits when in the presence of a large spacecraft. Summarized herein are the major assumptions used in the analysis, the heat balance equation for an elemental area of the astronaut enclosure, a description of the calculation procedure for obtaining azimuthal temperatures and average surface temperatures, and the details of the machine computation program.

The model used in this analysis is shown in Figure 40.

A. ASSUMPTIONS

The following assumptions were made:

1. Each of the 12 elements of the enclosure is in equilibrium (i.e., heat input equals the heat out).
2. There is no azimuthal heat flow from one element to the next and elements are independent of each other.
3. The internal heat generated by the astronaut is uniformly distributed and is equal to $Q_m/12$.
4. The spacecraft can be represented as a cylinder with a 7.5-foot radius and a 16.7-foot length, maintained at a uniform skin temperature of 70°F.
5. The flexible enclosure is a cylinder with a radius of 0.58 foot and a length of 6.4 feet.
6. The rigid enclosure is a cylinder with a radius of 1.5 feet and a length of 6.0 feet.
7. In all cases, the axis of the enclosure and the axis of the spacecraft are considered parallel; in all cases, the axis of the enclosure is considered to be perpendicular to the plane determined by the earth-to-sun line and the earth-to-enclosure line.
8. The effects of the circular ends of the cylinders are neglected.
9. All reflection and radiation is assumed to be diffuse.
10. The solar constant is 442 Btu/ft²-hr.
11. The albedo of the earth for solar radiation is 0.4.

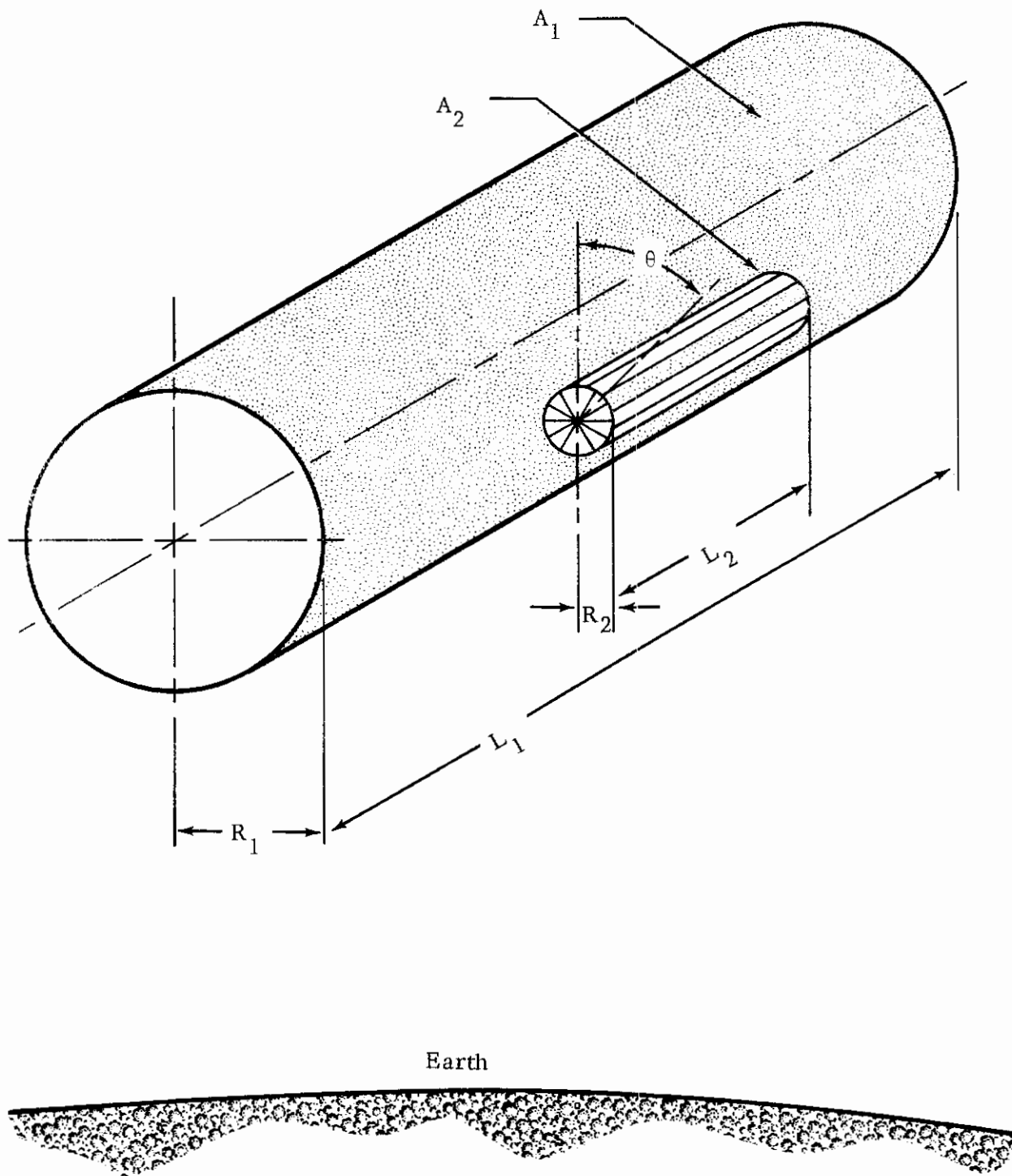


FIGURE 40. GEOMETRY FOR TYPICAL HEAT BALANCE

Contrails

12. The absorptivity of the earth for solar radiation is 0.6.
13. The emissivity of the craft and the enclosure is $\epsilon = 0.85$.
14. The absorptivity of the enclosure is equal to:
 - a. $\alpha_s = 0.17$ (for solar wavelengths) and
 - b. $\alpha = \epsilon = 0.85$ (for long wavelengths--spacecraft and earth).
15. The effect of the space enclosure on the spacecraft is negligible.

B. ANALYSIS

The heat balance equation for the astronaut enclosure is based on the scheme shown in Figure 40.

| Emitted Radiation Q_{radiated} | Absorbed Radiation Q_{input} | | |
|-----------------------------------------------|------------------------------------------------------------|----------------------------------|------|
| $\epsilon_2 A_2 \sigma T_2^4$ | $= \alpha_{2S} S A_{2P} \cos\theta$ | solar | (28) |
| | $+ \alpha_{2S} a S A_{2P} F_R$ | earth albedo | |
| | $+ \alpha_{2L} S \left(\frac{1-a}{4}\right) A_{2P} F_S$ | earthshine | |
| | $+ \alpha_{2S} (1-\alpha_{1S}) S \frac{2}{\pi} F_{21} A_2$ | solar reflected from spacecraft | |
| | $+ \alpha_{2L} \epsilon_1 \sigma T_1^4 F_{21} A_2$ | direct radiation from spacecraft | |
| | $+ \frac{1}{12} Q_{\text{int}}$ | interior heat generated | |

From this equation, the total emitted radiation and temperature for each segment can be calculated.

The flat plate view factors C_R and C_S for earth reflection and earthshine were taken from Stevenson and Grafton (1961) while those for sector-to-craft were calculated by numerical integration. For some of the sectors, the sector's view of the earth is impeded in whole or in part by its view of the craft; in which case, corrections to the flat plate view factors were made on a geometric basis.

Contrails

From the sum of the net outward heat flow for each section, the average heat flow over the external area of the enclosure was calculated. The effective average temperature which the skin of the space enclosure must reach to radiate the total energy emitted was calculated.

C. COMPUTATION PROGRAM

The analysis was programmed for machine computation on the General Electric 235 Datanet Computer System. The program listing is as follows:

SLIST

```
00000 C      TANG CALCULATES TEMP OF 12 SECTORS   E FIELD
00010      DIMENSION RFP(12,2),SFP(12),CCA(12,3),T(12,3),FR(9)
00020      1,QQ(12),QT(3),TAV(3)
00030      PI=3.14159
00040      W1=PI/180.
00050      SIGMA=.1712
00060      EPS1=EPS2=ALPH2L=.85
00070      ALPH1S=ALPH2S=.17
00080      TS4=((459.6+70.)*.01)**4
00090      RFP(1,1)=RFP(12,1)=0.
00100      RFP(2,1)=RFP(11,1)=.0380
00110      RFP(3,1)=RFP(10,1)=.1642
00120      RFP(4,1)=RFP(9,1)=.3721
00130      RFP(5,1)=RFP(8,1)=.6073
00140      RFP(6,1)=RFP(7,1)=.7831
00150      RFP(1,2)=.0002
00160      RFP(2,2)=.0059
00170      RFP(3,2)=.0188
00180      RFP(4,2)=.0310
00190      RFP(5,2)=.0353
00200      RFP(6,2)=.0302
00210      RFP(7,2)=.0172
00220      RFP(8,2)=.0050
00230      RFP(9,2)=.0005
00240      RFP(10,2)=RFP(11,2)=RFP(12,2)=0.
00250      SFP(1)=SFP(12)=0.
00260      SFP(2)=SFP(11)=.0280
00270      SFP(3)=SFP(10)=.1603
00280      SFP(4)=SFP(9)=.3790
00290      SFP(5)=SFP(8)=.6254
00300      SFP(6)=SFP(7)=.8157
00310      100 PRINT 150
00320      150 FORMAT("ISIZE,ICRAFT,IDAY ")
00330      READ:ISIZE,ICRAFT,IDAY
00340      ICRAFT=ICRAFT+1
00350      IDAY=IDAY+1
00360      S=442.
00370      EAL=.4*S
00380      ESH=(1.-.4)/4.*S
00390      GO TO (65,66),IDAY
00400      65 S=EAL=0.
```

Contrails

```
00410      66 DO 210 I=1,12
00420      DO 210 J=1,4
00430      210 CCA(I,J)=0.
00440      GO TO (201,202),ISIZE
00450      201 R2=.58
00460      XL2=6.4
00470      GO TO 203
00480      202 R2=1.5
00490      XL2=6.
00500      203 DO 130 J=6,9
00510      ANG=1.5*PI-(W1*30.*FLOATF(J)-15.)
00520      E=SQRTF((7.5+R2)**2+R2**2-2.*(7.5+R2)*R2*COSF(ANG))
00530      OME=ASIN(7.5/E)-ASIN(R2/E*SINF(ANG))
00540      130 FR(J)=MIN1F(1.,.5+(PI*.5-OME)/2./ASIN(4000./1.15/4300.))
00550      GO TO (204,205), ICRAFT
00560      205 GO TO (206,207),ISIZE
00570      206 CCA(1,1)=CCA(12,1)=1.944
00580      CCA(2,1)=CCA(11,1)=1.849
00590      CCA(3,1)=CCA(10,1)=.493
00600      CCA(4,1)=CCA(9,1)=.285
00610      CCA(5,1)=CCA(8,1)=.0246
00620      GO TO 204
00630      207 CCA(1,1)=CCA(12,1)=4.712
00640      CCA(2,1)=CCA(11,1)=3.801
00650      CCA(3,1)=CCA(10,1)=1.393
00660      CCA(4,1)=CCA(9,1)=.289
00670      204 DO 9 I=1,12
00680      IF(I-9) 8,9,8
00690      8 CCA(I,2)=CCA(XMODF(I+3,12),1)
00700      9 CONTINUE
00710      CCA(9,2)=CCA(12,1)
00720      DO 31 I=1,12
00730      IF(I-6) 30,31,30
00740      30 CCA(I,3)=CCA(XMODF(I+6,12),1)
00750      31 CONTINUE
00760      CCA(6,3)=CCA(12,1)
00770      QQ(1)=0.
00780      DO 28 L=2,7
00790      28 QQ(L)=200.+FLOATF(L-1)*100.
00800      DO 29 L=8,10
00810      29 QQ(L)=500.+FLOATF(L-7)*500.
00820      A2=PI*R2*XL2/6.
00830      AC=2.*SINF(15.*W1)*R2*XL2
00840      AS=AC*S
00850      PRINT 4
00860      L=0
00870      2 L=L+1
00880      PRINT 32,QQ(L)
00890      32 FORMAT(1H1/"INTERNAL HEAT =",F7.0," BTU/HR"/)
00900      DO 25 ISUN=1,2
```

Contrails

```
00910      GO TO (213,214),ICRAFT
00920 213 PRINT 215,ISIZE,ISUN
00930 215 FORMAT("SIZE =",I2,3X,"NO CRAFT  ISUN =",
00940 1 I2// "SECTOR  TEMP, DEG F"//)
00950      ICI=3
00960      GO TO 216
00970 214 PRINT 3,ISIZE,ISUN
00980 3 FORMAT("SIZE =",I2,"  ISUN =",I2/21X,"TEMP, DEG F"/
00990 1 "SECTOR  ICAP=1  ICAP=2  ICAP=3"//)
01000      ICI=1
01010 216 DO 40 ICAP=ICI,3
01020      QT(ICAP)=0.
01030      DO 10 I=1,12
01040      XI=I
01050      Q=QQ(L)/12.
01060      GO TO (121,123),ISUN
01070 121 GO TO (120,122,122),ICAP
01080 122 Q=Q+AS*MAX1F(0.,COSF(W1*(30.*XI-15. ))) *ALPH2S
01090      GO TO 120
01100 123 Q=Q+AS*MAX1F(0.,COSF(W1*(30.*XI-105. ))) *ALPH2S
01110 120 Q=Q+CCA(I,ICAP)*EPS1 *SIGMA*TS4*ALPH2L
01120      GO TO (6,7,17), ICAP
01130 6 GO TO (12,11),ISUN
01140 7 GO TO (14,20),ISUN
01150 14 IF(I-9) 13,13,20
01160 13 IF(I-3) 20,20,12
01170 17 GO TO (20,11),ISUN
01180 11 IF(I-6) 20,20,12
01190 20 Q=Q+2./PI*S*CCA(I,ICAP)*(1.-ALPH1S)*ALPH2S
01200 12 GO TO (112,52,22),ICAP
01210 52 IF(I-9) 113,113,42
01220 113 IF(I-5) 112,112,114
01230 114 Q=Q+FR(I)*AC*ESH*SFP(I)*ALPH2L
01240      GO TO (116,115), ISUN
01250 116 Q=Q+FR(I)*AC*EAL*RFP(I,ISUN)*ALPH2S
01260      GO TO 42
01270 112 Q=Q+AC*ESH*SFP(I)*ALPH2L
01280 115 Q=Q+AC*EAL*RFP(I,ISUN)*ALPH2S
01290      GO TO 42
01300 22 Q=Q+MAX1F(0.,(AC*SFP(I)-CCA(I,ICAP)))*ESH*ALPH2L
01310      Q=Q+MAX1F(0.,(AC*RFP(I,ISUN)-CCA(I,ICAP)))*EAL*ALPH2S
01320 42 QT(ICAP)=QT(ICAP)+Q
01330      T2=(Q/(A2*EPS2*SIGMA))**.25
01340      T2=T2*100.-459.6
01350 10 T(I,ICAP)=T2
01360      TAV(ICAP)=(QT(ICAP)/(12.*A2*EPS2*SIGMA))**.25
01370 40 TAV(ICAP)=TAV(ICAP)*100.-459.6
01380      DO 24 I=1,12
01390 24 PRINT 1,I,(T(I,ICAP),ICAP=ICI,3)
01400 1 FORMAT(I4,3X,3F10.1)
```

Contrails

```
01410      PRINT 41,(TAV(ICAP),ICAP=ICI,3)
01420      41 FORMAT(/"RADI-"/"ATIVE"/"T AVG =",3F10.1)
01430      PRINT 4
01440      4 FORMAT(1H1)
01450      GO TO (67,25),IDAY
01460      25 CONTINUE
01470      67 IF(L-10) 2,100,100
01480      END
01490      FUNCTION ASIN(X)
01500      ASIN=ATANF(X/SQRTF(1.-X*X))
01510      RETURN
01520      END
```

Contrails

APPENDIX II

HEAT TRANSFER COEFFICIENT OF OXYGEN GAS TO SKIN

A. OXYGEN PROPERTIES

In this analysis, we estimate the heat transfer coefficient (h) which might be achieved in a flexible space enclosure.

$$P = 3.7 \text{ psia}$$

$$T \sim 90^\circ\text{F}$$

$$\text{Pr} = 0.71$$

$$C_p = 0.22 \text{ Btu/lb}^\circ\text{F}$$

$$\mu = 13 \times 10^{-6} \text{ lbm/sec-ft}$$

$$\rho = 0.021 \text{ lbm/ft}^3$$

B. MODEL

Annulus

$$\text{Cross-sectional width} = 0.5 \text{ ft}$$

$$\text{Length} = 6.7 \text{ ft}$$

$$\text{Diameter} = 1 \text{ ft}$$

$$\text{Inside area (modeling skin area)} = \pi DL = \pi \times 1 \times 6.7 = 21 \text{ ft}^2$$

$$\text{Cross-sectional area} = (0.5/12)(\pi \times 1) = 0.13 \text{ ft}^2$$

$$\text{Effective diameter for Re calculation} = 4 \times \text{cross section}/L \times \text{heat transfer area} = 1 \text{ in} = 0.083 \text{ ft}$$

$$\text{Re} = \rho V D_e / \mu = 135V$$

Let $V = 5 \text{ ft/sec}$, $\text{Re} = 675$, flow is laminar.

$$\text{CFM} = \text{cross-sectional area} \times \text{velocity} = 0.13 \times 5 \times 60 = 39$$

From the laminar flow correlations of Kays and London, for this case, $h = 1.05 \text{ Btu/hr-ft}^2^\circ\text{F}$. Actually, the value of h does not increase, particularly with V in this range (e.g., for $V = 15 \text{ ft/sec}$, $\text{Re} = 2000$, $h = 1.12$).

Contrails

One could increase h by decreasing the cross-sectional area, but a width of 0.5 inch is rather small and closer tolerances would tend to cause the coolant to channel.

APPENDIX III

MAXIMUM EFFECTIVE ABSORPTANCE OF AN INFINITE V-GROOVE

To determine the maximum effect on the absorptance or emittance in a fold, we examined the flux absorbed on a small differential area near the point of a V-groove. The absorbed flux consists of two components, the direct solar radiation, S (of long wavelength radiation), and the diffusively reflected component of radiation from the opposite wall, W_s .

Consider the V-groove shown in Figure 41, with direct solar radiation, S . The absorbed radiation, U , is given by:

$$U = \alpha_s S + \alpha_s W_s F_{dA-W_s} \quad (29)$$

where the view area of the element dA to the opposite wall is given by:

$$F_{dA-W_s} = \frac{1}{2} (1 + \cos\theta) \quad (30)$$

The radiance of the opposite wall is given by:

$$W_s = (1 - \alpha_s) S + (1 - \alpha_s) \frac{1}{2} (1 + \cos\theta) \quad (31)$$

Substituting equation 31 into 29 and rearranging yields:

$$U = \alpha_s S \left[1 + \frac{(1 - \alpha_s) \frac{1}{2} (1 + \cos\theta)}{1 - \frac{1 - \alpha_s}{2} (1 + \cos\theta)} \right] \quad (32)$$

By definition, the effective absorptance is given by $\alpha_{as} = \frac{U}{S}$; therefore,

$$\alpha_{as} = \alpha \left[1 + \frac{\frac{1}{2} (1 - \alpha_s) (1 + \cos\theta)}{1 - \frac{1}{2} (1 - \alpha_s) (1 + \cos\theta)} \right] \quad (33)$$

This expression can also be written in terms of the long wavelength absorptance which is also equal to the emittance, ϵ :

$$\epsilon_a = \epsilon \left[1 + \frac{\frac{1}{2} (1 - \epsilon) (1 + \cos\theta)}{1 - (1 - \epsilon) (1 + \cos\theta)} \right] \quad (34)$$

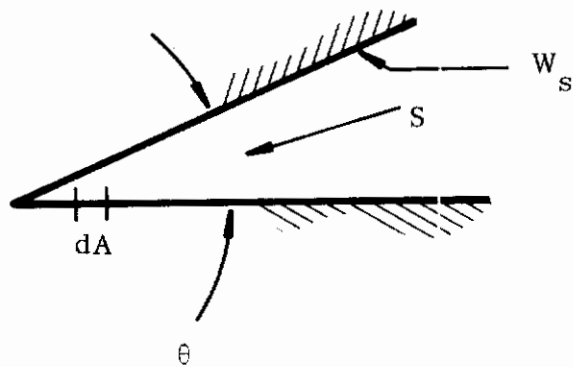


FIGURE 41. SPACE SUIT FOLD

Contrails

The effective solar absorptance was calculated for $\alpha_s = 0.17$; the effective emittance was calculated for $\epsilon = 0.85$; and the ratio of α_{as}/ϵ_a was calculated. The results are summarized below and on Figure 20.

| <u>θ</u> | <u>α_{as}</u> | <u>ϵ_a</u> | <u>α_{as}/ϵ_a</u> |
|----------------------------|---------------------------------|--------------------------------|--------------------------------------------|
| 0 | 1.0 | 1.0 | 1.0 |
| 30 | 0.755 | 0.991 | 0.76 |
| 60 | 0.450 | 0.958 | 0.47 |
| 90 | 0.291 | 0.920 | 0.32 |
| 120 | 0.214 | 0.882 | 0.24 |
| 180 | 0.17 | 0.85 | 0.20 |

Contrails

APPENDIX IV

ANALYSIS OF LOUVER PERFORMANCE

In this analysis we are concerned with (1) the heat which can be dissipated by a louver system, and (2) the temperatures of the baseplate and the louvers. Two analyses are presented: (1) for open louvers with the sun overhead or without sunlight, and (2) closed louvers with the sun overhead or without sunlight. The analysis takes into account the specular reflection of energy from one side of each louver vane and diffuse reflection from the baseplate and from the opposite side of each louver vane. The model used in the analysis for open louvers is shown in Figure 42.

A. ASSUMPTIONS

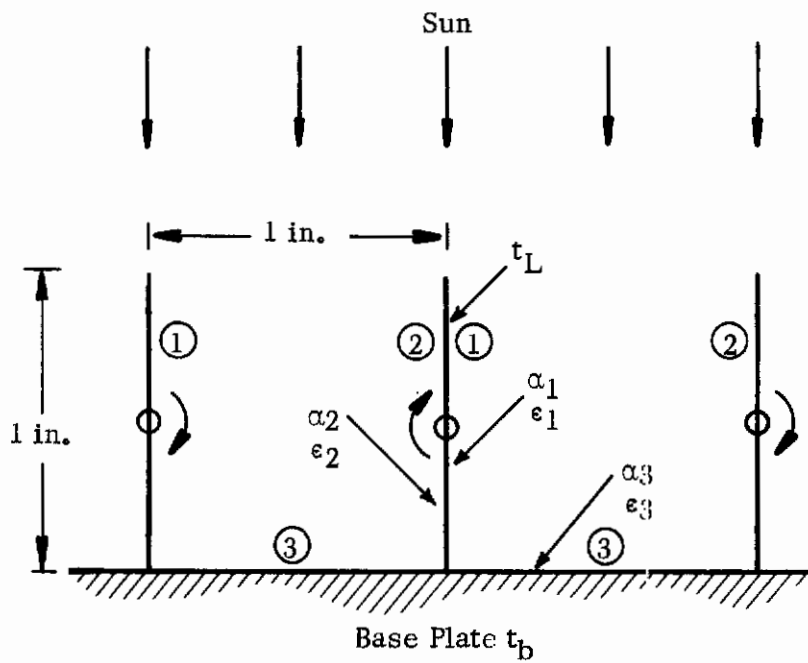
The following assumptions were made:

1. The baseplate and one side of the louvers are diffuse reflectors.
2. The other side of the louvers are specular reflectors.
3. All surfaces are diffuse emitters.
4. The reflectivity of all surfaces for all wavelengths is $\rho = (1 - \alpha)$.
5. The area of one side of the louver is equal to the area of the base (i.e., $A_1 = A_2 = A_3 = A_L$).

B. ANALYSIS FOR OPEN LOUVERS

1. Louver Heat Balance

$$\begin{aligned}(\epsilon_1 + \epsilon_2) \sigma T_L^4 &= \alpha_1 (1 - \alpha_3) F_{3-1} S && \text{solar reflected} \\ & && \text{from baseplate} \\ & && \text{to surface (1)} \\ &+ \alpha_2 (1 - \alpha_3) F_{3-2} S && \text{solar reflected} \\ & && \text{from baseplate} \\ & && \text{to surface (2)} \\ &+ \epsilon_1 \epsilon_3 F_{3-1} \sigma T_b^4 && \text{direct from} \\ & && \text{baseplate to} \\ & && \text{surface (1)} \\ &+ \epsilon_2 \epsilon_3 F_{3-2} \sigma T_b^4 && \text{direct from} \\ & && \text{baseplate to} \\ & && \text{surface (2)}\end{aligned}$$



Surface 1 is a specular reflector

Surfaces 2 and 3 are diffuse reflectors

All surfaces are diffuse emitters

FIGURE 42. MODEL FOR OPEN LOUVERS

| | |
|--------------------------------------------------------------------|-------------------------------------------------------------------|
| $+ \epsilon_1 \epsilon_2 F_{2-1} \sigma T_L^4$ | direct from louver surface (2) to surface (1) |
| $+ \epsilon_2 \epsilon_1 F_{1-2} \sigma T_L^4$ | direct from louver surface (1) to surface (2) |
| $+ S(1 - \alpha_3)(1 - \alpha_1) \alpha_2 F_{3(1)-2}$ | solar reflected from (3) and re-reflected from (1) onto (2) |
| $+ \epsilon_2 (1 - \epsilon_1) F_{3(1)-2} \epsilon_3 \sigma T_b^4$ | baseplate radiation re- flected from (1) onto (2) |
| $+ \epsilon_2 (1 - \epsilon_1) F_{2(1)-2} \epsilon_2 \sigma T_L^4$ | side (2) radiation re- flected from (1) back onto side (2) |

2. Baseplate Heat Balance

| | |
|--------------------------------------------------------------------|---------------------------------------------------|
| $\epsilon_3 \sigma T_b^4 = S \alpha_3$ | direct solar |
| $+ \epsilon_3 F_{1-3} \epsilon_1 \sigma T_L^4$ | direct from (1) |
| $+ \epsilon_3 F_{2-3} \epsilon_2 \sigma T_L^4$ | direct from (2) |
| $+ \epsilon_3 F_{2(1)-3} (1 - \epsilon_1) \epsilon_2 \sigma T_L^4$ | radiation from (2) re- flected in (1) onto (3) |
| $+ q_b$ | heat generated per unit of area in baseplate |

The view areas for both direct diffuse radiation and for specular re-reflected radiation were calculated by the method of crossed strings for the geometry shown in Figure 42. (Infinitely long vanes were assumed.) The view areas are:

| | |
|------------------|----------------------|
| $F_{3-1} = 0.3$ | $F_{1-3} = 0.3$ |
| $F_{3-2} = 0.3$ | $F_{3(1)-2} = 0.085$ |
| $F_{2-1} = 0.38$ | $F_{2(1)-2} = 0.24$ |
| $F_{1-2} = 0.38$ | $F_{2(1)-3} = 0.085$ |
| $F_{2-3} = 0.3$ | |

The equations were programmed for solution by machine computation and solved for a range of q_b .

C. ANALYSIS FOR CLOSED LOUVERS

When the louvers shown in Figure 42 are closed, the heat balance equations become:

1. Louver Heat Balance

$$(\epsilon_2 + \epsilon_1) \sigma T_L^4 = S \alpha_2 + \epsilon_1 \epsilon_3 \sigma T_b^4$$

2. Baseplate Heat Balance

$$q_b = \frac{\epsilon_1 \epsilon_3}{\epsilon_1 + \epsilon_3 - \epsilon_1 \epsilon_3} (\sigma T_b^4 - \sigma T_L^4)$$

REFERENCES

- Bader, Frank, 1965, Considerations for Temperature Control of Aircrewman through Water Cooled Garments, SLS-121-65, Johns Hopkins Applied Physics Laboratory, Silver Spring, Maryland, pp 6.
- Beaumont, W. van, and R. W. Bullard, 1965, "Sweating: Direct Influence of Skin Temperature," Science, 147, 1465-1467.
- Benzinger, T. H., 1961, "The Diminution of Thermo-Regulatory Sweating during Cold-Reception at the Skin," Physiology, 47, 1683-1688.
- Bowen, J. D., 1963, Thermal Transport System for a Space Worker's Garment, AMRL Memorandum M-49, Aerospace Medical Research Laboratories, Wright-Patterson AFB, Ohio, pp 9.
- Burton, D. R., and L. Collier, 1964, The Development of Water Conditioned Suits, Tech. Note No. Mech. Eng. 400, Royal Aircraft Establishment, Farnborough, Hants, England, pp 54.
- Burton, D. R., 1965, The Thermal Assessment of Personal Conditioning Garments, Tech. Report 65263, Royal Aircraft Establishment, Farnborough, Hants, England, pp 40.
- Burton, D. R., and L. Collier, 1965, The Performance of Water Conditioned Suits, Tech. Report 65004, Royal Aircraft Establishment, Farnborough, Hants, England, pp 43.
- Cramer, K. R., and T. F. Irvine, 1963, Attenuation of Nonuniform Suit Temperatures for Space Suits in Orbit, AMRL-TDR-63-80, pp v + 9.
- Felder, J. W., and A. P. Shlosinger, 1963, Research on Methods for Thermal Transport in a Space Worker's Garment, AMRL-TDR-63-90, Aerospace Medical Research Laboratories, Wright-Patterson AFB, Ohio, pp v + 70.
- Fixler, S. Z., 1966, "Satellite Thermal Control Using Phase-Change Materials," J. Spacecraft, 3, 1362-1368.
- Jennings, D. C., 1966, "Water-Cooled Space Suit," J. Spacecraft, 3, 1251-1256.
- Katzoff, S., 1967, Heat Pipes and Vapor Chambers for Thermal Control of Spacecraft, Paper No. 67-310, AIAA Thermophysics Specialist Conference, New Orleans, Louisiana, pp 23.
- Kincaid, W. C., 1965, Apollo Portable Life-Support System--Development Status, Paper 65-AV-45, Aviation and Space Conference, Los Angeles, pp 5.
- Leatherman, R. A., 1963, Component Thermal Control Via Heat of Fusion Radiator, ASME Paper 63-AHGT-12, Aviation and Space, Hydraulic, and Gas Turbine Conference and Products Show, Los Angeles, California, pp 8.

Contrails

Little, Arthur D. Inc., 1964, Basic Investigations of Multi-Layer Insulation Systems, Report No. NASA CR-54191, Contract NAS3-4181.

Little, Arthur D. Inc., 1966, Advanced Studies on Multi-Layer Insulation Systems, Report No. NASA CR-54929, Contract NAS3-6283.

Parmer, J. F., and D. L. Buskirk, 1967, The Thermal Radiation Characteristics of Spacecraft Temperature Control Louvers in the Solar Environment, Paper No. 67-307, AIAA Thermophysics Specialist Conference, New Orleans, Louisiana, pp 9.

Peterson, J. A., C. Cafaro, A. P. Shlosinger, and K. F. Sterrett, 1965, Analytical Review of Passive Mass Transfer of Water Vapor in a Space Suit, NSL 65-87-1, Northrup Space Laboratory, pp ii + 52.

Plamondon, J. A., 1964, Analysis of Movable Louvers for Temperature Control, Jet Propulsion Laboratory Technical Report No. 32-555, pp iii + 13.

Richardson, D. L., 1965, Study and Development of Materials and Techniques for Passive Thermal Control of Flexible Extravehicular Space Garments, AMRL-TR-65-156, Aerospace Medical Research Laboratories, Wright-Patterson AFB, Ohio, pp x + 82.

Robinson, S., 1963, Pediatrics, October, Part II, 691-702.

Shlosinger, A. P., and W. Woo, 1965, Feasibility Study of Integral Heat Sink Space Suit Concepts, Northrup Space Laboratories, NSL 65-87-2, pp iii + 22.

Stevenson, J. A., and J. C. Grafton, 1961, Radiation Heat Transfer Analysis for Space Vehicles, ASD Technical Report 61-119, Part I, Aeronautical Systems Division, Wright-Patterson AFB, Ohio, pp xiv + 426.

Sparrow, E. M., 1965, Radiation Emission, Absorption and Transmission Characteristics of Cavities and Passages, Symposium on Thermal Radiation of Solids (San Francisco, March 1965), S. Katzoff, Ed., NASA SP-55, 103-115.

Sparrow, E. M., and S. H. Lin, 1964, "Absorption of Thermal Radiation in a V-Groove Cavity," Int. J. of Heat and Mass Transfer, 5, 1111-1115.

Welch, B. E., et al., 1963, Effect of Ventilating Air Flow on Human Water Requirements, AD 426008, USAF School of Aerospace Medicine, Aerospace Medical Division, Brooks AFB, Texas, pp iii + 11.

Whisenhunt, G. B., and R. A. Knezek, 1962, A Thermal Protection System for Extra-Vehicular Space Suits, ARS Lunar Missions Meeting, Cleveland, Ohio, pp 11.

Contrails

Zerlaut, G. A., Y. Harada, and E. H. Tompkins, 1965, "Ultraviolet Irradiation in Vacuum of White Spacecraft Coatings," Symposium on Thermal Radiation of Solids, S. Katzoff, Ed., NASA SP-55, ML TDR-64-159, Scientific and Technical Information Division, National Aeronautics and Space Administration, Washington, D. C., 391-420.

Contrails

UNCLASSIFIED
Security Classification

| DOCUMENT CONTROL DATA - R&D | | |
|-----------------------------------------------------------------------------------------------------------------------------------------------------------------------------------------------------------------------------------------------------------------------------------------------------------------------------------------------------------------------------------------------------------------------------------------------------------------------------------------------------------------------------------------------------------------------------------------------------------------------------------------------------------------------------------------------------------------------------------------------------------------------------------------------------------------------------------------------------------------------------------------------------------------------------------------------------------------------------------------------------------------------------------------------------------------------------------------------------------------------------------------------------------------------------------------------------------------------------------------------------------------------------------------------------------------------------------------------------------------------------------------------------------------------------------------------------------------------------------------------------------------------------------------------------------------------------------------------------------------------------------------------------------------------------------------------------------------------------------------------------------------------------------------------------------------------------------------------------------------------|-----------------------------------------------------------------------------------------------------------------------------------------------------------------------------|-------------------------------|
| (Security classification of title, body of abstract and indexing annotation must be entered when the overall report is classified) | | |
| 1. ORIGINATING ACTIVITY (Corporate author) Arthur D. Little, Inc. Acorn Park Cambridge, Massachusetts 02140 | 2 a. REPORT SECURITY CLASSIFICATION Unclassified | |
| | 2 b. GROUP | |
| 3. REPORT TITLE STUDY OF TECHNIQUES AND MATERIALS FOR PASSIVE THERMAL CONTROL OF RIGID AND FLEXIBLE EXTRAVEHICULAR SPACE ENCLOSURES | | |
| 4. DESCRIPTIVE NOTES (Type of report and inclusive dates) Final Report, February 1966-May 1967 | | |
| 5. AUTHOR(S) (Last name, first name, initial) Richardson, David L. | | |
| 6. REPORT DATE December 1967 | 7 a. TOTAL NO. OF PAGES 114 | 7 b. NO. OF REFS 28 |
| 8 a. CONTRACT OR GRANT NO. AF 33(615)-3533 b. PROJECT NO. 7164 c. Task No. 716412 d. | 9 a. ORIGINATOR'S REPORT NUMBER(S) 9 b. OTHER REPORT NO(S) (Any other numbers that may be assigned this report) AMRL-TR-67-128 | |
| 10. AVAILABILITY/LIMITATION NOTICES Distribution of this document is unlimited. It may be released to the Clearinghouse, Department of Commerce, for sale to the general public. | | |
| 11. SUPPLEMENTARY NOTES | 12. SPONSORING MILITARY ACTIVITY Aerospace Medical Research Laboratories, Aerospace Medical Division, Air Force Systems Command, Wright-Patterson AFB, Ohio | |
| 13. ABSTRACT This program encompassed an analytical and experimental investigation of passive and semi-passive thermal control techniques for rigid and flexible extravehicular space enclosures in 300 nautical mile earth orbits. The results of the orbit analysis indicate that when an astronaut in a flexible enclosure (soft space suit) works on the surface of a large spacecraft, the temperatures on his external surface are markedly increased over those which occur when he is not near the spacecraft. Moreover, passive thermal control of the astronaut is not possible when he is near the spacecraft. The techniques investigated for thermally coupling an astronaut with his thermal control system include liquid cooled undergarments, gas cooling, and heat transfer to the cooled walls of his enclosure. Techniques were investigated for increasing the conductance through soft space suit insulations by compressing the insulation. The insulation of a cylindrical section of a space suit arm was measured under both compressed conditions (3.7 psia) and uncompressed conditions in simulated noon and earth-umbra orbit positions. The range of conductance increased from 0.26 Btu/ft ² -hr°F uncompressed to 0.81 Btu/ft ² -hr°F compressed. Measurements were made in simulated noon and earth-umbra orbit positions of the thermal heat dissipating capability of a louver system which was designed for operation in the sun. A 6-inch square model had a net heat flow from the louvers for the four orbit conditions tested (open and closed in the sun and in the shade). The louver operation controls maintained the louver baseplate temperature in the range from 73.9 to 84.7°F for a steady heat dissipation rate of 95.5 Btu/ft ² -hr while operating in the shade. | | |

DD FORM 1473
1 JAN 64

UNCLASSIFIED
Security Classification

| 14. | KEY WORDS | LINK A | | LINK B | | LINK C | |
|-----|---------------------------------------------------------------------------------------------------------------------------------------------|--------|----|--------|----|--------|----|
| | | ROLE | WT | ROLE | WT | ROLE | WT |
| | <p>Extravehicular space enclosures, flexible and rigid</p> <p>Passive thermal control</p> <p>Insulations</p> <p>Thermal control louvers</p> | | | | | | |

INSTRUCTIONS

1. **ORIGINATING ACTIVITY:** Enter the name and address of the contractor, subcontractor, grantee, Department of Defense activity or other organization (*corporate author*) issuing the report.
- 2a. **REPORT SECURITY CLASSIFICATION:** Enter the overall security classification of the report. Indicate whether "Restricted Data" is included. Marking is to be in accordance with appropriate security regulations.
- 2b. **GROUP:** Automatic downgrading is specified in DoD Directive S200.10 and Armed Forces Industrial Manual. Enter the group number. Also, when applicable, show that optional markings have been used for Group 3 and Group 4 as authorized.
3. **REPORT TITLE:** Enter the complete report title in all capital letters. Titles in all cases should be unclassified. If a meaningful title cannot be selected without classification, show title classification in all capitals in parenthesis immediately following the title.
4. **DESCRIPTIVE NOTES:** If appropriate, enter the type of report, e.g., interim, progress, summary, annual, or final. Give the inclusive dates when a specific reporting period is covered.
5. **AUTHOR(S):** Enter the name(s) of author(s) as shown on or in the report. Enter last name, first name, middle initial. If military, show rank and branch of service. The name of the principal author is an absolute minimum requirement.
6. **REPORT DATE:** Enter the date of the report as day, month, year; or month, year. If more than one date appears on the report, use date of publication.
- 7a. **TOTAL NUMBER OF PAGES:** The total page count should follow normal pagination procedures, i.e., enter the number of pages containing information.
- 7b. **NUMBER OF REFERENCES:** Enter the total number of references cited in the report.
- 8a. **CONTRACT OR GRANT NUMBER:** If appropriate, enter the applicable number of the contract or grant under which the report was written.
- 8b, 8c, & 8d. **PROJECT NUMBER:** Enter the appropriate military department identification, such as project number, subproject number, system numbers, task number, etc.
- 9a. **ORIGINATOR'S REPORT NUMBER(S):** Enter the official report number by which the document will be identified and controlled by the originating activity. This number must be unique to this report.
- 9b. **OTHER REPORT NUMBER(S):** If the report has been assigned any other report numbers (*either by the originator or by the sponsor*), also enter this number(s).
10. **AVAILABILITY/LIMITATION NOTICES:** Enter any limitations on further dissemination of the report, other than those

imposed by security classification, using standard statements such as:

- (1) "Qualified requesters may obtain copies of this report from DDC."
- (2) "Foreign announcement and dissemination of this report by DDC is not authorized."
- (3) "U. S. Government agencies may obtain copies of this report directly from DDC. Other qualified DDC users shall request through _____."
- (4) "U. S. military agencies may obtain copies of this report directly from DDC. Other qualified users shall request through _____."
- (5) "All distribution of this report is controlled. Qualified DDC users shall request through _____."

If the report has been furnished to the Office of Technical Services, Department of Commerce, for sale to the public, indicate this fact and enter the price, if known.

11. **SUPPLEMENTARY NOTES:** Use for additional explanatory notes.
12. **SPONSORING MILITARY ACTIVITY:** Enter the name of the departmental project office or laboratory sponsoring (*paying for*) the research and development. Include address.
13. **ABSTRACT:** Enter an abstract giving a brief and factual summary of the document indicative of the report, even though it may also appear elsewhere in the body of the technical report. If additional space is required, a continuation sheet shall be attached.

It is highly desirable that the abstract of classified reports be unclassified. Each paragraph of the abstract shall end with an indication of the military security classification of the information in the paragraph, represented as (TS), (S), (C), or (U).

There is no limitation on the length of the abstract. However, the suggested length is from 150 to 225 words.
14. **KEY WORDS:** Key words are technically meaningful terms or short phrases that characterize a report and may be used as index entries for cataloging the report. Key words must be selected so that no security classification is required. Identifiers, such as equipment model designation, trade name, military project code name, geographic location, may be used as key words but will be followed by an indication of technical content. The assignment of links, roles, and weights is optional.